OVERACTIVE CDK2 IN THE PROGRESSION AND TREATMENT OF CANCER

By

STEPHAN CHRISTOPHER JAHN

A DISSERTATION PRESENTED TO THE GRADUATE SCHOOL
OF THE UNIVERSITY OF FLORIDA IN PARTIAL FULFILLMENT
OF THE REQUIREMENTS FOR THE DEGREE OF
DOCTOR OF PHILOSOPHY

UNIVERSITY OF FLORIDA

2013

To my family, my friends, the Gator Nation, and all of the fish I have yet to catch

ACKNOWLEDGEMENTS

I first want to thank the people that helped me get here. My family has always been extremely supportive throughout my schooling and there is no way I would have come this far without their help. They know what it means to me to be a Gator, and have made sure that I was able to achieve that dream. I would also like to thank my friends and professors at Saginaw Valley State University, particularly Dr. David Karpovich, who served as my undergraduate honors thesis advisor and has continued to provide knowledge and support since.

I next would like to thank all of those that helped me navigate through graduate school. My mentor, Dr. Brian Law, has given me a wonderful opportunity in his lab, and has taught me much of what I know about being an academic scientist. Dr. Mary Law and Dr. Patrick Corsino taught me many of the techniques I have utilized and Brad Davis kept the lab running. My other committee members: Dr. Jeffrey Harrison, Dr. Nicole Horenstein, Dr. Thomas Rowe, and Dr. Peter Sayeski, have provided me with a lot of valuable feedback on my data and Dr. Rowe spent considerable time helping me with protein purification. Dr. Horenstein provided time and resources in helping with organic synthesis.

I finally need to thank those that have supported me outside of the lab. My fellow Lutheran Gators have truly changed my life in the last few years and I am proud to call them my friends. Most of all, I thank Stephani. While we study vastly different areas and rarely understand the intricacies of each other's work, she somehow understands the big picture of what I have done better than I do and continues to give more support and love than I could ever need. Thank you.

TABLE OF CONTENTS

page

LIST OF FIGURES

LIST OF ABBREVIATIONS

APC	Adenomatous Polyposis Coli
APC/C	Anaphase Promoting Complex/Cyclosome
BRCA	Breast Cancer
BRK	Breast tumor Kinase
Bub	Budding uninhibited by benzimidazoles
CAK	Cdk Activating Kinase
Cdc	Cell division cycle
Cdh1	Cdc20 homolog 1
Cdk	Cyclin dependent kinase
CIN	Chromosomal Instability
CTX	Cholera toxin
D1K2	Cyclin D1/Cdk2 fusion protein
D1K2(kd)	Kinase Dead D1K2
D1K2(ke)	Inactive D1K2
D1K2 CL1	D1K2 Clone 1
D1K4	Cyclin D1/Cdk4 fusion protein
DAPI	4',6-diamidino-2-phenylindole
DMEM	Dulbecco’s Modified Eagle’s Medium
DMSO	Dimethyl Sulfoxide
E2F	E2 promoter binding Factor
EGF/R	Epidermal Growth Factor/Receptor
EK2	Cyclin E/Cdk2 fusion protein
EMT	Epithelial to Mesenchymal Transition
FBS	Fetal Bovine Serum

GFP-NPM	Green Fluorescent Protein tagged Nucleophosmin
GST-Cdh1	Glutathione tagged Cdh1
HCN	Hydrocortisone
Her2	Human epidermal growth factor receptor 2
HGF	Hepatocyte Growth Factor
HPV	Human Papilloma Virus
IL6	Interleukin 6
ITS	Insulin Transferrin Selenium
LPA/R	Lysophosphatidic Acid/Receptor
Mad	Mitotic arrest deficient
MCC	Mitotic Checkpoint Complex
Mek	MAP/ERK Kinase
MMTV	Mouse Mammary Tumor Virus
MPM2	Mitotic Protein Monoclonal 2
NPM	Nucleophosmin
PBS	Phosphate Buffered Saline
PCM	Pericentriolar Matrix
PDGF/R	Platelet Derived Growth Factor/Receptor
Plk	Polo-like Kinase
PSF	Polypyrimidine tract binding protein-associated Splicing Factor
PSF(12M)	Non-phosphorylatable mutant PSF
Rb	Retinoblastoma
RTK	Receptor Tyrosine Kinase
SAC	Spindle Assembly Checkpoint
SDS-PAGE	Sodium Dodecyl Sulfate Polyacrylamide Gel Electrophoresis

SFPQ	Splicing Factor Proline Glutamine rich
TGF-β	Transforming Growth Factor Beta
TNFα	Tumor Necrosis Factor Alpha
WT-PSF	Wildtype PSF

Abstract of Dissertation Presented to the Graduate School
of the University of Florida in Partial Fulfillment of the
Requirements for the Degree of Doctor of Philosophy

OVERACTIVE CDK2 IN THE PROGRESSION AND TREATMENT OF CANCER

By

Stephan Christopher Jahn

May 2013

Chair: Brian Law
Major: Medical Sciences—Physiology and Pharmacology

Cyclin dependent kinase 2 (Cdk2) is commonly overactive in human cancers. This has previously been shown to cause a deregulation of the cell cycle through Rb phosphorylation and subsequent tumorigenesis. Here, we discuss a number of other effects that overactive Cdk2, particularly when in complex with Cyclin D1, has on cells and how this may possibly lead to tumor progression. Phosphorylation of Rb leads to increased expression of the spindle assembly checkpoint protein, Mad2, and therefore strengthens it. Conversely, this hyperphosphorylation prevents cell cycle arrest due to the tetraploidy checkpoint, rendering cells susceptible to polyploidy and subsequent aneuploidy. Cooperating with this mechanism of chromosomal instability, Cyclin D1/Cdk2 complexes are shown to phosphorylate Nucleophosmin and Cdh1, two proteins that play integral roles in the centrosome replication pathway. Cells expressing a Cyclin D1/Cdk2 fusion protein, D1K2, also exhibit failed cytokinesis, decreased ability to bundle supernumerary centrosomes, and phosphorylation of the multifunctional protein, PSF.

Likely through a number of these mechanisms, overactive Cdk2 also promotes an epithelial to mesenchymal transition, which is characterized by a change in mitogenic

signaling pathways and an increased sensitivity to small molecule inhibitors of the newly activated pathways. Together, these results show that Cyclin D1 overexpression and overactive Cdk2 likely play a number of roles in the initiation, development, and progression of human cancers. The data presented here raise questions regarding our current understanding and treatment of tumors with overactive Cdk2, and offer insight into possible new directions in the fight against this disease.

CHAPTER 1
BACKGROUND

Introduction

Cancer is a disease that pervades our society. This uncontrolled cell growth starts at the single cell level but can quickly form a tumor large enough to affect human life. Cellular proliferation is normally well controlled and additional mechanisms exist to prevent abnormal growth, should a mutation occur. Traditional cancer treatments target tumor cells by preferentially killing these rapidly proliferating cells. However, these therapies tend to have significant side effects, making some cancer treatments nearly as terrible as cancer itself.

Recent advances have marked a shift in the treatment paradigm. Targeted therapies promise to exploit fundamental differences between tumor and normal cells at the molecular level, oftentimes hitting the root cause of the abnormal growth. These drugs are developed using rational, biochemical means rather than the simple growth inhibitory screens of the past, requiring researchers to have a greater understanding of cancer biology. Without basic research, these advances would not be possible.

This study examines the role of Cdks, particularly Cdk2, in the initiation and progression of cancer. It was found that overactive Cdk2 alters many of the cellular growth-control mechanisms, leading to tumor initiation and causes changes in the number of chromosomes contained in cells, which in turn can spur tumor progression. It also examines the intracellular targets of Cdk2 and discusses changes that occur in pro-growth signaling during the transition from a localized, epithelial phenotype, to an invasive, mesenchymal phenotype during cancer evolution. These results will hopefully prove useful in developing better, more specific cancer therapies.

Breast Cancer Overview

Each year there are approximately 230,000 cases of breast cancer in the United States, resulting in almost 40,000 deaths annually. One in eight women will be diagnosed with breast cancer at some point in their life. This makes breast cancer the second most common human cancer behind prostate cancer, and the second deadliest cancer behind lung cancer in terms of numbers of deaths [1]. Breast cancers arise due to many reasons, both acquired and familial. Mutations in the BRCA1 and BRCA2 genes, both encoding proteins important in DNA repair, are strong risk factors for developing breast cancer in a lifetime. Inherited mutations such as these only account for 5-10% of all cases, however [2]. While no specific environmental factors have been identified, other risk factors include obesity, use of exogenous estrogen or progesterone, and not having children or having them later in life, among many others (reviewed in [3]).

Most breast tumors are removed through surgery. However, surgery may not remove the entire tumor and cannot remove any metastases. Treatment therefore often also includes radiation and targeted or classic chemotherapy. Specific treatment regimens are determined by the specific type of breast cancer being treated.

Just as cancers differ wildly from one site to another (i.e. breast vs. colon cancer), breast cancers as a group are also extremely heterogeneous. Classified into five types with a total of eighteen further subtypes based on location and tissue type, tumors are also subdivided based on their molecular profile. Most important among these differences is the expression of the estrogen, progesterone, and Her2 receptors. These receptors normally control cellular growth and all, some, or none of them may be expressed in tumor cells. If one of these receptors is expressed, the cells are many

times still reliant on the pro-growth signals generated by them. This offers a therapeutic target, and perhaps the best example of this is tamoxifen, an estrogen receptor antagonist and widely used treatment against estrogen receptor positive tumors [4]. However, if a tumor has become no longer dependent on these pro-growth signals and does not express any of these receptors, treatment is much more difficult. As a result, these “triple negative” breast cancers have much lower rates of survival (reviewed in [5]).

Cell Cycle Control Through Cdks

The process of cellular proliferation consists of a precisely controlled series of events known as the cell cycle. After a cell in the human body divides, each daughter cell must prepare itself for the next mitotic division by replicating its DNA in S-phase. This results in a repeating sequence of DNA synthesis and mitosis alternating with gap-phases, giving the cell cycle the canonical G1, S, G2, M pattern. However, this does not proceed unchecked. Normal cells contain checkpoints that ensure cells only divide when appropriate, which involves both internal and external pro-growth signals as well as internal quality controls. While a large number of proteins contribute to cell cycle control, Cyclin Dependent Kinases (Cdks) are responsible for the majority of this regulation.

The Cdks are a family of serine/threonine kinases that received their name due to the fact that they are only active when bound to one of a family of activating proteins known as the Cyclins. Different Cyclins are produced at different points of the cell cycle, activating different Cdks and leading to cell cycle progression (reviewed in [6]) (Figure 1-1). The process is stopped by a fail-safe mechanism involving the E2F transcription factors. The E2F family controls the transcription of many proteins

including Cyclin A [7] and Cyclin E [8], as well as those responsible for DNA replication [9]. The pocket protein family, including Rb, p107, and p130 [10] inhibits E2F by binding and preventing transcription [11,12].

When a cell receives an external pro-growth signal, it causes the production of Cyclin D1 [13]. Cyclin D1 is the classic binding partner of Cdk4 [14] and Cdk6 [15], activating their kinase activity and inducing Rb phosphorylation [16]. This releases E2F and increases the expression of Cyclins A [7] and E [8]. These associate with Cdk2 [17], which further phosphorylates Rb [18], driving the cell into and through S phase (Figure 1-2). Cyclin A persists and complexes with Cdk1 until early mitosis [19], when a switch to Cyclin B occurs until the end of mitosis [20].

Cdk regulation is not limited to Cyclin levels, however. Kinase activity is also controlled by post-translational modifications and the binding of Cdk inhibitory proteins. Cdks require an activating phosphorylation event on a residue in their activation loop by a Cyclin dependent kinase activating kinase (CAK) [21,22]. Additionally, Cdk1 contains an inhibitory phosphorylation site that is phosphorylated by WEE1 [23] and removed by Cdc25 [24]. Cdks may also be inhibited by the binding of a member of the cip/kip family of proteins, including $p21^{cip}$ [25], $p27^{kip}$ [26], and $p57^{kip2}$ [27], or a protein from the INK4 family, which includes $p15^{INK4B}$ [28], $p16^{INK4A}$ [29], $p18^{INK4C}$ [30], and $p19^{INK4D}$ [31]. In most cases these proteins are constantly produced, presenting a surmountable barrier to cell cycle progression, however p21 is a p53 dependent gene that responds to DNA damage [32].

While each Cdk appears to play an important role in the cell cycle, studies have shown that there is a large amount of redundancy built into the system. For instance,

knockout of Cdk4 has little effect on cell proliferation [33], and Cdk6 knockout mice show little difference to normal mice [34]. Even Cdk2, which on the surface appears to play an indispensable role, when knocked out in mice leads only to errors in meiosis [35] due to the fact that Cdk1 can substitute for Cdk2, binding Cyclin E and phosphorylating normal Cdk2 substrates [36]. Combined knockout of Cdk2, Cdk4, and Cdk6 result in mouse embryos that develop past day 12 and cell lines derived from these embryos are viable [37].

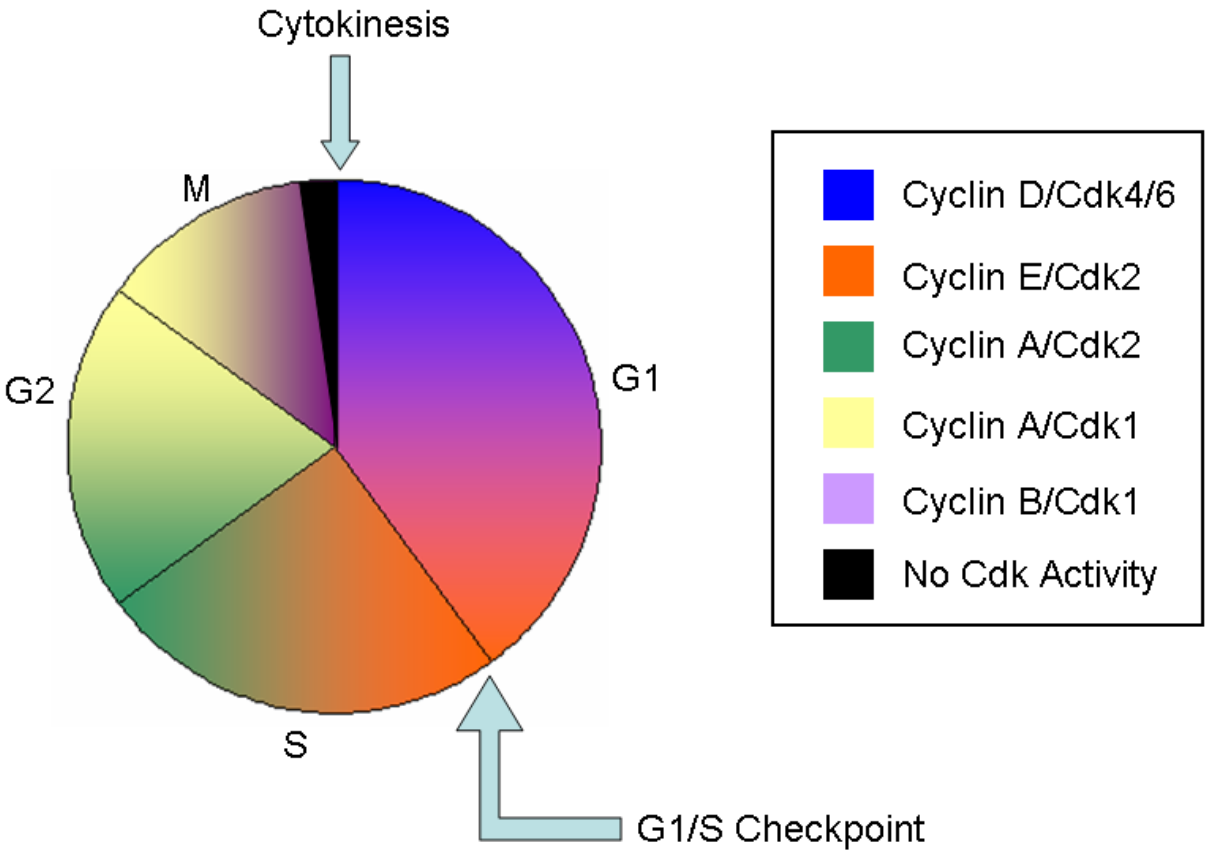

Figure 1-1. Cyclin expression controls Cdk activity. Cyclin D activates Cdk4 and Cdk6 in G1. Cyclin E/Cdk2 activity pushes the cell through the G1/S transition at which point Cyclin A levels increase to become the predominant Cdk2 binding partner. Cyclin A activates Cdk1 during G2 into the beginning of mitosis when Cyclin B binds to Cdk1. Degradation of Cyclin B marks the beginning of mitosis termination and there is no Cdk activity during cytokinesis.

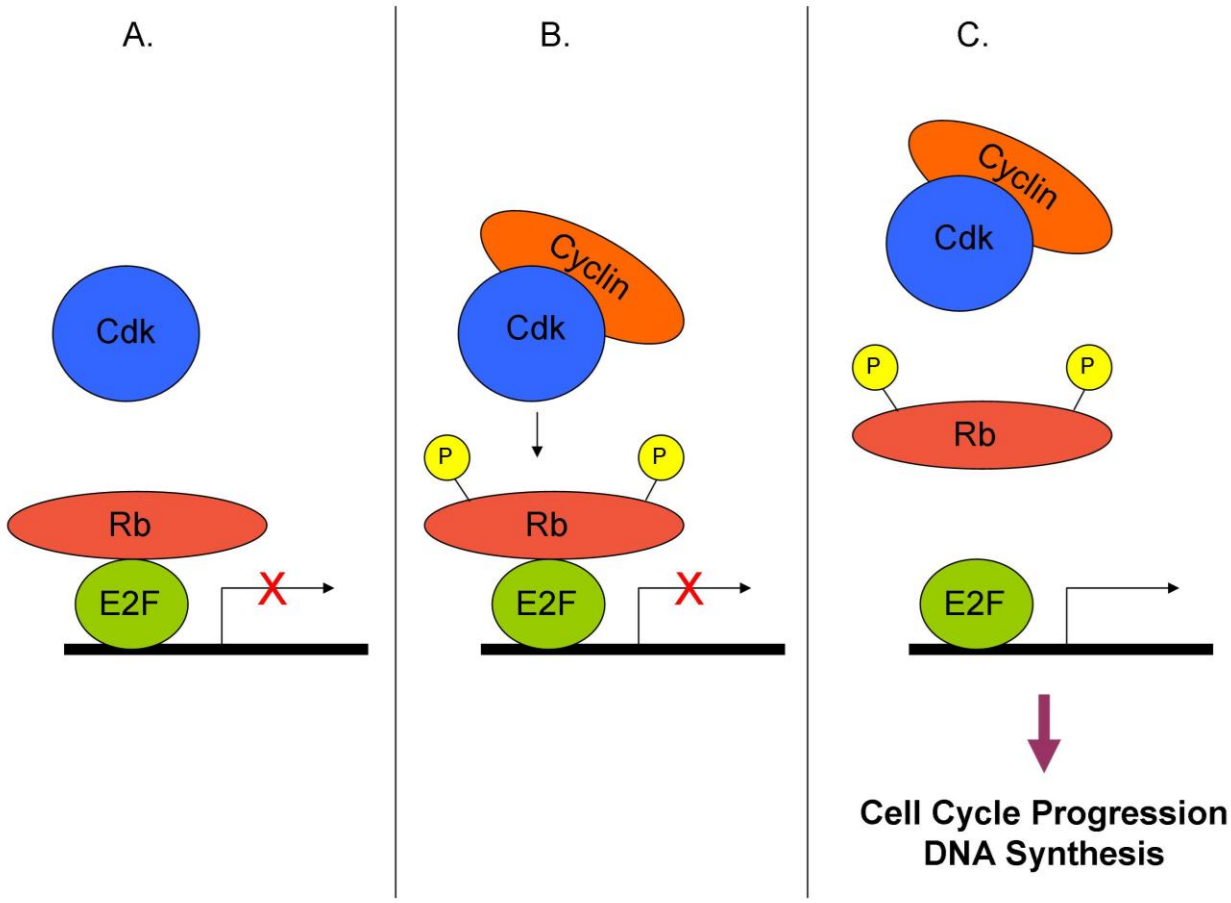

Figure 1-2. Cyclin/Cdk complexes promote the G1/S transition through phosphorylation of Rb. A) Without Cyclin expression, Rb sequesters E2F, blocking transcription. B) Upon Cyclin binding, the Cdk phosphorylates Rb. C) Phosphorylated Rb releases E2F, allowing transcription of genes required for DNA synthesis and cell cycle progression.

Cdks in Cancer

While Cdks may be able to replace other missing Cdks, they are not able to compensate when one becomes overactive, as is common in cancer. This may occur through multiple mechanisms including activating mutation [38] or loss of Cdk inhibitory protein expression or activity. p21 has been found to be mislocalized, residing in the cytoplasm rather than the nucleus where most Cdk activity occurs, in some breast cancers [39]. Being a p53 dependent gene, p21 is also not properly upregulated in most cancers since p53 is the most common mutation in all cancers [40,41]. This prevents p53 mediated cell cycle arrest in cells with a de-regulated cell cycle due to a lack of Cdk inhibition.

Perhaps the most common mechanism of Cdk overactivation is Cyclin overexpression. Cyclin E upregulation has been linked to both lung [42] and breast cancer [43], leading to a poorer prognosis in patients [44]. Additionally, a cleaved form of Cyclin E found in breast [45] and bladder [46] cancers, known as low molecular weight Cyclin E, produces greater Cdk2 activation than does the wild type protein [47].

Cyclin D1 is also commonly upregulated in breast cancer, being found at high levels in approximately 50% of all mammary tumors [48], particularly in estrogen and progesterone receptor positive tumors [49]. The simplest outcome of this phenomenon is overactivation of Cdk4 and Cdk6. Cyclin D1 overexpression also leads to an increase of Cdk4 protein levels [50] and high Cyclin D1 levels can lead to indirect increases in Cdk2 and Cdk1 activity. With the concomitant increase in Cyclin D1/Cdk4/6 complexes with p21 and p27, there will be a resulting decrease in levels of free Cdk inhibitory proteins, leading to a less inhibited pool of Cdk1 and Cdk2.

Cyclin D1/Cdk2 Complexes in Cancer

While the redundancy in the Cyclin-Cdk system, as already discussed, may prove beneficial to organisms lacking a functional Cdk gene, it can also lead to unintended phosphorylation events by non-canonical Cyclin/Cdk complexes, particularly when a Cyclin is expressed at more than a 1:1 ratio compared to its canonical Cdk partner. One example of this is Cyclin D1. The upregulation of Cyclin D1 reviewed above can also lead to the formation and activation of Cyclin D1/Cdk2 complexes [51,52]. In order to study these complexes in isolation from increased Cyclin D1/Cdk4 or Cdk6 complexes, our lab generated a D1K2 fusion protein in which a FLAG-tagged Cyclin D1 is located at the N-terminus and is attached by a flexible linker to a His_6-tagged Cdk2 on the C-terminus and it was found that one possible advantage of D1K2 activation as opposed to overactivation of Cyclin E/Cdk2 or Cyclin D1/Cdk4 complexes is an overlapping set of substrates [53]. Studies in transgenic mice with mammary specific expression of D1K2 under the control of the Mouse Mammary Tumor Virus (MMTV) promoter showed that this complex is capable of producing spontaneous tumor formation [54]. Cell lines isolated from these tumors showed hyperphosphorylation of pocket proteins, upregulation of E2F dependent genes, excretion of pro-growth factors, and resistance to the growth-inhibitory effects of TGF-β.

A number of studies have shown the physiological relevance of this D1K2 fusion protein. Cyclin D1/Cdk2 complexes were identified in nine out of thirteen breast cancer cell lines [48]. Additionally, an elegant experiment in which the endogenous Cdk2 gene was knocked out followed by a subsequent knock in of a FLAG-tagged Cdk2 gene to the same locus resulted in the exogenous protein being produced at endogenous levels, resulting in a non-tumorigenic model [55]. In these mice, Cyclin D1 was found to readily

form complexes with Cdk2, showing that Cyclin D1/Cdk2 complexes may play a normal physiological role in addition to situations where it is overexpressed.

Cdk Inhibitors as Cancer Therapeutics

With Cdks playing such a pivotal role in the cell cycle, which when deregulated is the driving force behind cancer cell proliferation, these kinases present a clear therapeutic target (discussion of Cdk inhibitors for the treatment of HPV infected tumors is discussed in Appendix A). Several Cdk inhibitors have been discovered and those that have been developed the furthest have been ATP competitive inhibitors. Being kinases, Cdks require the binding of ATP, the source of the transferred phosphate group. A compound that occupies the ATP binding site will block ATP binding and, in turn, block kinase activity. The most notable ATP competitive inhibitors to date are flavopiridol and roscovitine. Flavopiridol, isolated from a natural product [56], is a pan-Cdk inhibitor in that it inhibits all Cdks relatively equally, with IC_{50} values below 1 μM [57]. Inhibition leads to decreased Cyclin D1 levels, increased differentiation, and induces apoptosis (reviewed in [58]). It has advanced into the clinic, being used in Phase I and Phase II clinical trials [59-62]. Likewise, roscovitine has also progressed into Phase I clinical trials [63,64], however it shows more specificity than flavopiridol, inhibiting Cdk1 and Cdk2 much more potently than the other Cdks [65].

While most drug development focuses on discovering compounds that are as specific as possible in order to limit off target effects, the Cdks offer a unique circumstance. As already discussed, redundancy in the Cdk system allows other Cdks to substitute for a missing Cdk. Therefore, inhibiting a single Cdk may not be sufficient to halt the cell cycle of cancer cells, possibly explaining the relatively greater clinical

success of flavopiridol and roscovitine over more selective inhibitors such as CVT313, a Cdk2 inhibitor [66].

Our lab has taken an entirely different approach to inhibiting Cdks, developing a family of non-ATP competitive inhibitors. Using in silico molecular docking, compounds were discovered that induce Cdk aggregation, reducing the effective levels of intracellular Cdks, and reducing Cdk kinase activity. These aggregates form and are collected into aggresomes before degradation. This results in decreased Rb phosphorylation, lower E2F dependent transcription, and cell cycle arrest [67]. One compound identified in this screen, NSC117024, was more potent in inhibiting cellular proliferation than the other compounds and did not appear to induce aggregation. The further characterization of this compound is included in the current study and is located in Appendix B.

The Spindle Assembly Checkpoint in Cancer

Discovery

In 1902, Theodore Boveri proposed that cancers could derive from “a certain abnormal chromosome constitution, which in some circumstances can be generated by multipolar mitoses” [68]. Since little was known about the cell cycle, and the spindle assembly checkpoint (SAC) had not been discovered, he did not know he was implying that cancer cells have a weakened SAC. While studying the effects of radiation on mitosis in 1970, Zirkle was one of the first to notice that even a small aberration in the alignment of chromosomes at the metaphase plate induced a delay in anaphase [69]. With the discovery of microtubule agents including paclitaxel (1967) [70] and nocodazole (1976) [71], researchers were equipped with the tools needed to induce this delay and discovered that it was triggered by the failure of the mitotic spindles to

correctly attach to the chromosomes. Today, it is known that the SAC is a complex mechanism for monitoring attachment of microtubules to centromeres during mitosis wherein even a single anomaly will prevent the release of proteins essential for the progression of mitosis, and that deficiencies in the ability to prevent improper division can lead to chromosomal instability (Figure 1-3).

Mechanism of Mitotic Inhibition

The final event in initiating cell division at the metaphase to anaphase transition is the cleavage of Cohesin, which is the protein responsible for holding sister chromatids together after they replicate in S-phase. The end result of an activated SAC is the delay of the protease Separase in cleaving Cohesin. Separase is sequestered and inhibited by Securin, whose degradation is controlled by the Anaphase Promoting Complex/Cyclosome (APC/C) (Figure 1-4). The activating subunit of the APC/C, Cdc20, is bound at the kinetochore of improperly attached chromosomes in a group of proteins known as the Mitotic Checkpoint Complex (MCC) also containing Bub3, BubR1, and Mad2 (reviewed in [72]) (Figure 1-5).

Spindle Assembly Checkpoint Control

The SAC checkpoint operates using a “fail-safe” mechanism in that rather than being initiated if a problem arises in the formation of the spindle poles, it is automatically activated prior to spindle formation and is then shut off once all connections are properly made. Upon nuclear envelope breakdown as cells enter mitosis, Mad1 binds to the unattached kinetochores. Mad1 then recruits Mad2 and the remainder of the MCC [73]. Experimental data support two models of release from the SAC. It is currently unclear which the predominant mechanism is, but both are likely to be relevant in vivo.

Attachment model

The attachment model requires all chromatids to be attached to a spindle, but does not account for correct versus incorrect attachments. When the plus-ends of microtubules attach to kinetochores, Mad2 is released from the MCC, signaling SAC inactivation. This is supported by the fact that using a laser to destroy the last unattached kinetochore results in checkpoint deactivation, despite leaving a tensionless microtubule [74].

Tension model

In this model, it is tension at the kinetochore that inactivates the SAC, rather than only the presence of microtubules. AuroraB senses tension at the kinetochore and controls the activity of MCAK, a microtubule severing protein, along with the DASH and Ndc80/Hec1 complexes [75]. This mechanism is able to detect incorrect spindle attachments. Syntelic attachment, the attachment of both kinetochores to one spindle pole, does not generate the tension required to satisfy the SAC, and mitosis is unable to proceed [76]. However, merotelic attachments, the attachment of one kinetochore to both spindle poles, do provide sufficient tension. This is alternatively detected by AuroraB through a separate, poorly understood mechanism [75].

Causes of a Weakened Checkpoint

With chromosomal instability being a hallmark of cancers and a weakened SAC being present in a majority of tumor cells, it would seem likely that the components of the SAC would have a high rate of mutation. While individual mutations have been identified, they are not widespread enough to be considered the cause of the defective checkpoint, and in fact a large number of tumors show no mutations at all [77]. Contrarily, the expression levels of proteins involved in the checkpoint are often

misregulated and even minor changes have the ability to weaken the SAC sufficiently to induce tumorigenesis. The most common proteins to be misregulated appear to be Mad2 [78] and BubR1 [79] and in many cases they correlate with aneuploidy and a poor prognosis. Other proteins found to have aberrant expression levels include Bub1 [80] [81] and Mad1 [82]. It does not appear to matter whether the proteins are up- or downregulated as many have been found to have changes in both directions in different forms of cancer and even different tumors of the same type. The SAC is likely sufficiently weakened in either case and the direction is determined by the conditions in individual tumor cells.

Therapeutic Targeting of the Spindle Assembly Checkpoint

Complete loss of spindle assembly checkpoint activity is not compatible with life as it leads to a catastrophic loss of chromosomes within a small number of divisions. Loss of BubR1 or Mad2 expression, or loss of BubR1 kinase activity, leads to apoptotic cell death within six cell divisions [83]. Cancer cells need to find a balance in which they are able to produce a small rate of chromosomal instability to allow for tumor progression but without losing complete control. Therapeutic strategies that either further abrogate the SAC or restore SAC function could preferentially kill cancer cells. Further weakening would create an unmaintainable level of chromosomal instability and restoration of SAC activity would arrest cancer cells that have underlying mechanisms causing a high rate of spindle mis-attachment.

Pharmacologic strategies

Kinases involved in the SAC present promising targets as there has been a large amount of success developing kinase inhibitors in the past. Aurora B, Mps1, Bub1, and BubR1 kinase activity are all required for a functional SAC (reviewed in [84] and [85]).

Indeed, an Aurora B inhibitor has already shown efficacy in treating cancer in mice [86]. Small molecules that block protein-protein interactions, such as the sequestration of Cdc20 by Mad2, could also eliminate SAC function.

Biological strategies

Since it is already known that knockdown of the Mad2 or BubR1 protein causes cell death in vitro, it is possible that a siRNA gene-therapy approach could be useful in treating cancer. siRNA mediated knockdown is generally more selective than pharmacological inhibitors and presents great potential. However, our knowledge of the in vivo use of these techniques has not reached the clinic and requires more work before that potential can be realized.

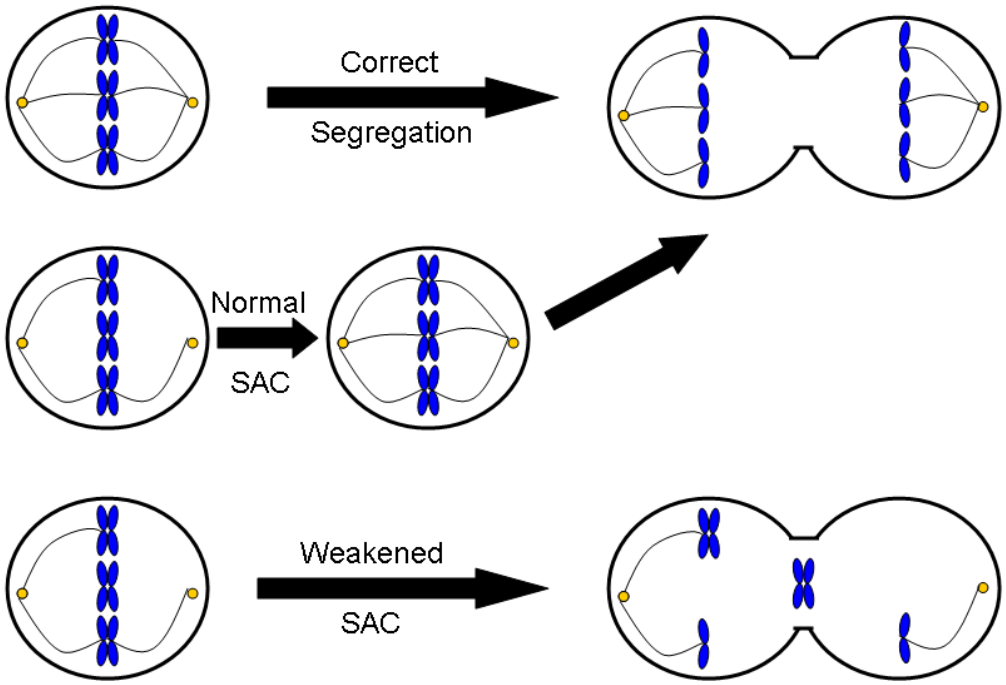

Figure 1-3. The spindle assembly checkpoint assures faithful chromosome segregation. Cells with a functional spindle assembly checkpoint arrest upon improper spindle attachment, allowing time for correct attachments to occur. Cancer cells with a weakened spindle assembly checkpoint proceed to cell division prior to correct spindle attachments being made, resulting in improper DNA segregation.

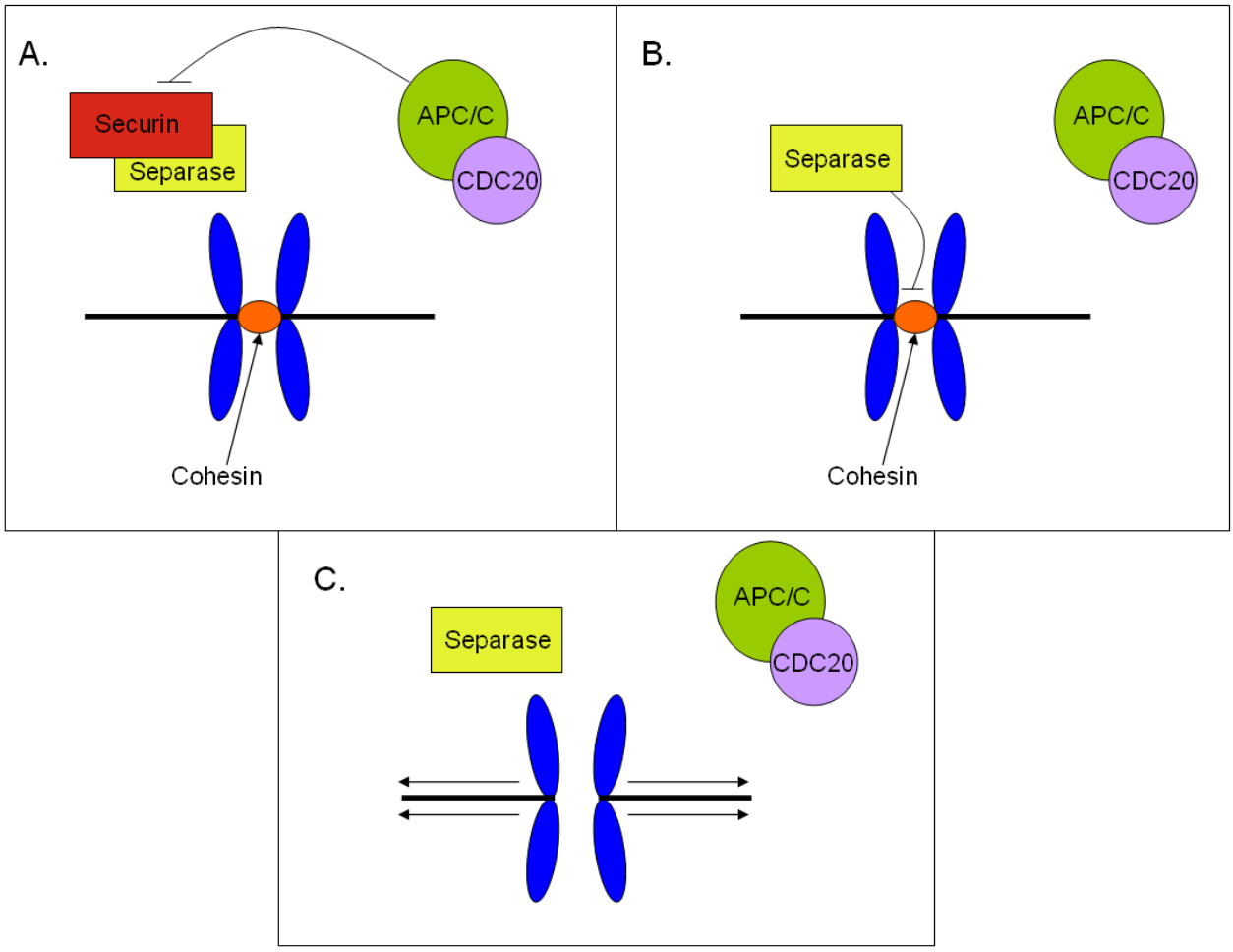

Figure 1-4. The spindle assembly checkpoint controls the separation of sister chromatids. A) APC/C in complex with CDC20 leads to degradation of Securin. B) Separase, no longer inhibited by Securin, causes the degradation of Cohesin. C) In the absence of Cohesin, tension on the spindle poles pull the sister chromatids apart.

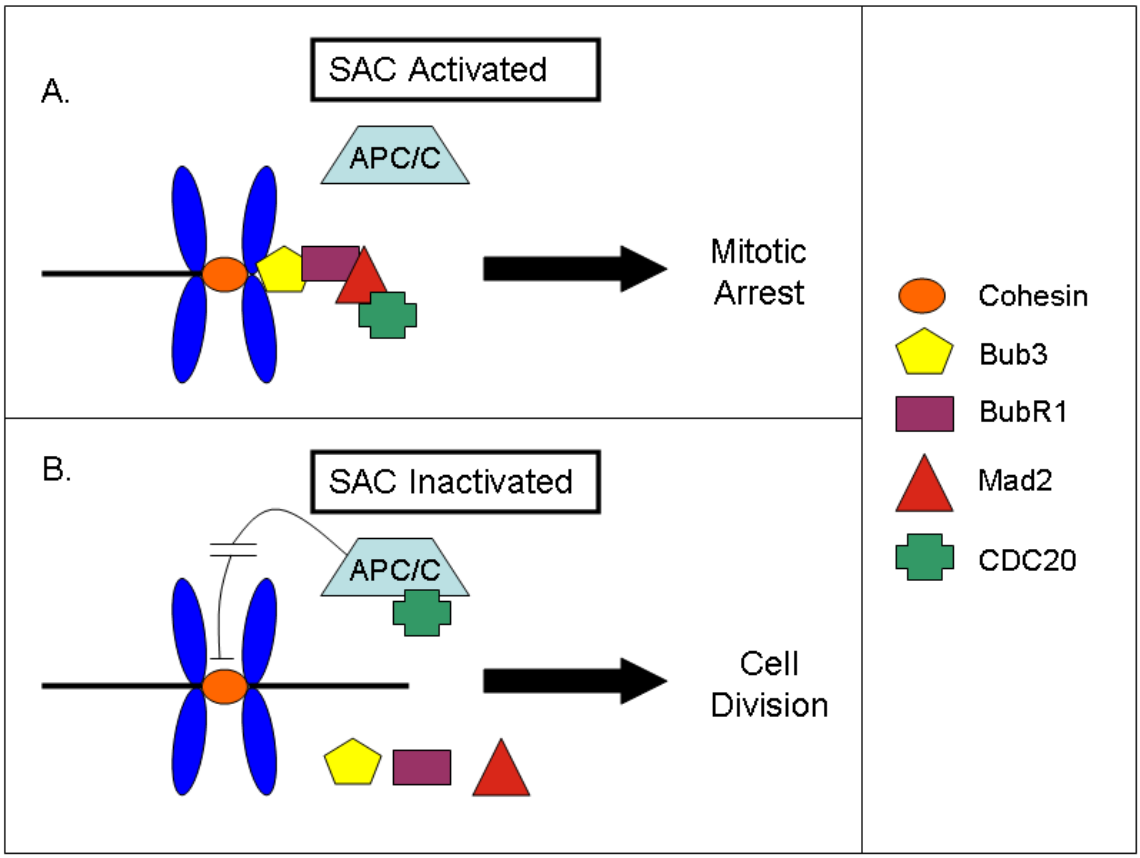

Figure 1-5. Microtubule attachment inactivates the spindle assembly checkpoint. A) In the absence of proper microtubule attachment, the mitotic checkpoint complex binds unattached kinetochores, sequestering CDC20 and preveting mitotic progression. B) Upon spindle attachment, the mitotic checkpoint complex disassembles along CDC20 to activate APC/C, leading to Cohesin degradation and cell division.

The Tetraploidy Checkpoint

Compared to the spindle assembly checkpoint, much less is known about the tetraploidy checkpoint. There has even been debate over its existence in the near-past [87]. Where the spindle assembly checkpoint is a fail-safe mechanism that is activated every time a cell enters mitosis and is not shut off until the spindles are properly assembled, the tetraploidy checkpoint is only activated in response to detection of an error. Presence of a 4N DNA content, i.e. four copies of each chromosome compared to the normal two, in the G1 phase of the cell cycle has been shown to cause a p53 mediated arrest via increased p21 levels and subsequent blockage of Rb phosphorylation [88], as illustrated in Figure 1-5. This leads to a G1 arrest that, if not quickly reversed, leads to senescence [89] or apoptosis [90] (Figure 1-6).

Tetraploidy can occur through multiple mechanisms including endoreduplication (the re-replication of DNA without entering mitosis), failed cytokinesis, mitotic failure, and cell fusion. The original discovery of the tetraploidy checkpoint was through the generation of tetraploid cells using pharmacological methods such as spindle poisons and cytokinesis inhibitors [88]. It was later published that the observed arrest was due to DNA damage caused by the drugs used and not the tetraploidy they induced [91]. In that study, it was found that high doses of many drugs caused large amounts of DNA damage, but that lower doses were able to induce tetraploidy without detectable levels of DNA damage. These cells proceeded through the cell cycle without arrest and it was concluded that nontransformed cells do not contain a tetraploidy checkpoint. It was not until later that it was discovered that, while the cells continued through the cell cycle, they arrested and died after subsequent division [92]. The observation is therefore likely a cell line-dependent phenomenon and the hTERT-RPE1 cells used simply

contain a weakened checkpoint. Additionally, while the mechanism of p53 activation is currently unknown, activation involves phosphorylation of p53 on Ser33 rather than Ser15, which is associated with DNA damage [93].

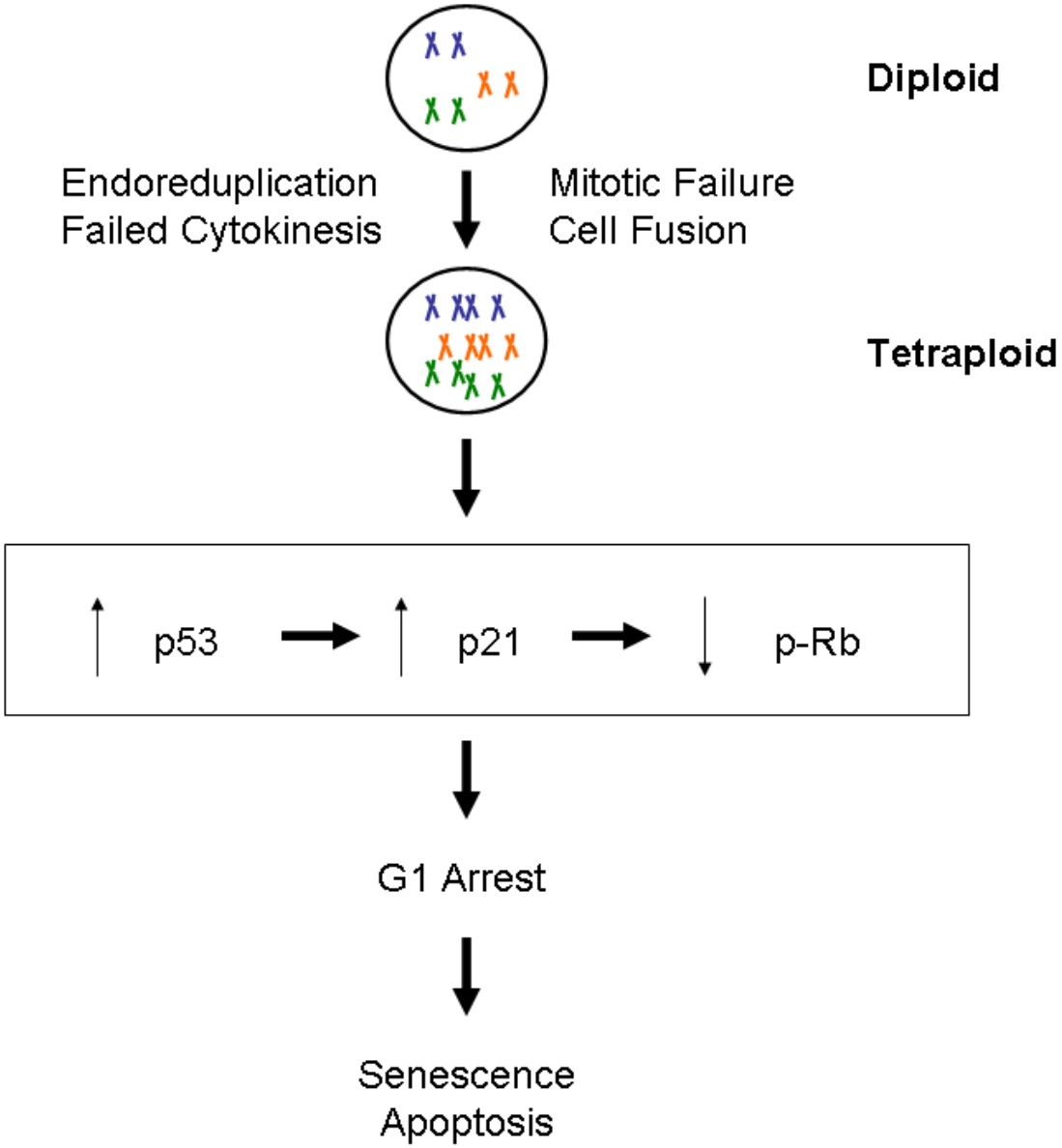

Figure 1-6. The tetraploidy checkpoint prevents the proliferation of tetraploid cells. Cells may become tetraploid through multiple mechanisms. When tetraploidy is sensed, p53 is activated, leading to increased levels of p21. Through its Cdk inhibitory actions, p21 results in a blockage of Rb phosphorylation, causing G1 arrest and subsequent senescence or apoptosis.

Chromosomal Instability in Cancer

Cancer, being the result of abnormal gene expression, suffers from major changes in cellular DNA. These changes are not one-time events, and continued instability of DNA has been classified as one of the hallmarks of cancer [94]. This instability manifests itself in two major forms: genetic instability and chromosomal instability (CIN). Genetic instability is classified as changes in the DNA sequence within chromosomes. These gene deletions, amplifications, and mutations are primarily due to defects in the DNA repair machinery (reviewed in [95]), such as BRCA1 and BRCA2, which are frequently mutated in hereditary breast cancers [96].

CIN on the other hand is the gain or loss of whole numbers of chromosomes and can also include chromosomal translocations. While the end results are similar, potential gain and loss of oncogenes and tumor supressors, the process involves the chromosomal structure in its entirety rather than the nucleotide sequence within it. These changes in DNA content can occur through many mechanisms. These include those that result in a doubling of the cellular genome, such as failed cytokinesis, monopolar mitosis, or endoreduplication, which consists of re-duplication of the genome without attempting mitosis, or those that cause small stochastic changes, including multipolar mitosis and lagging chromosomes (illustrated in Figure 1-7).

The most visible form, and one that was first proposed to be the cause of CIN in cancer by Theodore Boveri in 1902 [68], is multipolar mitosis. These events clearly cause a change in DNA content of the daughter cells and they were long assumed to be the driver of CIN. However, it was recently shown that the majority of these daughter cells are unviable in the long-term, not surviving past two or three future divisions [97]. It appears that these large-scale changes result in massive imbalances in gene

expression, resulting in cell death. Alternatively, it was found that lagging chromosomes resulted in small changes, usually one or two chromosomes at a time, and resulted in viable, aneuploid daughter cells [97].

Both multipolar mitoses and lagging chromosomes require supernumerary centrosomes. The centrosome, considered a cellular organelle, is the primary microtubule organizing center in the cell. Centrosomes consist of two smaller bodies, called centrioles, surrounded by a cloud of proteins known as the pericentriolar matrix, or PCM [98]. Exiting mitosis, each daughter cell contains one centrosome. In order to nucleate two spindle poles in the subsequent round of division, cells must duplicate the centrosome. The duplication process itself occurs through a complex, poorly understood mechanism beginning in S-phase (reviewed in [99]), however the initiation of duplication has been well studied. The start of centriole replication is controlled primarily by two kinases: Polo-like kinase 4 (Plk4) [100,101] and Cyclin Dependent Kinase 2 (Cdk2) [102,103].

Centrosome amplification is seen in the majority of cancers [104] and can arise through several different mechanisms. Overduplication can be caused by hyperactivity of the kinases controlling replication initiation, including Plk4 [100] and Cdk2 [105], or the overexpression of centrosomal components such as STIL [106] or HSAS-6 [107]. Interestingly, Plk4 [108], Cdk2 [42], and STIL [109] have already been found to be overactive or overexpressed in human cancers. While centrosome duplication is generally thought to be a templated process, de novo centrosome assembly can also occur both in transformed [110] and nontransformed [111] cells. Simple overexpression

of pericentrin, a major component of the PCM, is sufficient to induce de novo assembly and pericentrin is expressed at high levels in multiple forms of cancer [112,113].

Cells may also obtain extra centrosomes through mechanisms independent of the replication/assembly machinery. As cells normally enter mitosis with two centrosomes, anything that prevents those centrosomes from being segregated into two daughter cells will yield a G1 phase cell with an abnormal centrosome number of two. Subsequent replication results in four centrosomes and, potentially, four spindle poles. This may occur through a monopolar spindle due to improper centriole separation, cell fusion, or cytokinesis failure. Simple in its premise, yet remarkably complex in practice, cytokinesis can fail for any number of reasons.

Adenomatus Polyposis Coli (APC), often mutated in colon cancers [114], plays a role in anchoring the spindle poles. Mutations in this protein prevent formation of a cleavage plane, resulting in the failure of cytokinesis initiation [115]. Not to be confused with the protein APC, the Anaphase Promoting Complex/Cyclosome (APC/C) is an E3 ubiquitin ligase that is important in cytokinesis due to its degradation of several crucial proteins including Anillin [116], Cyclin B [20], Polo-like kinase 1 (Plk1) [117], and Aurora B [118]. Anillin acts as a linker between myosin, the motor that drives contraction, and the actin cytoskeleton [119] whereas Plk1 and Aurora B play roles throughout cytokinesis (reviewed in [120] and [121]). As outlined earlier in this chapter, Cyclin B degradation is the lead controller in mitotic progression. Incomplete Cyclin B degradation by the APC/C can lead to cytokinesis failure through multiple mechanisms including lagging chromosomes, due to a lack of Cohesin cleavage, which can physically block cytokinesis and cause furrow regression [122] and continued

phosphorylation of Myosin light-chain. Cdk1 is responsible for the inhibitory phosphorylation of Myosin and improper Cyclin B degradation prevents de-phosphorylation, Myosin activation, and subsequent cleavage furrow ingression [123].

Centrosome amplification by itself is not sufficient to induce multipolar mitosis as cells contain a mechanism for bundling extra centrosomes into two spindle poles. Centrosome clustering was first observed in the early 1980s [124] but was not well characterized until more recently. A genome-wide RNAi study identified 133 genes required for bundling of centrosomes [125]. Genes coding for proteins involved in regulation of the cytoskeleton and adhesion, signal transduction, and mitosis, including the spindle assembly checkpoint, were heavily represented.

A study in the same lab later characterized this bundling in cancer cell lines [97]. It was found that cancer cells are efficient at bundling even large numbers of centrosomes. This resulted in a relatively low rate of multipolar mitosis that could not account for the observed rates of CIN. Additionally, time-lapse microscopy showed that the progeny of these multipolar divisions rarely survived past the next round of mitosis and only a small percent were viable indefinitely. Alternatively, rates of lagging chromosomes increased along with centrosome number. While the cells were able to bundle the centrosomes into two spindle poles before cytokinesis, it did not occur until after spindle pole formation. Therefore, there was a high rate of merotely, the connection of one kinetochore to both spindle poles, which results in a failure to properly segregate the chromatid. Upon completion of cytokinesis, this chromatid is either forced into one daughter cell, with a 50/50 chance of it being the correct one, or is crushed and destroyed during abscission.

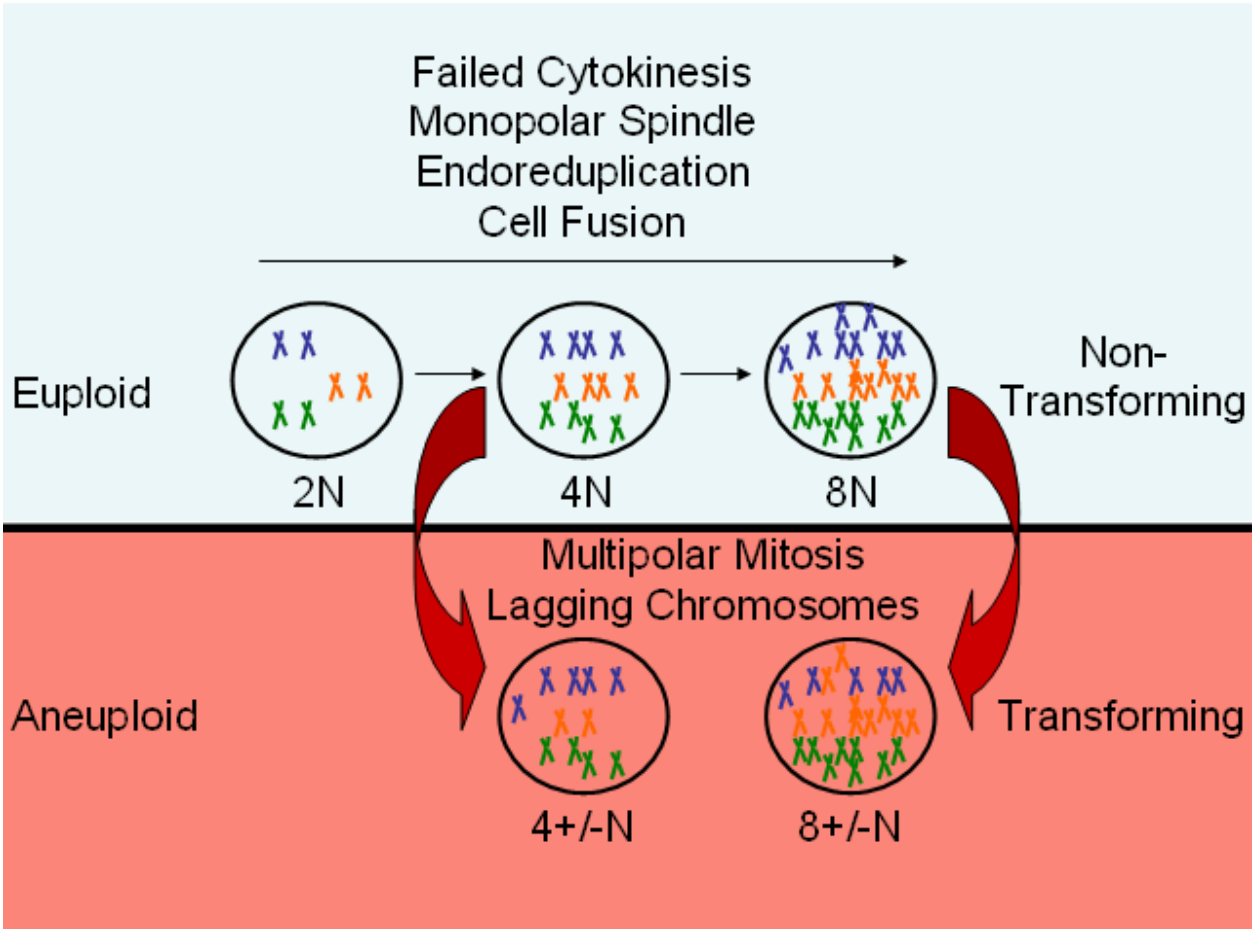

Figure 1-7. Diagram showing the basic process of chromosomal instability. Phenomena including failed cytokinesis, monopolar spindles, endoreduplication, and cell fusion cause genome doubling, which is not sufficient to cause cellular transformation. However, these process can lead to multipolar mitoses and lagging chromosomes, resulting in aneuploidy, which is capable of causing cellular transformation.

Consequences of CIN

Chromosomal instability in cancer is a sort of “chicken or the egg” paradox. Approximately 70% of all solid tumors present with CIN [126], but it is not currently clear whether CIN is predominantly the underlying cause of the cancer, or simply an effect of another root cause. As has been mentioned earlier, many proteins that are oftentimes mutated in cancers have a role in maintaining genome stability. Should a mutation in one of these genes initiate CIN, this could in turn cause many changes throughout the genome that ultimately result in transformation. Indeed, aneuploidy caused by CIN is capable of initiating tumorigenesis [127] and under- or overexpression of proteins involved in the spindle assembly checkpoint are capable of producing tumors [128,129].

On the other hand, many of the same mutations that are thought to be drivers of transformation through cell-cycle deregulation, such as Rb, also result in CIN [130,131]. The addition of CIN in a tumor introduces a process very similar to evolution. With an ever-changing genome, cells within the tumor have the ability to find the chromosome content best suited for proliferation. It is also a built in mechanism for generating drug resistance. Clinically, CIN correlates with poor prognosis [132], and multidrug resistance is seen in cell lines and tumors with CIN both in vitro and in vivo [133].

Targeting CIN

While CIN may make cancers more resistant to certain cytotoxic treatments, it also opens the door for more specific anti-cancer treatments. Being a hallmark of cancer [94], it is a fundamental difference between cancer cells and normal cells, leading to the possibility of it being exploited for treatment. Inhibition of Aurora B weakens the SAC and, in turn, strengthens the connections between microtubules and kinetichores. This results in improper spindle attachments and increases the rate of

CIN [134]. In cancer cells that already are chromosomally unstable, this increase may lead to unsustainable rates of CIN, and the increased rate may be multiplied due to the fact that these cells likely have centrosome amplification and will have a higher rate of spindle misattachment. Aurora B inhibitors have shown anti-tumor activity in the clinic, including tumors refractory to other treatments (reviewed in [135]).

Centrosome bundling presents an intriguing possibility for targeting cancer cells as well. Considering that normal cells contain only two centrosomes, blocking the process of clustering extra centrosomes should be inconsequential to their proliferation and viability. On the other hand, as mentioned, multipolar mitosis leads to a very high rate of cell death [97]. Therefore, blocking centrosome bundling would likely lead to cancer cell death while not harming the normal tissue. The majority of proteins involved in clustering serve other roles in the cell, creating the potential for unintended effects of their inhibition [125]. However, the protein HSET, a kinesin [136], is not required for normal cell division [137], but is required for centrosome bundling [125]. Knockdown of HSET causes apoptosis in cell lines at approximately the rate of centrosome amplification [125]. There is currently not a small molecule inhibitor of HSET available, but the development of one could hold great promise for the treatment of cancer.

Purpose of the Current Study

This study examines the cellular effects of overactive Cdk2, particularly through Cyclin D1/Cdk2 complexes. The various chapters investigate different consequences of constitutive Cdk2 activity. Through Rb phosphorylation, Cyclin D1/Cdk2 strengthens the SAC while weakening the tetraploidy checkpoint. The end result is a condition permissive to polyploidy and aneuploidy.

As already mentioned, Cdk2 and other Cdks have many more roles in the cell than simply phosphorylating Rb. It is shown that Cyclin D1/Cdk2 phosphorylates two of the proteins already discussed, NPM and Cdh1, as well as a novel Cdk2 target, polypyrimidine tract binding protein-associated splicing factor (PSF). While the functional consequence of this phosphorylation is currently unknown, several possibilities are discussed.

These phosphorylation events not only lead to chromosomal instability, but also to a change in cellular phenotype. Tumors initiated by Cyclin D1/Cdk2 complexes show invasive and morphological characteristics of the epithelial to mesenchymal transition and this transition is accompanied by a striking shift in mitogenic signaling. Together, these data exemplify the complexity of cancer. Cyclin D1/Cdk2 complexes, very common yet often overlooked, can have dramatic effects on tumor development. These experiments seek to shine light on these effects, increasing the scientific understanding of their role in tumorigenesis, hopefully leading to new and better treatments.

CHAPTER 2
CONSTITUTIVE CDK2 ACTIVITY PROMOTES ANEUPLOIDY WHILE ALTERING THE SPINDLE ASSEMBLY AND TETRAPLOIDY CHECKPOINTS

Introduction

Included in the updated Hallmarks of Cancer [94], unstable DNA is a common characteristic of many solid cancers. This instability can take the form of genetic instability, changes in the DNA nucleotide sequence, or chromosomal instability (CIN), changes in the number of whole chromosomes, and this instability is both a tumor initiator [127] and a driver of tumor evolution [138]. The DNA content of cells can change through multiple mechanisms, either causing stochastic changes up or down or simple genome doubling. Phenomena including endoreduplication and failed cytokinesis induce an abnormal tetraploid, 4N, DNA content. Centrosome duplication can also occur concomitantly, and while a stable, true tetraploid DNA content is not sufficient to cause transformation [139], centrosome amplification can lead to multipolar mitoses, lagging chromosomes, and subsequent aneuploidy [97,140].

Many of the cellular mechanisms to protect the cellular genome are integrally linked to the cell cycle, and cancers with cell cycle mutations oftentimes have a high rate of chromosomal instability [128,141,142]. Cyclin D has been found to be overexpressed in approximately 50% of all breast cancers [48] and Nelsen et al. have shown that short term overexpression of Cyclin D1 is capable of initiating CIN, and that the process of chromosomal changes persists even after the exogenous Cyclin D1 is no longer being produced [143]. The molecular mechanism by which this occurs is unknown. Cyclin D1 is most commonly thought to be an activating partner of the Cyclin dependent kinases Cdk4 and Cdk6 and Cyclin D1/Cdk4 complexes have been shown to induce centrosome amplification in the presence of Ras mutations [144] and MEK2

deficiency [145]. Additionally, both Cdk4 and Cdk2 are required for the Nucleophosmin hyperphosporylation and subsequent centrosome amplification observed in p53 null cells [146].

While it may not generally be considered a canonical partner, Cyclin D1 has also been shown to form active complexes with Cdk2 [34,53]. Cdk2, which is normally active and bound to Cyclin E in late G1 through S phase and then with Cyclin A into late G2, is thought to play a critical role in the centrosome duplication cycle [102,103]. Therefore, it was unclear whether the results seen by Nelsen et al. were due to Cyclin D1 complexes with Cdk2, Cdk4, Cdk6, or any of the other Cyclin Dependent Kinases. Further studies showed that expression of Cdk2 is required for Cyclin D1-induced CIN, hinting to the importance of Cyclin D1/Cdk2 complexes, but not eliminating the possibility that Cyclin D1 is binding to another Cdk and causing CIN in a Cdk2-dependent mechanism [147].

We have previously published studies utilizing a Cyclin D1-Cdk2 fusion protein (D1K2), and transgenic mice expressing this protein under the control of the mammary-specific Mouse Mammary Tumor Virus (MMTV) promoter/enhancer develop spontaneous mammary tumors which are invasive, heterogeneous, and express markers associated with the basal-like subtype of breast cancer [53,54,148]. Here, we present analysis of the effect of D1K2 expression on the mitotic and tetraploidy checkpoints using tumor-derived cell lines and the nontransformed human mammary epithelial cell line, MCF10A, stably expressing D1K2. Our results show that D1K2 strengthens the mitotic checkpoint through upregulation of Mad2, increasing the anti-proliferative effects of paclitaxel. D1K2 expression also weakens the tetraploidy checkpoint, allowing polyploidization of cells that enter G1 as tetraploid through mitotic

slippage or failed cytokinesis. Long-term survival data of these cells raise intriguing questions regarding the treatment of cancers with overactive Cdk2.

Results

MMTV-D1K2 Mice Develop Aneuploid Mammary Tumors with a Compromised Tetraploidy Checkpoint

Cdk2 activation has previously been implicated in the induction of aneuploidy and genomic instability through the processes of centrosome overduplication and endoreduplication [146,149-153]. We previously observed aneuploidy in MMTV-D1K2 transgenic mice, suggesting that induction of tumorigenesis by Cyclin D1/Cdk2 complexes may involve these processes [54]. We examined hematoxylin and eosin (H&E) stained sections of MMTV-D1K2 tumors for evidence of aberrant mitosis. As indicated in Figure 2-1A, all primary MMTV-D1K2 tumors isolated exhibited mitoses that appeared abnormal. Metaphase spreads of cell lines derived from these tumors (Figure 2-1B) showed a high variance in DNA content. The presence of cells with a greater than 4N DNA content indicates a weakened tetraploidy checkpoint in these tumors.

Further, karyotype analysis of the tumor-derived cell lines showed high rates of trisomy and a bi-modal population with cells concentrating around diploid or tetraploid status (Figure 2-1C and data not shown). These results indicate a mechanism for genome doubling and the ability to bypass the p53-dependent tetraploidy checkpoint [88] in order to continue growth. This abnormal doubling would be expected to be paired with centrosome amplification, and the tumor cell lines do show high levels of centrosome amplification, ranging from 13.5 to 22.5% of individual cells showing supernumerary centrosomes marked by γ-tubulin staining (Figure 2-1D). These cells also exhibit multipolar mitoses, and a hydroxyurea-based centriole reduplication assay

[154] showed a small, not statistically significant, increase in the rate of centrosome amplification in the D1K2-T1 cell line from 19.5% to 22% (data not shown). This indicates that while D1K2 tumor cell lines possibly possess a mechanism to induce minor overduplication of centrioles, which is unsurprising due to the Nucleophosmin hyperphosphorylation seen in Figure 2-2A, it is likely not sufficient to account for the high rate of centrosome amplification observed. These cell lines also generate populations with 8N and 16N DNA content, as measured by flow cytometry, when grown in the presence of the spindle poisons nocodazole or paclitaxel, providing further evidence for the lack of a functional tetraploidy checkpoint.

MCF10A Cells Expressing D1K2 Have a Deregulated Cell Cycle and Increased Paclitaxel Sensitivity

Since tumors derived from the mouse model presumably have undergone further mutations during tumor development, we sought to create a model in which the direct effects of D1K2 activity could be studied. We stably transduced MCF10A cells with vectors encoding a Hygromycin control vector (Hygro), D1K2, or a kinase dead version of D1K2 (D1K2(KD)). A clonal cell line, D1K2 CL1, was derived from the polyclonal D1K2 expressing cell line in order to obtain cells expressing a homogenous amount of the transgene. Immunoblot of these cell lines (Figure 2-2A) shows intracellular D1K2 activity illustrated by hyperphosphorylation of Cdk substrates, including Rb and Nucleophosmin (NPM) in only those cell lines containing kinase active D1K2. Rb shows phosphorylation on sites preferred by Cdk4 (Ser249/Thr252, Ser780, and Ser795) as well as Cdk2 (Ser807/811), consistent with our previous findings [53]. Nucleophosmin is a substrate of the Cyclin E/Cdk2 complex and helps maintain control of centriole duplication [155]. It is unclear as to whether D1K2 phosphorylation of NPM leads to

centrosome amplification in vivo. In the in vitro model discussed below, NPM hyperphosphorylation does not lead to abnormal centrosome numbers, however these cells likely have redundant mechanisms to block overduplication [92,97] that may be compromised during tumor development.

Rb hyperphosphorylation, particularly of the Cdk4 phosphorylation sites mentioned above, causes cell-cycle deregulation [130] and analysis of growth rates showed a dramatic increase in proliferation of the D1K2 CL1 cell line compared to the Hygro control (Figure 2-2B, top panel). In addition, D1K2 expression increased the maximum confluent density of the cells, indicated by the approximately 4x higher maximum cell number reached by the D1K2 CL1 cell line. Treatment of these cell lines with paclitaxel yielded interesting results. D1K2 expressing cells replated after paclitaxel washout showed growth rates equal to or less than that of the comparably treated control over the first four days (Figure 2-2B, bottom panel). The untreated D1K2 CL1 cell line had a statistically significant increase in cell number compared to the Hygro cell line after 3 and 4 days. However, the difference in cell number of each cell line was not statistically different on days 3 and 4 after paclitaxel treatment, indicating a greater sensitivity to the growth inhibitory effects of the spindle poison. Subsequent growth, presumably after the effects of treatment had dissipated, recapitulated that seen in the untreated cells.

[^{3}H]Thymidine incorporation in the Hygro and D1K2 CL1 cell lines after treatment with increasing concentrations of paclitaxel for 72 hours also showed a differential response between the cell lines (Figure 2-2C). There was a statistically significant difference in proliferation in these cell lines, normalized to untreated controls, when

grown in the presence of 1.875 or 3.75 nM paclitaxel. Interestingly, the data in Figure 2B and 2C show that the difference in sensitivity to paclitaxel in the control and D1K2 expressing cells increases with time after exposure. Whereas nearly a 2 nM concentration was required to see a statistically significant difference after 72 hours of exposure in Figure 2-2C, the effects of paclitaxel were seen after 72 hours of treatment and a subsequent 72 hour washout period with only 1 nM paclitaxel in Figure 2B. Treatment with 1 μM paclitaxel for 72 hours, as required to generate tetraploid populations below, blocked nearly all proliferation (Figure 2-8).

D1K2 Kinase Activity Strengthens the Spindle Assembly Checkpoint

Flow cytometric analysis of the DNA content of Hygro and D1K2 CL1 cells treated with paclitaxel for 72 hours shows the appearance of a tetraploid, 8N, population in the cells expressing D1K2 but not in the control cells (Figure 2-3A, left and center panels). Cells expressing the kinase dead D1K2 fail to produce this 8N population (Figure 2-3A, right panel), indicating that the D1K2 kinase activity is required for the phenomenon rather than the fusion protein exerting its effects through protein/protein interactions, as has been discussed previously [53]. Similarly, co-treatment of the D1K2 CL1 cell line with the Cdk2 inhibitor CVT313 along with paclitaxel inhibited the development of this 8N population in a dose-dependent manner (Figure 2-3B). Thymidine incorporation experiments treating these cell lines with paclitaxel, CVT313, or a combination blocks proliferation. At the paclitaxel concentration used, a small amount of DNA synthesis remains and addition of CVT313 further decreases it, supporting the flow cytometry data (Figure 2-9).

As expression of the spindle assembly checkpoint (SAC) protein Mad2 has been shown to be E2F dependent [131] and its overexpression is capable of initiating

tumorigenesis and chromosomal instability [128], we examined Mad2 protein levels in our cell lines. Mad2 expression was found to be increased in the D1K2 CL1 cell line compared to the Hygro and D1K2(KD) cell lines (Figure 2-3C, left panel). This increased expression was confirmed to be due to D1K2 activity as partial Cdk2/D1K2 knockdown reduced Mad2 protein levels (Figure 2-3C, right panel). We also observed decreased Mad2 expression in the presence of CVT313 (Figure 2-9).

If high levels of Mad2 are responsible for a weakened SAC, leading to tetraploidy, restoration of Mad2 levels through a partial knockdown should block formation of an 8N population in the D1K2 CL1 cell line. However, we observed that Mad2 knockdown (analyzed in Figure 2-10) cooperated with D1K2 activity to increase the formation of this population (Figure 2-3D). Immunoblot analysis of cell lines treated with paclitaxel showed that, in all cases, Mad2 levels initially increased upon treatment but decreased nearly to zero upon long-term treatment (Figure 2-3E). Presumably, all of the utilized cell lines treated with paclitaxel eventually suffer a failure of the SAC and undergo mitotic slippage, reentering the G1 phase of the cell cycle as 4N. Increased Mad2 expression due to D1K2 activity appears to strengthen the SAC, delaying mitotic slippage, protecting against tetraploidy, and providing a potential mechanism for the increased sensitivity to paclitaxel seen in Figure 2. As further evidence of a strengthened SAC, the D1K2 CL1 cell line shows much greater MPM2 staining, a mitotic marker, than does the Hygro cell line after treatment with paclitaxel (Figure 2-10).

Quantification of centrosome numbers showed amplification due to paclitaxel treatment. Whereas the untreated D1K2 CL1 cell line showed an approximately 5%

rate of centrosome amplification (>2 centrosomes/cell), that rate increased to 22% upon 72 hour paclitaxel treatment. Surprisingly, co-treatment with CVT313 failed to block this amplification and instead resulted in a further increase to 45% (Figure 2-11). This is presumably due to the observed decrease in Mad2 levels upon CVT313 treatment (Figure 2-9), weakening the spindle assembly checkpoint, allowing a greater number of cells to enter G1 with two unduplicated centrosomes, which will then become four. While Cdk2 inhibition via CVT313 is sufficient to block subsequent DNA replication (Figure 2-3B), it does not appear to be sufficient to block centrosome duplication. It is possible that a lower kinase activity level is required to initiate centrosome duplication compared to DNA replication. Another explanation for the results could be that Cdk4 is substituting for the inhibited Cdk2 in the centrosome duplication machinery, as has been previously seen [146], but is unable to do so in the DNA replication process.

D1K2 Activity Weakens the Tetraploidy Checkpoint

A p53 dependent tetraploidy checkpoint has been shown to arrest cells that contain a 4N DNA content in G1 phase through increased production of p21 and the subsequent blockage of Rb phosphorylation [88]. If all of the MCF10A cell lines undergo mitotic slippage as our data suggest, the mechanism that prevents the control cells from becoming 8N must act in G1 or at the G1/S transition. Stable knockdown of p53 (analyzed in Figure 2-12) cooperated with D1K2 to increase the 8N population (Figure 2-4A), providing further evidence that cells are reentering G1 and DNA replication is being inhibited by a p53 dependent checkpoint.

To generate large populations of tetraploid cells and to examine the fidelity of the tetraploidy checkpoint in the absence of a SAC response, we utilized the cytokinesis inhibitor cytochalasin-B. Even more strikingly than is seen with paclitaxel treatment,

long-term treatment with cytochalasin-B induced a large 8N population in the D1K2 CL1 cell line that was much larger than that seen in the Hygro cell line (Figure 2-4B, left and center panels). Additionally, the 8N population persisted to 72 hours, whereas the small 8N population produced in the Hygro cell line after 24 and 48 hours appears to have reverted to 2N/4N or died after 72 hours. Elimination of the tetraploidy checkpoint through p53 knockdown produced results similar to that seen with D1K2 expression (Figure 2-4B, right panels). Photographs of treated cell lines show that untreated cell lines are mononucleate. Upon cytokinesis failure due to cytochalasin-B treatment, the Hygro cell line remains binucleate, whereas D1K2 expressing or shp53 cell lines progress to become multinucleate (Figure 2-4C). Interestingly, in the D1K2 CL1 cell line in which p53 is also knocked down, cytochalasin-B treatment not only produced a large 8N population, but also a substantial 16N population (Figure 2-4D) that was not seen in any of the other cell lines. It appears that constitutive Cdk2 activation or ablation of the tetraploidy checkpoint are sufficient to allow one extra round of DNA replication, but that both conditions must be met in order to permit a subsequent duplication.

D1K2 Expression Prolongs Rb Phosphorylation upon Tetraploidy Checkpoint Activation

Immunoblot analysis of MCF10A cell lines treated with cytochalasin-B for 24, 48, or 72 hours shows that both Hygro and D1K2 CL1 cell lines activate the tetraploidy checkpoint upon cytokinesis failure, illustrated by an increase in p53 expression (Figure 2-5A). At 24 hours, little decrease in Rb phosphorylation is shown in either cell line. After 48 hours of treatment, D1K2 CL1 exhibits higher levels of phosphorylated Rb compared to the Hygro cell line despite the D1K2 CL1 cell line having progressed further in the cell cycle and started to develop an 8N population due to its faster growth

rate. At 72 hours of treatment, Rb phosphorylation has been abolished in both cell lines, presumably arresting both. It is interesting to note that the D1K2 CL1 cell line shows higher levels of p53 after checkpoint activation than does the Hygro cell line, and it appears to increase further between 48 and 72 hours. The MCF10A shp53 cell line shows no induction of p53 and maintains Rb phosphorylation through 72 hours. These results are consistent with a model in which the tetraploidy checkpoint is activated in both Hygro and D1K2 CL1 cell lines. The initial activation is adequate to arrest the Hygro cell line at 4N, whereas D1K2 expression maintains Rb phosphorylation at levels sufficient for DNA replication. This further increase in DNA content intensifies the tetraploidy checkpoint, arresting these cells at 8N after the subsequent round of failed cytokinesis.

Long-term Outcome of Tetraploid Populations

In order to evaluate the long-term effects of tetraploidy, we sorted cells treated with cytochalasin-B for 72 hours using flow cytometry. 2N and 4N populations were isolated from MCF10A Hygro, D1K2 CL1, and shp53 cell lines as well as 8N populations from D1K2 CL1 and shp53. Cell viability and growth rates were observed the week following sorting by measuring Crystal Violet staining (Figure 2-6A). 4N and 8N populations showed a decreased rate of proliferation compared to the 2N population. The DNA profiles of these populations were examined one week after sorting and showed a near normal 2N/4N population, with the previous polyploid population markedly absent (Figure 2-6B). Additionally, D1K2 CL1 cells plated at single cell density prior to being treated with cytochalasin-B were monitored for survival (Figure 2-6C). The majority of cells visually confirmed to be multinucleate after cytochalasin-B treatment died (77%) or failed to divide (19%) in the 7 days following

washout. A small number of cells successfully divided once (4%) but their progeny failed to undergo subsequent divisions.

These data are consistent with cells that are able to briefly continue to proliferate with a polyploid DNA content due to the presence of D1K2 or absence of p53 but are not viable in the long-term. The post-sorting flow cytometry showing a normal population likely reflects a 2N population initially present in the 4N and 8N populations, due to imperfect sorting, that overtakes the polyploid populations over time. This also explains the growth curve data. Indeed, further flow cytometry analysis of sorted populations detects the presence of 2N cells in the 4N and 8N populations (data not shown).

Discussion

The generation of polyploid cells, followed by subsequent multipolar mitosis and lagging chromosomes, has been suggested as a potential mechanism of aneuploidy generation in tumors, a near universal commonality in cancers. The existence of a checkpoint that is able to detect the presence of a 4N DNA content in G1 phase cells has been known for some time. A number of studies have clearly shown the ability of tetraploidy to arrest the cell cycle [88,92,156,157], but the mechanism by which it senses tetraploidy is poorly understood. The effects of this checkpoint on the long-term viability of cells appear to be cell line specific. In a comprehensive study, it was found that multiple non-transformed cell lines that were treated with cytochalasin-B to induce tetraploidy were able to undergo several rounds of mitosis upon washout, but eventually exited the cell cycle or died. It was found that the response of transformed cells containing p53 mutations to tetraploidy also varied, ranging from death, to repeated cytokinesis failure, to indefinitely viable tetraploid cells [92].

Using in vivo and in vitro models, we have studied the role of constitutive Cdk2 activity, due to Cyclin D1/Cdk2 complexes, in polyploidization. Mice with mammary-specific expression of a D1K2 fusion protein generate spontaneous mammary tumors. These tumors are aneuploid, exhibit centrosome amplification, abberant mitosis, and have a sub-population of near tetraploid cells. This indicates that these cells harbor a mechanism for becoming tetraploid as well as a lack of a functional tetraploidy checkpoint. Indeed, treatment of cell lines derived from these tumors with the spindle poisons paclitaxel or nocodazole results in further genome amplification.

MCF10A, nontransformed human mammary epithelial cells, stably expressing the D1K2 fusion protein exhibit cell cycle deregulation caused by Rb hyperphosphorylation that results in an increase in population growth rates. Proliferation of this cell line in the presence of paclitaxel for 72 hours results in the formation of an 8N population that is not seen in similarly treated control cells. These results indicate that D1K2 is able to bypass a checkpoint that is present in MCF10A cells that serves to block paclitaxel induced polyploidization. We have previously shown that the D1K2 protein is capable of exerting effects through protein/protein interactions in addition to through its kinase activity, so we generated a cell line expressing a kinase-dead variant of D1K2. This cell line mirrors the control cell line when treated with paclitaxel, failing to generate an 8N population. Further, treatment of D1K2 expressing cells with the Cdk2 inhibitor CVT313 blocks tetraploidization, precluding the possibility that D1K2 weakens the SAC through activation of Cdk1 via sequestration of Cdk inhibitory proteins such as p21, and indicates that the effects of D1K2 are due to its kinase activity. However, since flow cytometry cannot discriminate between diploid 4N

cells arrested in G2/M and 4N cells that have entered G1, these data cannot distinguish between effects on the SAC or the tetraploidy checkpoint.

Transcription of the SAC effector protein Mad2 is E2F dependent and overexpression of Mad2 is capable of initiating tumorigenesis and chromosomal instabilility [128,131]. Inactivation of Rb leads to Mad2 upregulation [131], therefore similar results would be expected through D1K2 induced Rb hyperphosphorylation, which would effectively ablate cells of functional Rb. We showed that D1K2 expression and kinase activity lead to a concomitant increase in Mad2 expression. While Mad2 is crucial in the functioning of the SAC, and even small decreases in its expression weaken the SAC [158], it has been reported that increased Mad2 expression can also lead to an impaired SAC [159]. The observed increase in expression is possibly the cause of the enhanced paclitaxel sensitivity in D1K2 cells as previous studies have shown that Mad2 is required for paclitaxel sensitivity [160,161]. It has previously been reported that Mad2 overexpression does not increase the sensitivity of MCF10A cells to paclitaxel, however the experiments only examined treatments up to 36 hours [160]. We did not observe a differential effect at similar time points (data not shown) and the effects of Mad2 overexpression were not seen until after 72 hours. Partial knockdown of Mad2 in the D1K2 CL1 cell line failed to decrease sensitivity (data not shown), however we have observed this cell line to be much less adherent than the parental cell lines. Multiple studies have shown that cell adherence inversely correlates with paclitaxel sensitivity [162,163], so it is possible this effect masks that of decreasing Mad2 levels.

If D1K2 expression leads to paclitaxel induced polyploidization by weakening the SAC through Mad2 upregulation, restoration of Mad2 levels in D1K2 expressing cells would be expected to restore cell cycle arrest. However, partial knockdown of Mad2 to near basal levels cooperated with D1K2 expression to increase the generation of 8N cells upon paclitaxel addition. Furthermore, immunoblot analysis of Mad2 expression upon long-term paclitaxel treatment showed that Mad2 levels increased before decreasing dramatically, regardless of D1K2 expression. This indicates that the cell lines in this study will eventually suffer mitotic slippage and enter G1 in the tetraploid state. The increased Mad2 level in D1K2 expressing cells serves to strengthen the SAC and prevent this phenomenon. This is evidenced by an increase in MPM2 phosphorylation in the D1K2 CL1 cell line compared to the Hygro cell line after treatment with paclitaxel. Recognizing phosphorylated mitotic proteins, the MPM2 antibody is a mitotic marker commonly used as a measure of SAC strength [164,165]. Perhaps a certain level of increased Mad2 expression strengthens the SAC, but any further overexpression causes a weakening. This could explain the difference between the results seen in this study and those in which direct overexpression of Mad2 causes a weakening of the SAC [128,159].

These data point to the conclusion that D1K2 is promoting a tetraploid population by exerting its effects on the tetraploidy checkpoint. Indeed, knockdown of p53 leads to an even greater population of 8N cells in the D1K2 expressing cell line, indicating that a p53 dependent mechanism is hampering the formation of this tetraploid population. In order to look more closely at the tetraploidy checkpoint, we generated tetraploid cells through failed cytokinesis induced by cytochalasin-B. This resulted in the formation of

8N cells in D1K2 expressing and shp53 cell lines, but not in the control cell line. Interestingly, whereas the shp53 cell line developed an 8N population in the presence of cytochalasin-B, this is in contrast to the result seen previously in the presence of paclitaxel (Figure 2-4A). While the reason for this is unclear, it is possible that paclitaxel induced arrest in these cells independent of the SAC as has been seen previously [166]. This would also explain the apparent lack of a G2 arrest. p53 knockdown may induce the death of the 8N population through an unknown mechanism, or these cells may be capable of dividing normally in the presence of paclitaxel. Importantly, this is likely a drug-dependent effect and does not affect the conclusions drawn from the experiments with cytochalasin-B.

Visual examination of these cells showed that the majority of the control cells were binucleate, with the remainder being mononucleate. D1K2 and shp53 cells additionally had a high rate of multinucleation, with three or more nuclei. Presumably, control cells arrest after failed cytokinesis whereas if the tetraploidy checkpoint is abrogated or bypassed with p53 knockdown or D1K2 expression, respectively, the cells undergo another round of DNA replication and failed cytokinesis. Immunoblot analysis of lysates obtained from treated cells show that Rb phosphorylation is lost in the Hygro cell line after 48 hours of treatment, whereas the D1K2 CL1 cell line as well as the shp53 cell line maintain greater phosphorylation. After an additional 24 hours, Rb phosphorylation is lost in all cell lines other than shp53, indicating that D1K2 is not capable of bypassing the tetraploidy checkpoint indefinitely.

The ability of D1K2 to allow DNA replication of 4N cells is despite a greater increase in p53 induction, compared to the Hygro control. Levels of p53 appear to

increase further between 48 and 72 hours, at which point D1K2 is no longer able to promote further DNA replication, demonstrating the possibility that the tetraploidy checkpoint functions in a step-wise manner. To our knowledge, this is the first evidence that p53 induction is proportional to DNA content, with an 8N DNA content eliciting a greater response than 4N. While the mechanism of sensing ploidy is currently unknown, these data suggest that it is sensitive to total quantities of DNA. Similarly, knockdown of p53 is not sufficient to allow replication of DNA past the 8N state, indicating that cells have an alternative mechanism for stopping the cell cycle. Concomitant expression of constitutively active Cdk2 along with ablation of the tetraploidy checkpoint through p53 knockdown is capable of bypassing both systems, allowing further DNA replication.

Ultimately, the significance of tetraploidy is determined by the fate of the affected cells. If a tetraploid state is fatal to a tumor cell, treatments that induce it should be beneficial. If the cells remain viable and maintain a tetraploid DNA content or revert to a diploid state, it will have little consequence. However, if tetraploidy leads to aneuploidy, it may possibly have negative consequences clinically. Our results show that tetraploid MCF10A cells are not viable; dying, failing to divide, or dividing once to produce unviable progeny. Thus, it is expected that treatment of tumors having constitutively active Cdk2 with certain therapeutics will induce tetraploidy that will ultimately lead to tumor death, consistent, and possibly complementary, with our observation of increased paclitaxel sensitivity due to Mad2 upregulation. While we did not visibly observe its occurrence, we cannot rule out the possibility that MCF10A cells are able to revert from a tetraploid state to a diploid state and remain viable. This phenomenon of halving the

cellular chromosome content occurs in meiosis and has been observed in tetraploid hepatocytes [167], however the mechanism is unknown in the latter case. Even if a very small fraction of tumor cells are able to carry out this reduction and remain viable, it would likely be sufficient to cause tumor relapse, potentially with a dramatically different tumor phenotype. It will be interesting to explore this possibility in the future, as it holds substantial consequence to patient treatment.

It is important to note, however, that our model using the MCF10A cell line cannot account for effects on cells due to other genetic and epigenetic alterations that may exist in tumors. Our results indicate that tumors with p53 mutations along with Cdk2 activation may be particularly prone to polyploidy and its potential ramifications. While the concentration of paclitaxel used to induce polyploidy in this study is lethal to the vast majority of cells, a small number of viable cells remain 48 hours after drug washout (Figure 2-8). In treating a patient, a relapse of the tumor may occur due to this small surviving population that contains a potentially considerable difference in chromosome content.

These data have allowed us to put forth two models of how constitutive Cdk2 activity affects the mitotic and tetraploidy checkpoints. The hyperphosphorylation of Rb induced by D1K2 causes an upregulation of Mad2. This strengthens the mitotic checkpoint, delaying slippage into G1 with a tetraploid DNA content (Figure 2-7A). In this case, D1K2 expression serves to prevent additional rounds of DNA replication.

Once cells have reached G1 with a tetraploid DNA content, the p53 dependent tetraploidy checkpoint is induced. In our model (Figure 2-7B), this initial response is sufficient to arrest cells without D1K2 expression. Cells with constitutive Cdk2 activity

provided by D1K2 are capable of progressing to S phase, where they become octaploid. After a second failed cytokinesis, the tetraploidy checkpoint increases in strength, causing cell cycle arrest. Together, it appears that overactive Cdk2 produces competing effects in terms of the generation of polyploid cells when treated with spindle poisons. However, the preventive effects offered by a strengthened spindle assembly checkpoint are temporary, allowing a weakened tetraploidy checkpoint to be the dominant phenotype observed.

Materials and Methods

Cell Culture and treatments

Tumor-derived cell lines were obtained as described previously [54] and maintained in Dulbecco's Modified Eagle's Medium supplemented with 10% fetal bovine serum. MCF10A cell lines were maintained in the suggested [168] 50/50 mixture of Dulbecco's Modified Eagle's Medium and Ham's F12 medium supplemented with 5% horse serum, 20 ng/mL EGF, 100 ng/mL cholera toxin, 10 µg/mL insulin, and 500 ng/mL hydrocortisone (Sigma-Aldrich, St. Louis, MO). The parental MCF10A cell line was obtained from ATCC (Manassas, VA). Nocodazole, paclitaxel, CVT313 (238803; Calbiochem, Billerica, MA), and cytochalasin-B (C6762; Sigma-Aldrich) were dissolved in DMSO.

Stable Cell Line Generation

MCF10A Hygro, D1K2, and D1K2(KD) cell lines were generated using the pBabe vector system as described previously [53]. Stable knockdown cell lines were generated by co-transfecting shRNA constructs (Thermo Scientific, Waltham, MA) along with viral packaging plasmids PMD2G and PsPax2 obtained from Addgene (Cambridge, MA) into the 293T cell line using Lipofectamine Reagent (Invitrogen, Grand Island, NY).

Medium from the transfected 293T cell line was then used to infect the target cell line, which was subsequently selected using 10 µg/mL Puromycin.

Propidium Iodide Staining/Flow Cytometry

Following treatment, cells were removed from the plate by trypsin digestion, washed 3x with PBS, and resuspended in a solution containing 3.4 mM sodium citrate, 75 µM propidium iodide, 0.1% Triton X-100 and 5 µg/ml RNAse A. Samples were analyzed on a Becton Dickinson FACSort flow cytometer. A total of 10,000 cells were counted for each sample. Data were analyzed using the ModFit program (Verity Software House Inc., Topsham, ME).

Cell Sorting

Cells were trypsinized and resuspended in medium containing 5 µM DyeCycle Violet DNA dye (Invitrogen) and incubated at 37 ºC for 30 minutes. Cells were then incubated on ice until sorting was complete. Cells were sorted on a FACSAria instrument from BD Bioscience (San Jose, CA) according to DNA content based on absorbance of the dye.

Immunofluorescence Microscopy

D1K2 tumor cells for immunofluorescence studies were plated onto glass coverslips in 6-well plates. After treatment, the cells were fixed with a solution containing 90% methanol and 10% MES buffer (100mM MES, pH 6.9, 1mM EGTA and 1mM $MgCl_2$). The coverslips were subsequently incubated with antibody buffer (5% goat serum in phosphate-buffered saline (PBS)) in a humidified chamber for 1 hour. Primary antibody staining was performed using an antibody for γ-Tubulin (sc-17787; Santa Cruz Biotechnology, Inc., Santa Cruz, CA) at a 1:200 dilution in antibody buffer

for 2 hours. Following primary antibody incubation, the coverslips were washed three times with PBS, and incubated with a goat anti-mouse Cy3 secondary antibody (81-6515; Zymed, Carlsbad, CA) for 1 hour at a 1:200 dilution in antibody buffer. Following three additional washes with PBS, coverslips were mounted onto slides with Vectashield + 4', 6-diamidino-2-phenylindole (DAPI) (H-1200; Vector Laboratories, Burlingame, CA) to visualize nuclei. Images were captured using an upright microscope (Axioplan2; Zeiss, Thornwood, NY), and processed using Openlab 5.5 Improvision software.

MCF10A cell lines intended for immunofluorescence were plated in Petri dishes and treated with DMSO, paclitaxel, CVT313, or paclitaxel with CVT313 for 72 hours. Cells were then trypsinized, washed with PBS, and fixed with 2% paraformaldehyde in PBS. Cells were then quenched with 0.2% Tween 20 and 50 mM NH_4Cl in PBS. After washing with PBS, cells were resuspended in antibody buffer for 1 hour, at which time an antibody directed towards pericentrin (ab4448, Abcam plc, Cambridge, MA) was added at a 1:200 dilution for 2 hours. Cells were pelleted, washed with PBS, and resuspended in antibody buffer containing a 1:200 dilution of a goat anti-rabbit Cy3 antibody (81-6115, Zymed) for 1 hour. After PBS washing, the cells were resuspended in PBS containing 0.1% Triton X-100 and spread evenly across coverslips. Upon drying, coverslips were mounted onto slides with Vectashield + DAPI to visualize nuclei and centrosomes.

Analysis of Metaphase Spreads

Preparation of metaphase spreads were performed according to basic protocol 2 from Current Protocols in Cell Biology [169]. The chromosomes were stained with DAPI and visualized and photographed using fluorescence microscopy as described above.

Immunoblot Analysis

Immunoblotting was performed as described [170], employing antibodies to NPM, p-NPM[T199], p-Rb 780, 795, or 807/811 (3542; 3541; 9307; 9301; 9308; Cell Signaling Technology, Inc., Danvers, MA), p-Rb 249/252 (44-584; Bio-Source International, Grand Island, NY), FLAG (F-3165; Sigma-Aldrich), Mad2 (Ab70385; Abcam plc), Actin, Cdk2, Rb, p21, or p53 (sc-1616-R; sc-163; sc-7905; sc-3997; sc-100; Santa Cruz).

Growth Curves

For growth curves constructed using cell counts, cell lines were treated for 72 hours and then seeded at 10,000 cells/well in 6-well plates. Cells were subsequently trypsinized and counted in triplicate (three separate wells) daily using a hemacytometer. For growth curves constructed using Crystal Violet staining, cell lines were seeded 2,500 cells/well in 24-well plates. Cells were quantitated daily by fixation using 4% paraformaldehyde in PBS for 20 minutes, staining with 0.1% Crystal Violet (C0775; Sigma-Aldrich) in 30/70 methanol/water for 30 minutes, followed by 5 washes using water. After drying overnight, retained Crystal Violet was eluted using methanol and quantitated by measuring absorbance at 590 nm on a DU800 spectrophotometer (Beckman Coulter Inc., Brea, CA). Values were normalized to the absorbance observed on day 1. Samples producing absorbance higher than 2 were diluted with

additional methanol to lower absorbance readings below 2. Plotted values for these samples are back-calculated.

Paclitaxel washout experiment

Cells were plated at 200,000 cells/p100 dish. The number of cells in each dish was counted in replicate plates before treatment with paclitaxel, after 72 hours of treatment, or after 72 hours of treatment followed by a 48 hour washout period, using a hemacytometer.

Tetraploid cell fate analysis

Cells were plated at a single-cell density in 96-well plates. After incubating overnight, they were treated with 4.5 μg/mL cytochalasin-B for 72 hours, followed by drug washout. Cells were visually inspected to identify multinucleate cells (>2 nuclei) and their fate was determined by re-examination one week after drug washout.

[^{3}H]Thymidine Incorporation

[^{3}H]Thymidine incorporation assays were carried out as previously described [54,148], using a 2 hour [^{3}H]thymidine pulse.

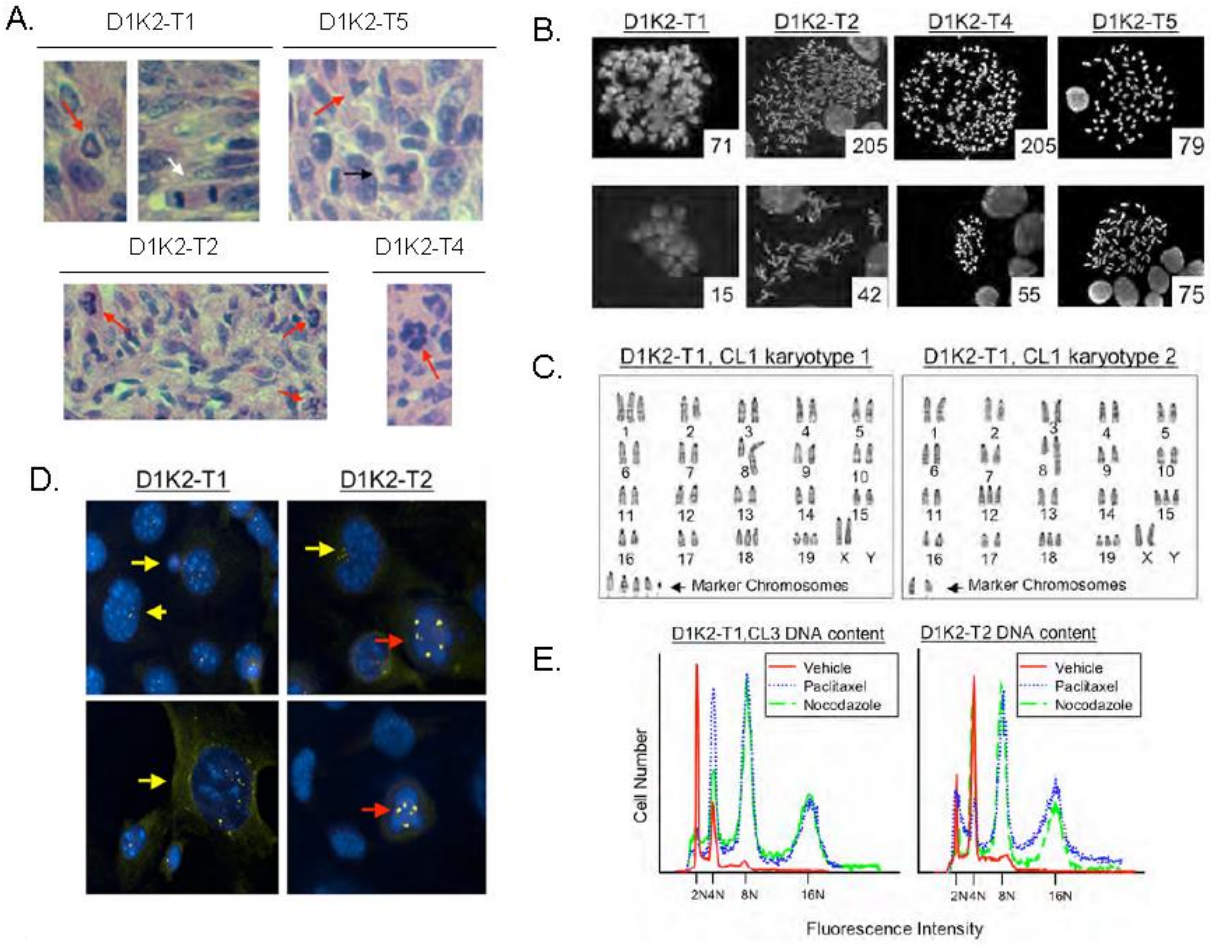

Figure 2-1. MMTV-D1K2 tumors and tumor-derived cell lines exhibit aberrant mitosis and CIN. A) H&E stained tumor tissue sections from tumors generated by injecting cancer cell lines isolated from MMTV-D1K2 tumors into the mammary glands of wild type FVB mice showing abberant mitoses (red arrows), a normal bipolar mitotic figure (white arrow), and a bipolar mitotic figure with lagging chromosomes (black arrow). B) Metaphase spreads of cells from the indicated MMTV-D1K2 cell lines. The number in the lower right-hand corner of each picture is the number of chromosomes in the associated spread. C) Karyotype analysis of metaphase chromosomes by G-banding. D) The indicated cell lines were analyzed by immunofluorescence microscopy with antibodies to γ-Tubulin (yellow). DAPI staining is shown in blue. Yellow arrows denote cells with abnormally high numbers of centrosomes (> 2). Red arrows show cells undergoing multipolar mitosis. E) The indicated cell lines were treated with 1 μM Paclitaxel, 1 μM Nocodazole, or the 0.1% DMSO vehicle for 72 hours. Treated cells were subjected to propidium iodide staining followed by flow cytometry.

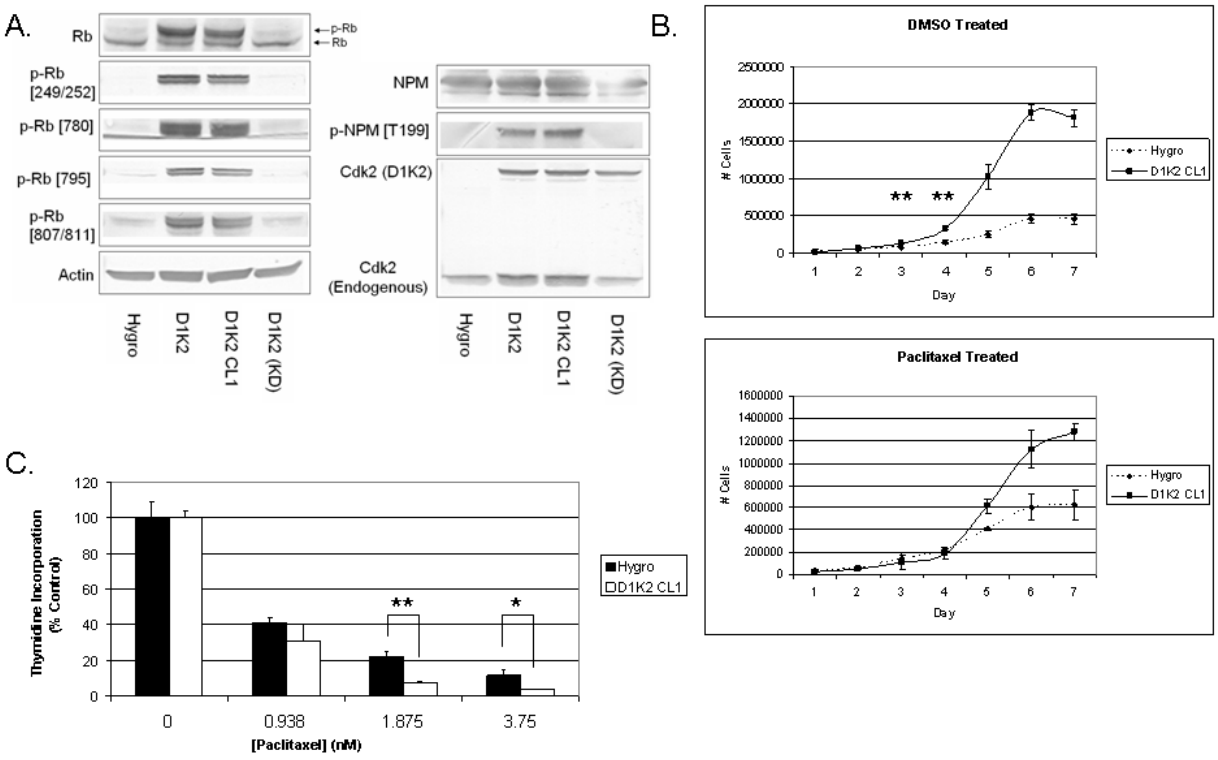

Figure 2-2. D1K2 phosphorylates Cdk2 substrates, increases growth rate, and sensitizes cells to paclitaxel. A) Immunoblot analysis of Cdk2 substrates in MCF10A cell lines expressing a vector control (Hygro), D1K2, a clonal line derived from the polyclonal line (D1K2 CL1), or a kinase-dead D1K2 mutant (D1K2(KD)) B) Growth curves of the indicated cell lines after being treated with 0.1% DMSO or 1 nM paclitaxel for 72 hours. Cells were then reseeded in 6-well plates and counted in triplicate each day for one week. C) [3H]Thymidine incorporation of the indicated cell lines treated with increasing concentrations of paclitaxel for 72 hours. Indicated values represent the average of three replicate samples. Error bars represent the s.d. of three replicates. * denotes $p < 0.05$ and ** denotes $p < 0.005$ using the unpaired t test.

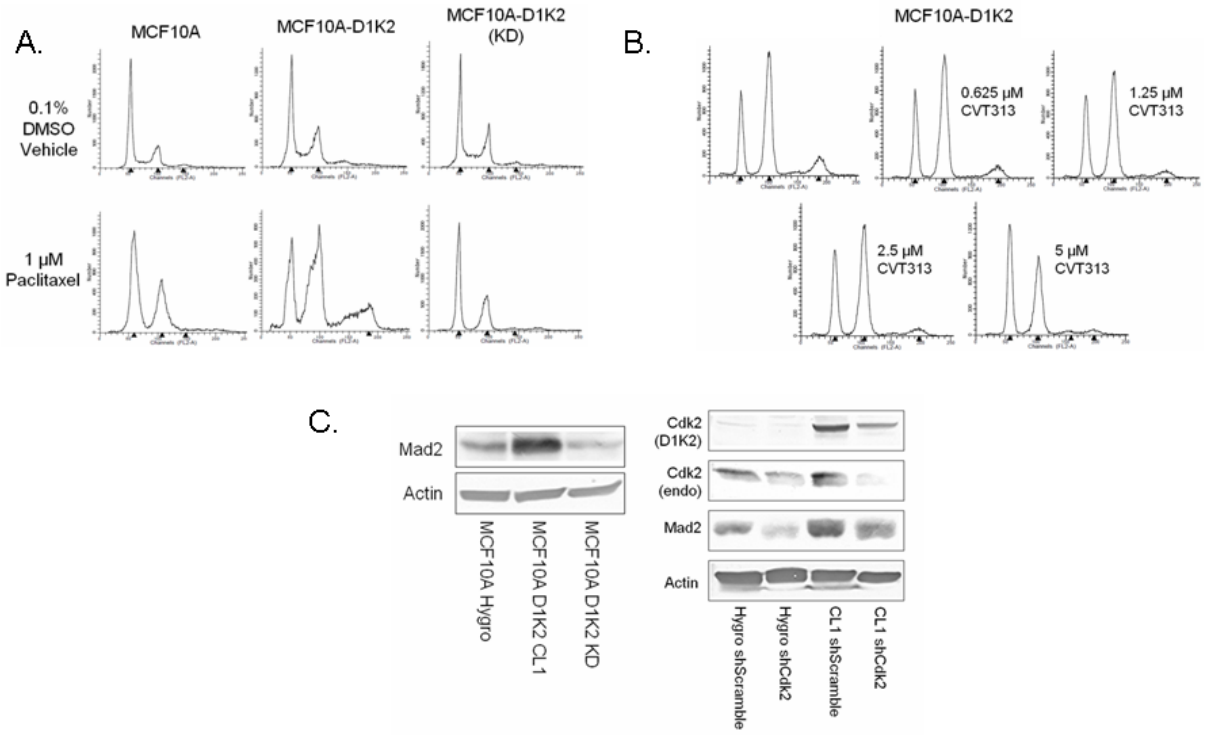

Figure 2-3. D1K2 kinase activity promotes polyploidy and upregulates Mad2 A) Flow cytometry analysis of the indicated cell lines after 72 hours of treatment with 0.1% DMSO or 1 μM paclitaxel. B) Flow cytometry analysis of the MCF10A D1K2 cell line treated with 1 μM paclitaxel and the indicated concentration of the Cdk2 inhibitor CVT313 for 72 hours. C) Immunoblot analysis of the indicated cell lines showing Mad2, Cdk2, and D1K2 expression. D) Flow cytometry analysis of the indicated cell lines after 72 hours of treatment with 0.1% DMSO or 1 μM paclitaxel. E) Immunoblot analysis of the indicated cell lines at various time points after constant treatment with 1 μM paclitaxel showing Mad2 expression levels. Flow cytometry profiles in all panels represent DNA content as measured by propidium iodide staining.

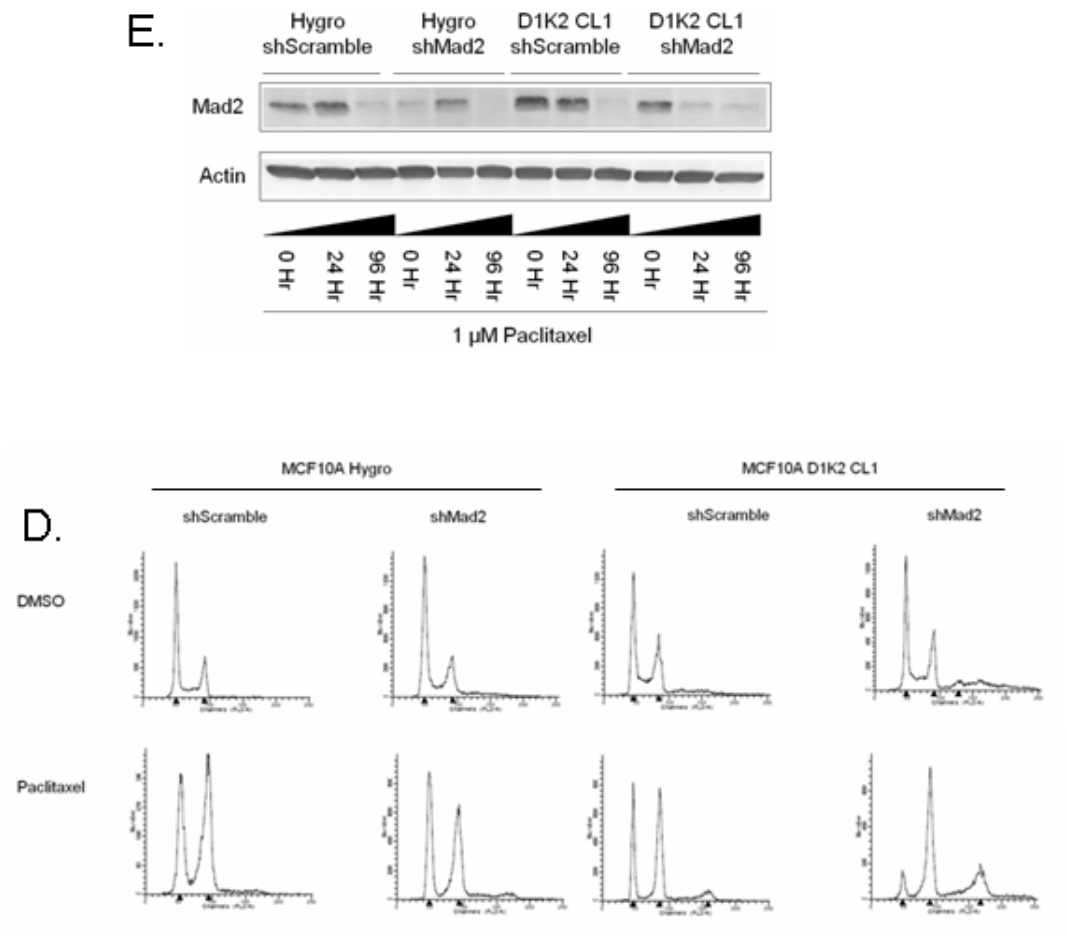

Figure 2-3. Continued

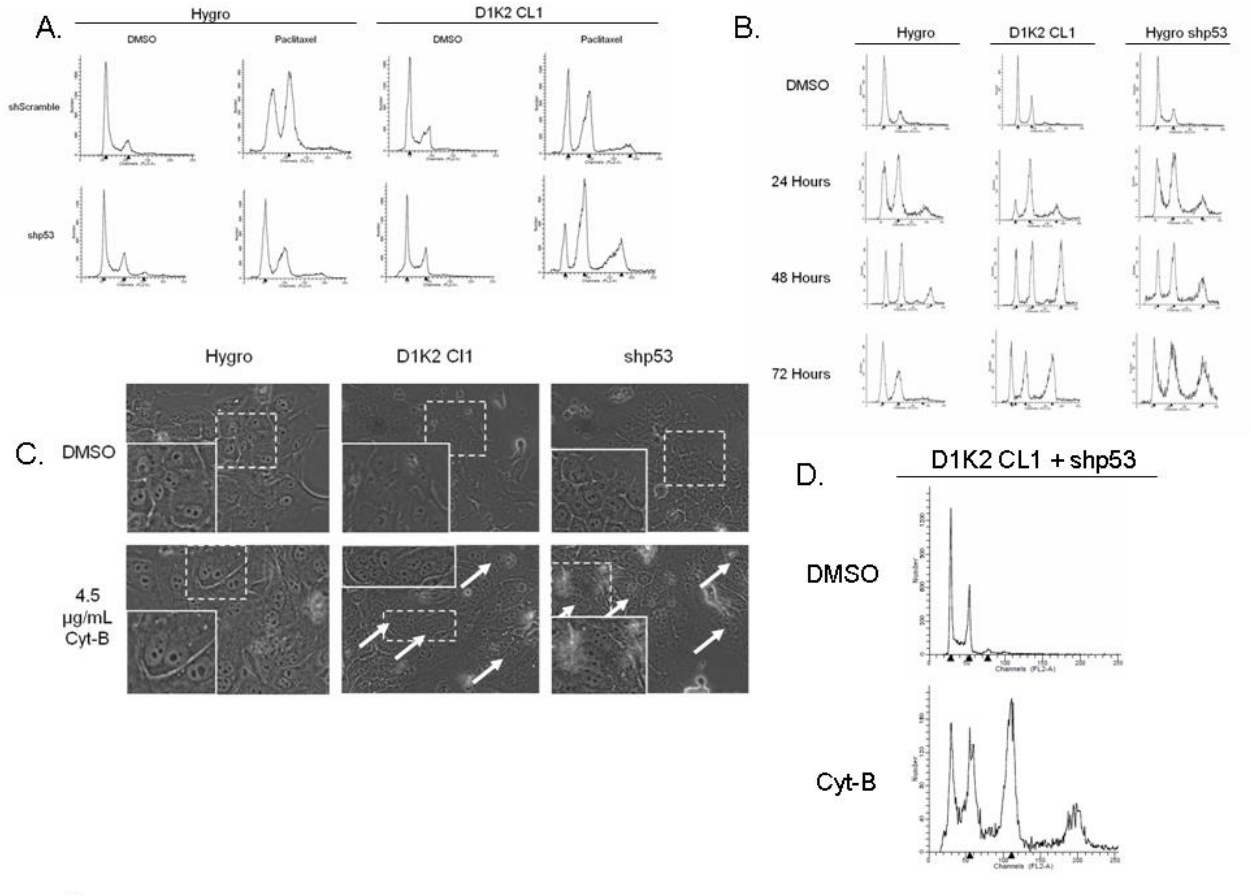

Figure 2-4. D1K2 weakens the tetraploidy checkpoint. A) Flow cytometry analysis of the indicated cell lines after 72 hours of treatment with 0.1% DMSO or 1 µM paclitaxel. B) Flow cytometry analysis of the indicated cell lines after 72 hours of treatment with 0.1% DMSO or after 24, 48, and 72 hours of treatment with 4.5 µg/mL cytochalasin-B. C) Micrographs of the indicated cell lines after 72 hours of treatment with 0.1% DMSO or 4.5 µg/mL cytochalasin-B. The dashed white boxes represent the location of the inset images in the solid white boxes. White arrows mark cells with more than two nuclei. D) Flow cytometry analysis of the MCF10A D1K2 CL1 shp53 cell line after 72 hours of treatment with 0.1% DMSO or 4.5 µg/mL cytochalasin-B. Note: X-axis values differ from previous flow cytometry profiles due to the lower detector voltage required to detect the 16N peak.

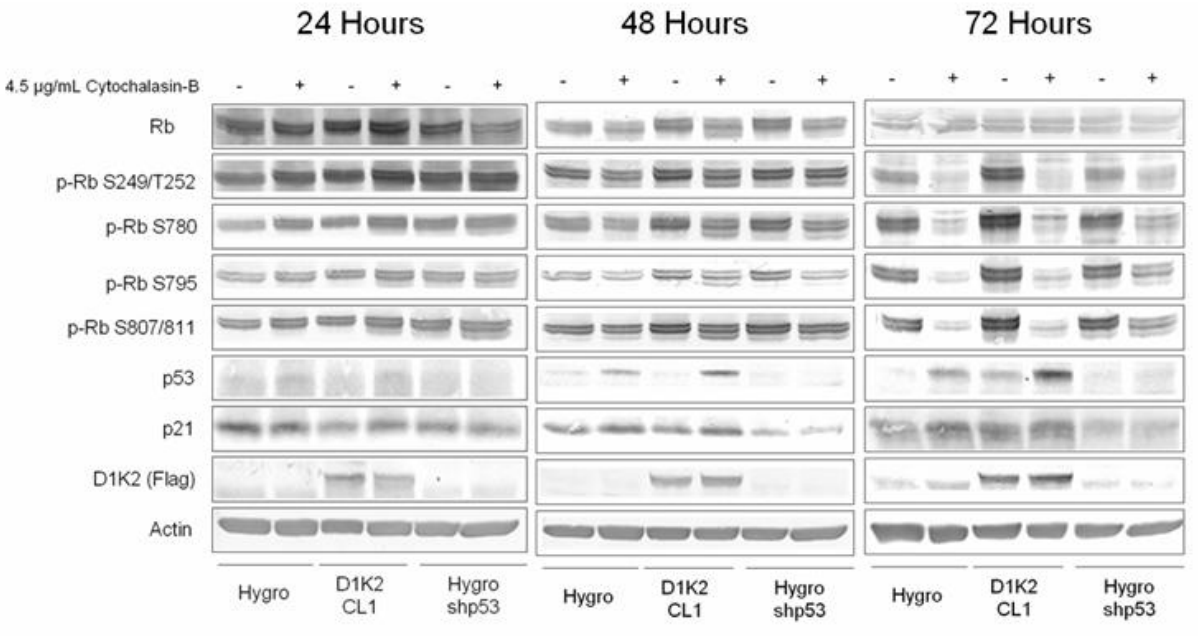

Figure 2-5. D1K2 and p53 knockdown sustain Rb phosphorylation in polyploid cells. Immunoblot analysis of the indicated cell lines after 24, 48, and 72 hours of treatment with either 0.1% DMSO or 4.5 µg/mL cytochalasin-B.

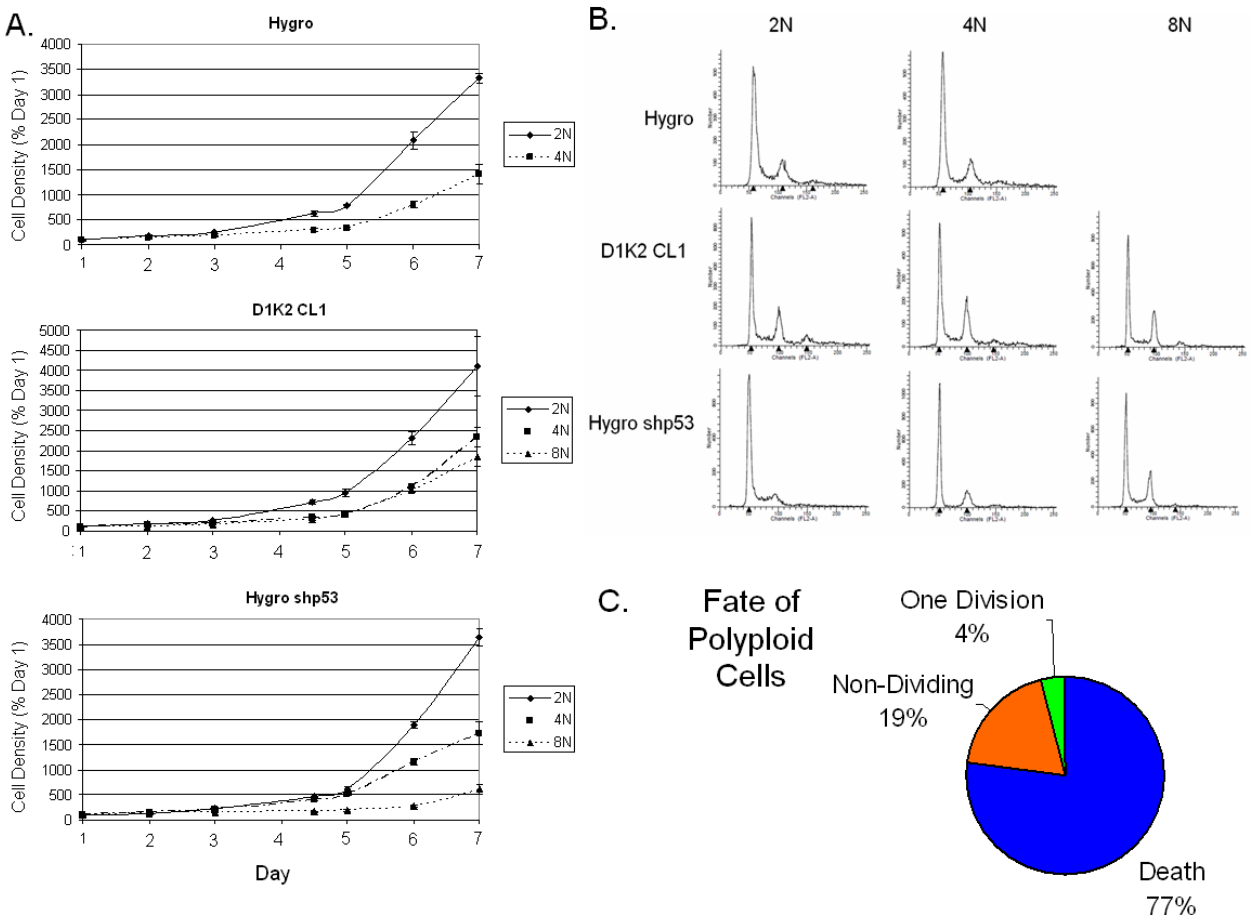

Figure 2-6. Long-term effects of polyploidy on MCF10A cell lines. A) Growth curves of the indicated cell lines after 72 hour treatment with 4.5 µg/mL cytochalasin-B and subsequent sorting based on DNA content. Cells were stained daily with Crystal Violet and washed. Residual Crystal Violet was eluted and the absorbance at 590 nm was determined. Plotted values represent absorbances normalized to day 1. Error bars represent the s.d. of three replicates. B) Flow cytometry analysis of the indicated cell lines one week after sorting based on ploidy (2N, 4N, 8N). C) Data obtained through the visual analysis of the fate of tetraploid D1K2 CL1 cells induced with cytochalasin-B for 72 hours.

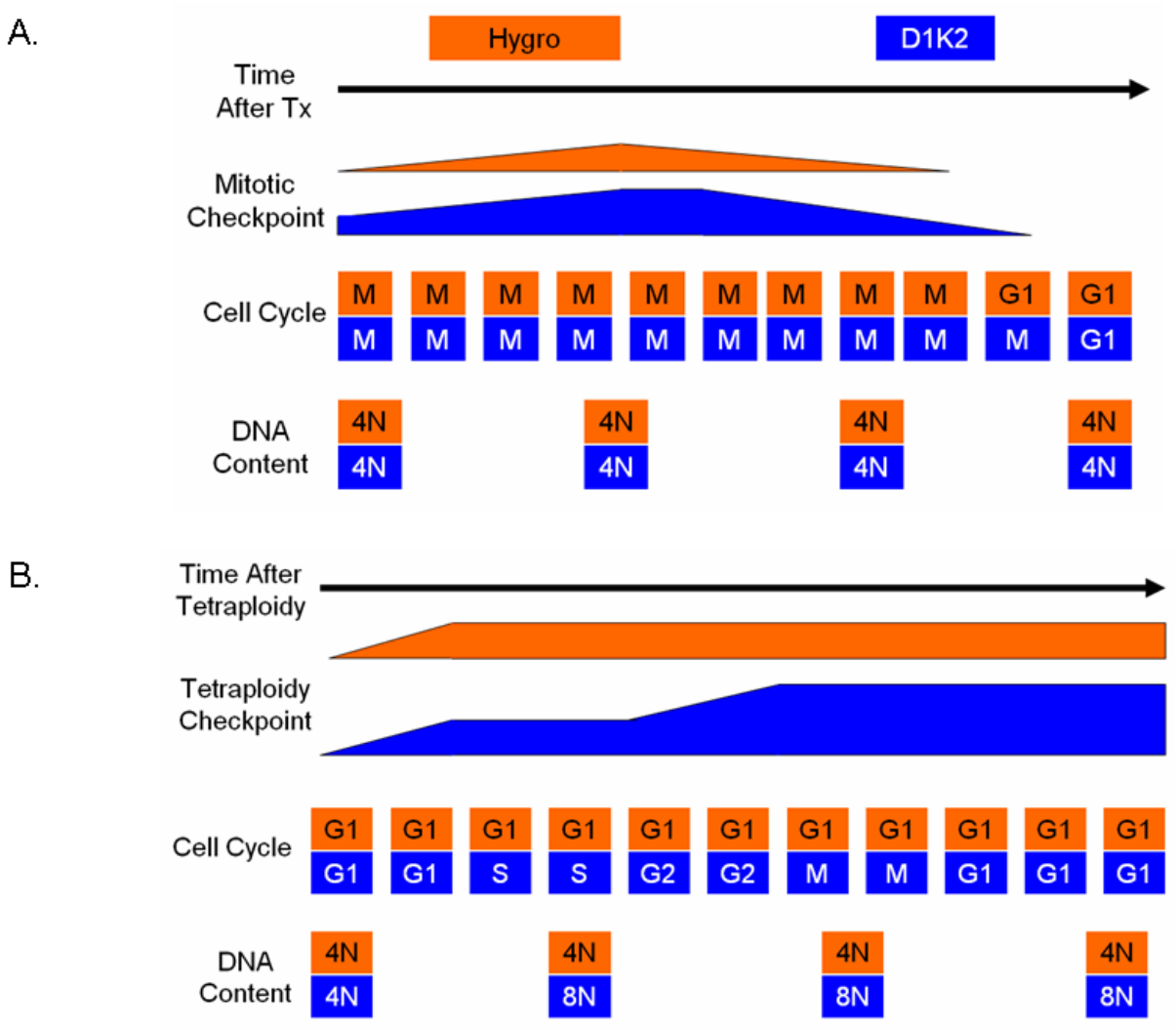

Figure 2-7. Current working models. A) The hyperphosphorylation of Rb induced by D1K2 causes an upregulation of Mad2. This strengthens the mitotic checkpoint, delaying slippage into G1 with a tetraploid DNA content. B) After tetraploidy occurs, an initial response of the tetraploidy checkpoint is sufficient to arrest cells without D1K2 expression. Cells with constitutive Cdk2 activity provided by D1K2 are capable of progressing to S phase, where they become octaploid. After a second failed cytokinesis, the tetraploidy checkpoint increases in strength, causing cell cycle arrest.

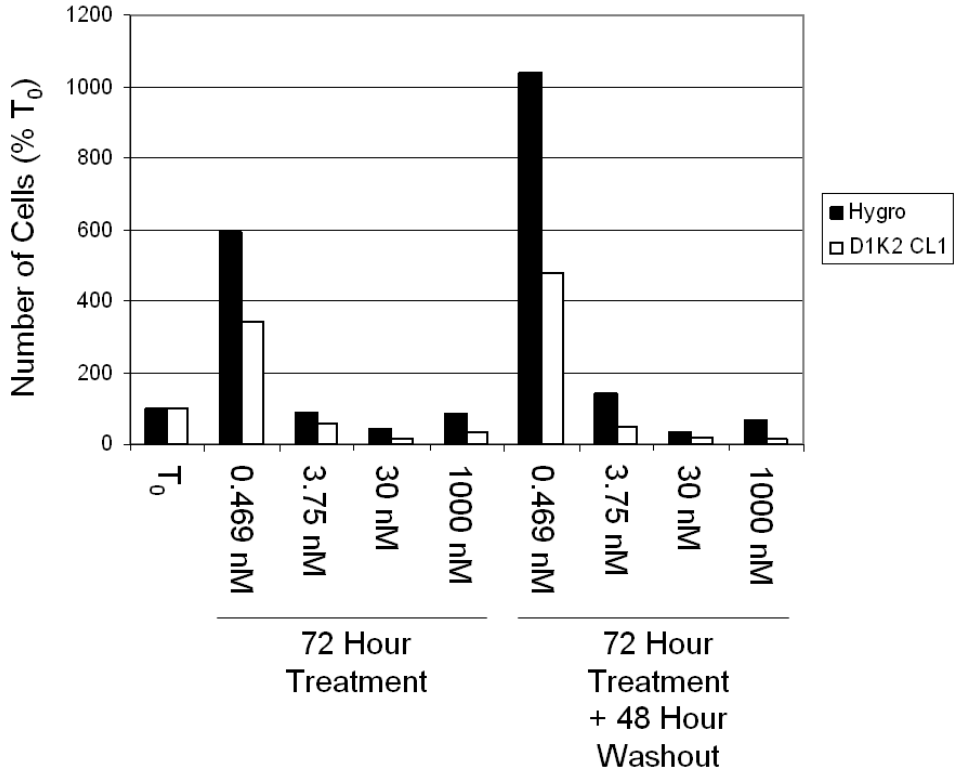

Figure 2-8. Viability of paclitaxel treated MCF10A cell lines. The Hygro and D1K2 CL1 cell lines were treated with the indicated concentration of paclitaxel for 72 hours, after which the number of cells remaining was counted using a hemacytometer. A parallel set of cells were incubated a further 48 hours after removal of paclitaxel before being counted. Cell numbers were normalized to the number of cells present upon starting paclitaxel treatment (T_0).

A.

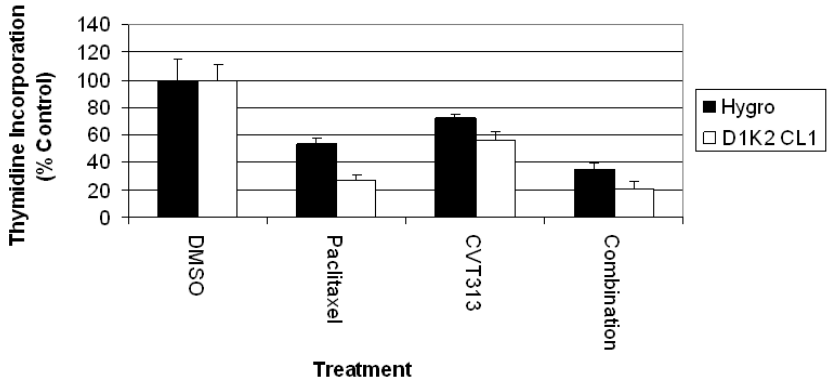

B.

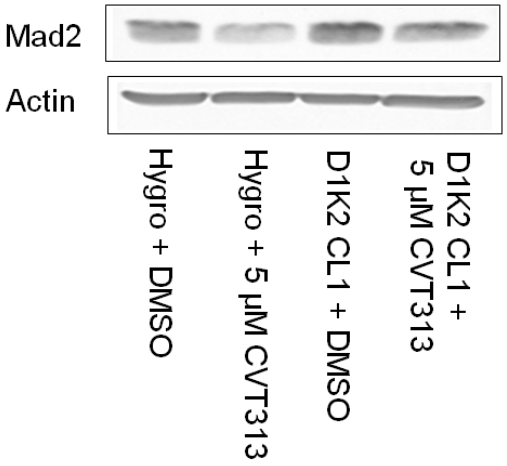

Figure 2-9. Effects of paclitaxel and CVT313 on MCF10A cell lines. A) [^{3}H]Thymidine incorporation of the indicated cell lines treated with 1 μM paclitaxel and/or 5 μM CVT313 for 24 hours. Indicated values represent the average of three replicate samples. Error bars represent the s.d. of three replicates. B) Immunoblot analysis of the indicated cell lines treated with or without 5 μM CVT313 for 24 hours. Actin serves as a loading control.

A.

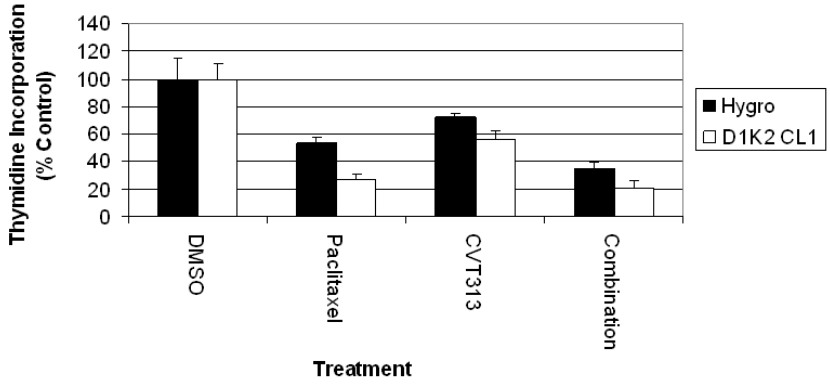

B.

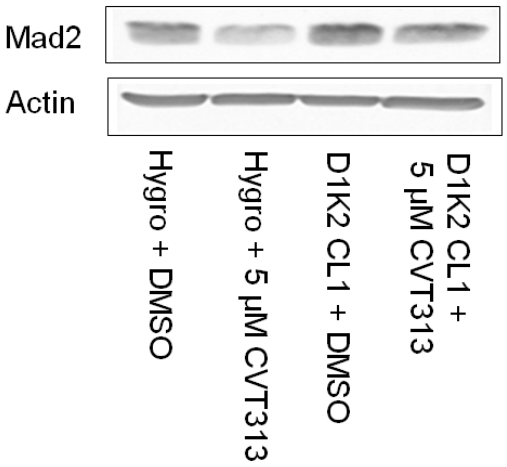

Figure 2-10. Analysis of Mad2 in the spindle assembly checkpoint. A) Immunoblot analysis of the indicated cell lines showing Mad2 expression levels before and after knockdown. B) Immunoblot analysis of p-MPM2 levels in the indicated cell lines after treatment with DMSO or 1 µM paclitaxel for 24 hours.

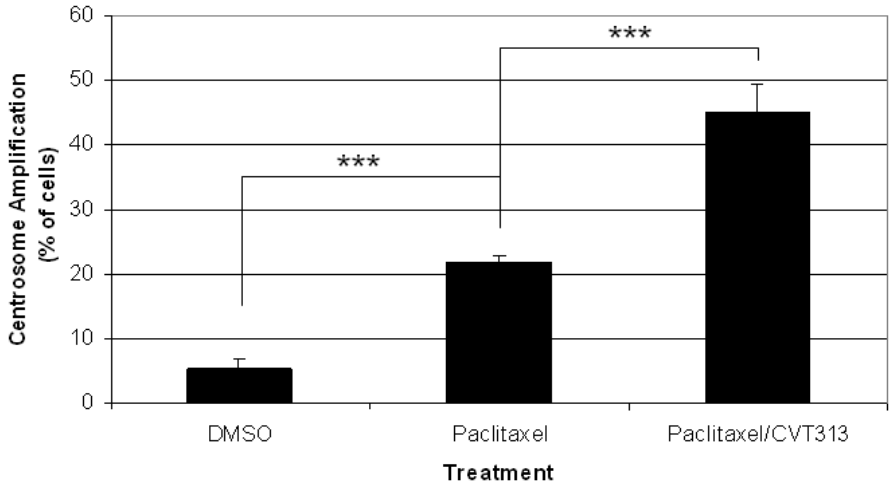

Figure 2-11. Centrosome amplification in MCF10A cell lines in the presence of paclitaxel and CVT313. Rate of centrosome amplification (>2 centrosomes/cell) in the MCF10A D1K2 CL1 cell line treated with vehicle control, 1 μM paclitaxel, or 1 μM paclitaxel along with 5 μM CVT313. Number of centrosomes were scored visually by immunofluorescence using an antibody directed toward pericentrin. Indicated values represent the average of three replicate samples. Error bars represent the s.d. of three replicates. *** denotes $p < 0.001$ using the unpaired t test.

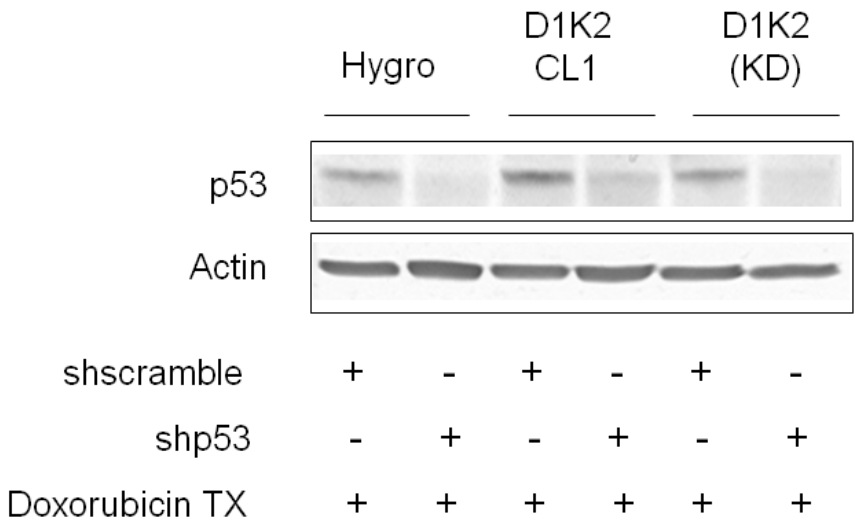

Figure 2-12. Analysis of p53 knockdown efficiency. Immunoblots of the indicated cell lines showing p53 expression. p53 was induced in all cell lines by treatment with 0.5 µg/mL doxorubicin for 8 hours. Actin serves as a loading control.

CHAPTER 3
CDK2 ACTIVATION INDUCES CHROMOSOMAL INSTABILITY THROUGH MULTIPLE MECHANISMS

Introduction

In the previous chapter, the role of overactive Cdk2, in the form of D1K2, in permitting CIN was discussed. Our data show that not only does D1K2 create an environment conducive to CIN through weakening of the tetraploidy checkpoint, but it also actively promotes CIN through multiple mechanisms. It has been discussed that the mechanisms of CIN rely primarily on centrosome amplification and here we show that D1K2 kinase activity results in supernumerary centrosomes both through over amplification and failed cytokinesis. Additionally, expression of D1K2 reduces the rate of centrosome bundling, resulting in a higher incidence of multipolar mitosis.

The process of centrosome duplication is quite complex, involving a large number of proteins throughout the cell cycle (reviewed in [99]). Nucleophosmin (NPM) is a crucial part of this process, binding to unreplicated centrosomes and releasing upon being phosphorylated by Cyclin E/Cdk2 on threonine 199, permitting centrosome duplication [155]. Interestingly, D1K2 appears capable of phosphorylating this site, with equal or greater strength, than the endogenous Cyclin E/Cdk2 complex in vitro.

We also show that D1K2 is capable of phosphorylating the activating subunit of the Anaphase Promoting Complex/Cyclosome (APC/C), Cdh1. Cdh1 is inactivated when phosphorylated and its active form is responsible for the degradation of many proteins responsible for centrosome duplication [171]. Cdh1 bound to the APC/C is also intricately involved in cytokinesis. Hyperphosphorylation of Cdh1 by D1K2 could lead to centrosome amplification directly through over-amplification, or through failed cytokinesis. Indeed, not only do we see centrosome amplification in cells expressing

D1K2, but also instances of failed cytokinesis. These results show additional mechanisms by which D1K2 is capable of producing CIN.

Results

Cellular Cyclin D1/Cdk2 Complexes can Phosphorylate NPM

As mentioned above, Nucleophosmin localizes to centrosomes and plays a critical role in their duplication during the cell cycle. Cdk2 phosphorylates Nucleophosmin on T199 and phosphorylation of this site initiates centrosome duplication. Cyclin E/Cdk2 complexes are thought to catalyze this phosphorylation event in normal cells [172]. Complexes of Cdk6 with the viral Cyclin, K-Cyclin, are also capable of phosphorylating Nucleophosmin on T199 and inducing centrosome amplification [173]. This raises the possibility that other transformation-associated Cyclin/Cdk complexes may be able to perform this function. We executed an experiment to determine which Cyclin D1 or Cyclin E/Cdk complexes are capable of phosphorylating Nucleophosmin on T199. NMuMG cells were treated with recombinant adenoviruses encoding Flag-tagged Cyclins and His_6-tagged Cdks in the indicated combinations (Figure 3-1A). Of these combinations, only coexpression of Cyclin D1 and Cdk2 and Cyclin E and Cdk2 significantly increased Nucleophosmin phosphorylation relative to the control adenovirus treatment. The combinations that did not increase Nucleophosmin concentration might have been inactive because of the inability of the particular combination to form complexes.

Various Cyclin/Cdk fusion proteins phosphorylate NPM

Overall, these results underscore the high degree of promiscuity among Cyclins and Cdks and indicate that in breast cancers where individual Cyclins such as Cyclin E, D, or A are overexpressed [174-177] it is difficult to determine which of the resulting

Cyclin/Cdk complexes mediate the oncogenic effects of the individual Cyclins that are overexpressed. The Cyclin D1-Cdk fusion protein (D1K2) was designed to specifically model the functions of Cyclin D1/Cdk2 complexes [53]. We have now designed vectors encoding N-terminally FLAG tagged and C-terminally His_6-tagged Cyclin D1-Cdk4 (D1K4) and Cyclin E-Cdk2 (EK2) fusion proteins to specifically model the functions of the respective Cyclin/Cdk complexes. These vectors were transfected into 293T cells and the fusion proteins were isolated from the cell lysates using anti-FLAG-agarose and the immunoprecipitates subjected to Rb kinase assays. The kinase assays were analyzed by immunoblot with phospho-specific antibodies to Rb (Figure 3-1B). In these assays the D1K2, D1K4, and EK2 fusion proteins exhibited kinase activity toward Rb and showed preferences in their phosphorylation of different sites. A kinase dead mutant of D1K2 (D1K2(KD)) did not exhibit kinase activity in this assay. These novel Cyclin-Cdk fusion proteins were cotransfected with Nucleophosmin fused to Green Fluorescent Protein (GFP-NPM) or Myc-tagged Cdh1. In agreement with the results of Figure 3-1A, D1K2 and EK2 induced Nucleophosmin phosphorylation on T199 (Figure 3-1C).

Cellular Cyclin D1/Cdk2 Complexes can Phosphorylate Cdh1

Like Nucleophosmin, the APC/C regulatory subunit Cdh1 has been shown to be a substrate for Cyclin E/Cdk2, and Cyclin E/Cdk2-dependent phosphorylation inhibits its association with APC/C, thus inhibiting APC/C activity. Heterozygous deletion of Cdh1 results in a high frequency of tumors, including breast tumors, and CIN [171]. This suggests that Cdh1 phosphorylation by D1K2 could explain its ability to induce breast tumors that exhibit CIN. Cyclin E/Cdk2-dependent phosphorylation of Cdh1 causes a decrease in its electrophoretic mobility [178], therefore we examined whether D1K2 or

kinase dead D1K2 mutants altered the mobility of Cdh1 in coexpression experiments. Transfection experiments in 293T cells were carried out in which Cdh1 was coexpressed with D1K2 or previously described kinase dead mutants of D1K2. D1K2(KD) is catalytically inactive due to a mutation in the ATP binding site of the Cdk2 domain. D1K2(KE) is kinase dead due to a mutation corresponding to a Lysine 114 to Glutamate mutation of Cyclin D1. This mutation prevents the intramolecular activation of Cdk2 by the Cyclin D1 domain and prevents regulatory phosphorylation of the Cdk2 domain [53]. D1K2 coexpression induced a mobility shift of Cdh1 relative to the control while both kinase dead D1K2 mutants were without effect (Figure 3-2A). This shift in Cdh1 mobility correlated with the phosphorylation of endogenous Rb. Cdh1 overexpression increased endogenous Rb expression. The significance of this observation is unknown.

D1K2 Phosphorylates NPM and Cdh1 in Untransformed Cells

We wanted to determine whether similar results would be obtained in nontumorigenic NMuMG cells therefore these cells were infected with control adenovirus (Ad.GFP) or adenoviruses encoding D1K2 or kinase dead D1K2. D1K2 expression induced a shift in the mobility of endogenous Cdh1 that was not observed with expression of kinase dead D1K2 (Figure 3-2B). Similarly, D1K2 but not D1K2(KD) increased the phosphorylation of endogenous Nucleophosmin on Thr^{199} even though both proteins were expressed at equivalent levels based on immunostaining with the FLAG antibody.

Various Cyclin/Cdk Complexes Bind to Cdh1

We next wanted to investigate if various Cyclin/Cdk complexes and the D1K2, D1K4, and EK2 fusion proteins could form stable complexes containing Cdh1. Myc-

tagged Cdh1 was coexpressed with various Cyclin/Cdk complexes or the Cyclin-Cdk fusion proteins and the lysates were subjected to immunoblot analysis (Figure 3-2C, left panel) or immunoprecipitated using an antibody to the Myc epitope tag followed by immunoblot analysis of the immunoprecipitates (Figure 3-2C, right panel). The ratio of the upper Cdh1 band to the lower Cdh1 band in the crude lysates was highest in the samples coexpressing D1K2, and Cyclin D1/Cdk2 and Cyclin E/Cdk2 complexes. Cdh1 coimmunoprecipitated with D1K2, D1K2(KD), D1K2(KE), D1K4, EK2, and Cyclin D1/Cdk2, Cyclin D1/Cdk4, and Cyclin E/Cdk2 complexes (Figure 3-2C, right panel). Interestingly, endogenous Cdk2 coimmunoprecipitated with Cdh1 when it was expressed alone, and also when Cdh1 was coexpressed with various other Cyclin/Cdk complexes and fusion proteins. Endogenous Cyclin E, Cyclin D1, or Cdk4 were not observed in Cdh1 immunoprecipitates suggesting that Cdh1 has the highest affinity for Cdk2.

D1K2 Directly Phosphorylates NPM and Cdh1 In Vitro

The results in Figs. 3-1C and 3-2A-D suggest that the D1K2 fusion protein can phosphorylate Nucleophosmin and Cdh1, but it is possible that D1K2 induces the phosphorylation of these proteins through indirect mechanisms. We performed in vitro kinase assays using purified GST-Nucleophosmin and GST-Cdh1 as the substrate for D1K2, or as a control, D1K2(KD) to determine whether D1K2 could directly phosphorylate Cdh1 and Nucleophosmin. The kinase assays were analyzed by autoradiography (Figure 3-2D, left panel) and immunoblot (Figure 3-2D, right panel). D1K2 phosphorylated Nucleophosmin. Some phosphorylation was observed in the D1K2(KD) control, but this was less than that observed with D1K2, and the immunoblots indicate that three to four fold more D1K2(KD) was present in the kinase assays than

D1K2. D1K2 catalyzed robust phosphorylation of Rb and very little phosphorylation was observed with D1K2(KD). This suggests that D1K2 can directly phosphorylate Nucleophosmin, but that another Nucleophosmin kinase may also coimmunoprecipitate with D1K2. A phospho-Thr199 Nucleophosmin immunoblot showed a pattern similar to the autoradiogram indicating that the phosphorylation occurs on this site during the kinase reactions, although this does not rule out the phosphorylation of other sites as well. Cdh1 kinase assays were limited by low concentrations of Cdh1, but a longer exposure of the autoradiogram showed that D1K2, but not D1K2(KD) was able to phosphorylate GST-Cdh1. A band that migrates just beneath GST-Cdh1 was observed in all of the lanes containing D1K2, but not in the lanes containing D1K2(KD). This band migrates at the same molecular size as D1K2 and is likely due to D1K2 autophosphorylation. Immunoblot with a GST antibody shows the relative levels of the GST fusion proteins in the assays. GST and GST-Nucleophosmin are present in similar abundance (note that GST-Nucleophosmin comigrates with FLAG-tagged D1K2). GST-Rb is present at lower levels than GST-Nucleophosmin and GST-Cdh1 is barely detectable by immunoblot with an antibody to GST.

Cells Expressing D1K2 Undergo Failed Cytokinesis

Time-lapse video microscopy of the D1K2-T2 cell line that was described previously [54] showed that there was an observable rate of failed cytokinesis. A number of cells were seen to enter mitosis, complete cytokinesis to varying degrees, but fuse back together prior to abscission. These cells appear to survive and frequently undergo a subsequent successful mitosis and cytokinesis. Individual video frames from a representative example are in Figure 3-3.

D1K2 Reduces the Rate of Supernumerary Centrosome Bundling

The frequency at which multipolar mitosis occurs relies not only on the process of centrosome amplification, but also the rate at which these supernumerary centrosomes are effectively bundled to preserve a bipolar mitosis. Initially, no statistically significant difference in the frequency of multipolar mitosis in MCF10A Hygro and D1K2 CL1 were seen, being 6.6 and 8%, respectively (Figure 3-4A). However, these mitotic figures represent the cell population that is in metaphase, whereas when cells have entered anaphase and are actively segregating their DNA, a large difference is seen between these cell lines. In this case, the Hygro control cell line showed a 2.33% rate of multipolar anaphase whereas the D1K2 expressing cells showed a 10.67% rate (Figure 3-4A). These different mitotic stages are illustrated in Figure 3-4B. These data indicate that D1K2 increases the frequency of multipolar cell division not through raising the number of spindle poles, but by preventing the amelioration of the basal rate of multipolar spindle formation.

D1K2 Induces EMT

In the course of producing the D1K2 expressing MCF10A cell lines used in this study, it was noticed that a few weeks after transduction the D1K2 cells took on a noticeably different, elongated morphology, appearing more mesenchymal than the parental MCF10A, a cuboidal, epithelial cell line (Figure 3-5A). Analysis of proteins commonly used as markers of Epithelial to Mesenchymal Transition (EMT) showed evidence that a partial EMT had occurred (Figure 3-5B). There was a noticeable switch from E- to N-cadherin as well as slight increases in snail and slug.

These results agree with those of the in vivo D1K2 tumor studies our lab has previously published [54,179]. In those studies, it was found that tumors induced by

D1K2 expression contained regions of spindle-shaped cells that were highly invasive, indicative of EMT. Again, the order of the cause and effect in this situation is in question as CIN induced by D1K2 can certainly cause changes that could cause EMT, however it has been found that Rb depletion can result in an effect similar to EMT [180]. Overactive Cdk2 could have the same consequential effect as Rb depletion, leading to the observed morphological change.

Discussion

Overactive Cdk2 has a number of effects on cells. In previous literature and in this study, it has been seen to phosphorylate Rb, causing a number of downstream effects. Cdk2 complexed with Cyclin D1 or E is also able to phosphorylate other substrates as well. Here we have shown that NPM, controlling the process of centrosome replication, is phosphorylated on T199 by Cyclin D1/Cdk2 and Cyclin E/Cdk2 complexes, but not by Cyclin D1/Cdk1, Cyclin D1/Cdk4, or Cyclin E/Cdk4 complexes. Similarly, these results were recapitulated using fusion proteins allowing the Cyclin/Cdk complexes to be more precisely controlled. The D1K2 and EK2 fusion proteins were capable of phosphorylating NPM, but the D1K4 and D1K2(KD) proteins were not.

When these complexes were analyzed for their ability to phosphorylate Cdh1, an activating subunit of the APC/C, comparable results were seen. It was shown that D1K2 is capable of phosphorylating Cdh1 and that all Cyclin/Cdk combinations and fusion proteins bind Cdh1 with the exception of Cyclin D1/Cdk4 in cells. The ability of D1K2 to phosphorylate NPM and Cdh1 was also confirmed through an in vitro kinase assay.

Phosphorylation of substrates leads to a variety of downstream effects in cells expressing D1K2. We observed a D1K2 tumor-derived cell line undergoing failed cytokinesis and it appears that D1K2 blocks the bundling of supernumerary centrosomes. MCF10A cells expressing D1K2 did not form multipolar spindles more frequently than control cells, but did have a higher incidence of multipolar anaphase. While the control cells were capable of bundling multipolar spindles in order to undergo bipolar division, the D1K2 expressing cells are not. The mechanism for this is currently unknown, although it is possibly due to the temporal shortening of mitosis due to Mad2 overexpression that has previously been seen [159]. In this case, D1K2 would not be directly interfering with the bundling machinery; it would simply not allow it enough time to occur. Cell attachment is also very important in the organization of spindle poles [125] and it is our experience that the MCF10A D1K2 CL1 cells are less adherent than the Hygro cell line, so this cannot currently be ruled out as a possible cause of the failed bundling as well.

Finally, D1K2 expression is capable of causing a morphology switch that shares characteristics with EMT. MCF10A expressing D1K2 had a more elongated shape with fewer cell-cell contacts than did cells without D1K2 or a kinase dead variant, and immunoblots showed a partial cadherin switch. It is unclear how these changes occur. It is possible that it is due to increased expression of E2F dependent genes, or it could be a manifestation of chromosomal instability.

Materials and Methods

Cell Culture

The 293T and D1K2-T2 cell lines were grown in DMEM + 10% FBS. MCF10A cell lines were maintained in the suggested [168] 50/50 mixture of Dulbecco's Modified

Eagle's Medium and Ham's F12 medium supplemented with 5% horse serum, 20 ng/mL EGF, 100 ng/mL cholera toxin, 10 μg/mL insulin, and 500 ng/mL hydrocortisone (Sigma-Aldrich, St. Louis, MO).

Transient Transfection, Transduction Using Recombinant Adenoviruses, and Stable Cell lines

Transient transfections were performed using 293T cells and Lipofectamine (Invitrogen, Carlsbad, CA) as described previously [170]. Recombinant adenoviruses encoding the kinase active and kinase dead Cyclin D1-Cdk2 fusion proteins (D1K2, D1K2(KD), and D1K2(KE)), Flag-Cyclin D1, Flag-Cyclin E, Cdk1-His_6, Cdk2-His_6, and Cdk4-His_6 have been described [53,181] and infection of cell cultures was performed as described previously [53].

Expression Vectors and the Construction of Genes Encoding the Cyclin D1-Cdk4 (D1K4) and Cyclin E-Cdk2 (EK2) Fusion Proteins

Expression vectors encoding Myc-tagged Cdh1 (Addgene plasmid 11595) and Green Fluorescent Protein-Flag-tagged Nucleophosmin (Addgene plasmid 17578) were described previously [182,183] and purchased from Addgene Inc., Cambridge, MA. Construction of vectors encoding Cyclin D1-Cdk4 and Cyclin E-Cdk2 fusion proteins were based on the Cyclin D1-Cdk2 (D1K2) fusion protein described previously [53]. The Cyclin E cDNA described previously [181] was used to replace the Cyclin D1 encoding region of D1K2 produce the Cyclin E-Cdk2 (EK2) fusion protein. Likewise, the Cdk4 cDNA described previously [181] was used to replace the Cdk2 coding region of D1K2 to produce the Cyclin D1-Cdk4 (D1K4) fusion protein. The cDNA sequences encoding the EK2 and D1K4 proteins were submitted to Bio Basic Inc. (Markham,

Ontario, Canada) who synthesized the cDNAs, subcloned them into the EcoR1 and XbaI sites of pcDNA3, and sequence verified the resulting constructs.

Affinity Purification and Analysis of Cyclin/Cdk-Containing Complexes, and Immunoprecipitation

Purification of D1K2 and D1K2(KD) was performed as described [53] by sequential chromatography using Talon resin (BD Biosciences Clontech, Palo Alto, CA) with elution by imidazole followed by anti-FLAG-agarose resin (Sigma-Aldrich) with elution by FLAG peptide (Sigma-Aldrich). Immunoprecipitations were performed using 4 µg/tube of the Myc-tag antibody 9E10 (Santa Cruz Biotechnology, Inc.) and the immunoprecipitates were collected using Protein G-sepharose (Invitrogen), and the immunoprecipitates were washed and analyzed by immunoblot.

Immunoblot Analysis

Immunoblotting was performed as described [170], employing antibodies to NPM, phospho-NPM[T199], Cyclin B1, and phospho-Cdk1[T161] (Cell Signaling Technology, Inc., Danvers, MA). All other antibodies used were purchased from commercial sources and listed previously [53,54,170,184,185].

Immunofluorescence Microscopy

Cells for immunofluorescence studies were plated onto glass coverslips in 6-well plates. After treatment, the cells were fixed with a solution containing 90% methanol and 10% MES buffer (100mM MES, pH 6.9, 1mM EGTA and 1mM MgCl2). The coverslips were subsequently incubated with antibody buffer (5% Goat Serum in phosphate-buffered saline (PBS)) in a humidified chamber for 1 hour. Primary antibody staining was performed using an antibody for γ-Tubulin (sc-17787; Santa Cruz

Biotechnology, Inc., Santa Cruz, CA), pericentrin (ab4448), or INCENP (ab23956; Abcam plc, Cambridge, MA), at a 1:200 dilution in antibody buffer for 2 hours. Following primary antibody incubation, the coverslips were washed three times with PBS, and incubated with a goat anti-Mouse Cy3 secondary antibody (81-6515; Zymed, Carlsbad, CA) and/or goat anti-rabbit 488 antibody (A11008; Invitrogen) for 1 hour at a 1:200 dilution in antibody buffer. Following three additional washes with PBS, coverslips were dried and mounted onto slides with Vectashield + 4', 6-diamidino-2-phenylindole (DAPI; H-1200; Vector Laboratories, Burlingame, CA) to visualize nuclei. Images were captured using an upright microscope (Axioplan2; Zeiss, Thornwood, NY), and processed using Openlab 5.5 Improvision software.

In Vitro Kinase Assays

Kinase assays were performed as described [170]. GST-Rb was purchased from Santa Cruz Biotechnology, Inc. GST-NPM and GST-Cdh1 were purchased from Abnova (Taipei, Taiwan). Two micrograms each of GST, GST-Rb, GST-NPM, and 1 microgram of GST-Cdh1 were present in each reaction. The amount of each kinase assay subjected to autoradiography represents 38% of the total reaction volume. The amount of each kinase assay analyzed by immunoblot was 10% of each reaction.

Video Microscopy

D1K2-T2 cells were plated in a FluoroDish (World Precision Instruments, Sarasota, FL) and imaged for 48 hours on a Leica TCS SP5 confocal microscope while grown in a climate controlled environment.

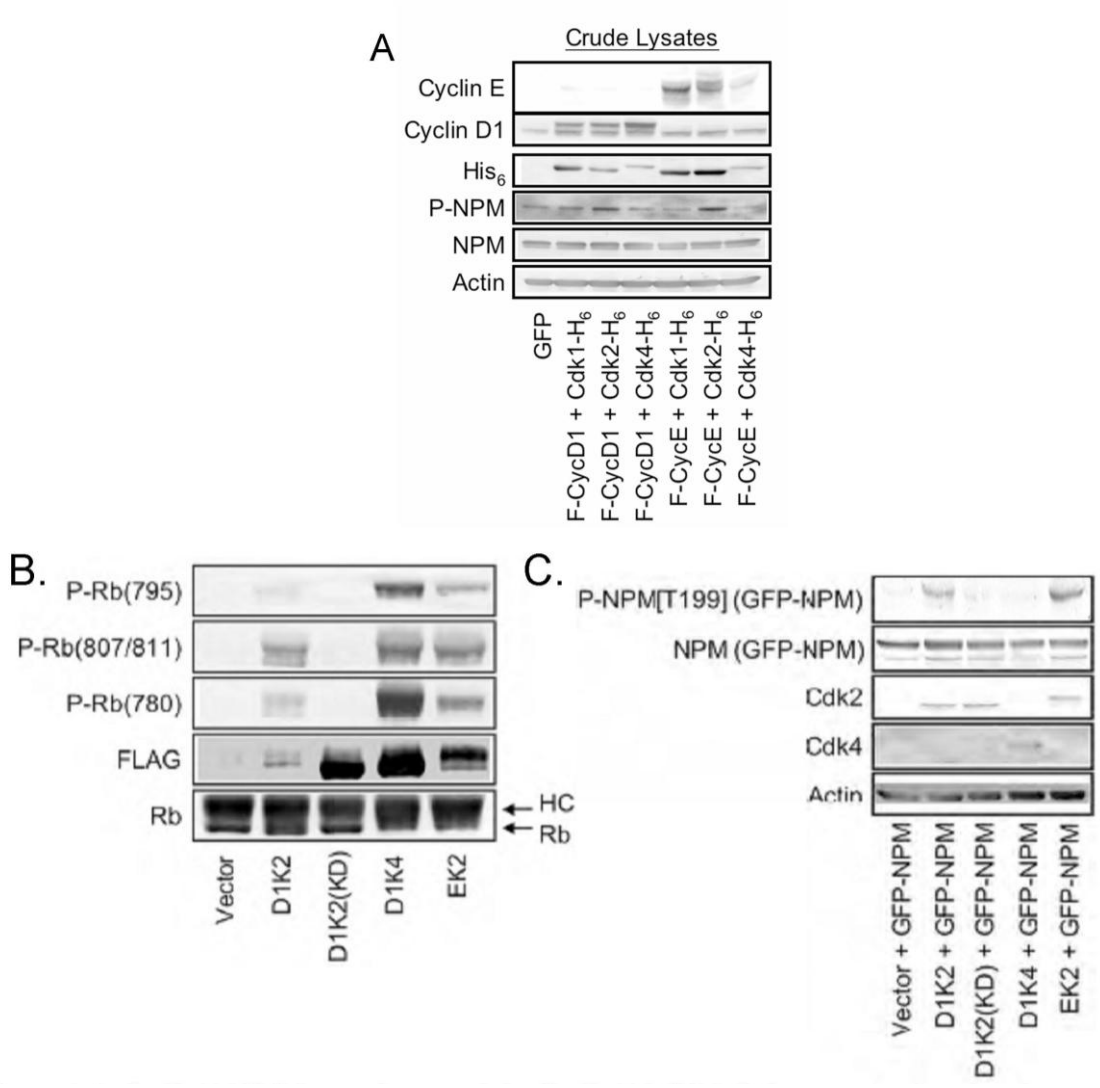

Figure 3-1. Cyclin D1/Cdk2 complexes and the Cyclin D1-Cdk2 fusion protein phosphorylate Nucleophosmin. A) Immunoblot analysis of crude lysates (left panel) and affinity purified Cyclin/Cdk complexes (right panel) from NMuMG cells transiently transfected with constructs coding for the indicated proteins. B) Immunoblot analysis of an in vitro kinase assay using Cyclin/Cdk fusion proteins purified from 293T cells transiently transfected with vectors encoding the indicated proteins. HC represents the heavy chain of the antibody used in the immunoprecipitation. The band labeled Rb below is the Rb substrate present in the kinase assays. C) Immunoblot analysis of cell lysates obtained from 293T cells transiently transfected with constructs coding for the indicated proteins. "(GFP-NPM)" indicates that the bands shown represent the exogenously expressed GFP-Nucleophosmin rather than endogenous Nucleophosmin.

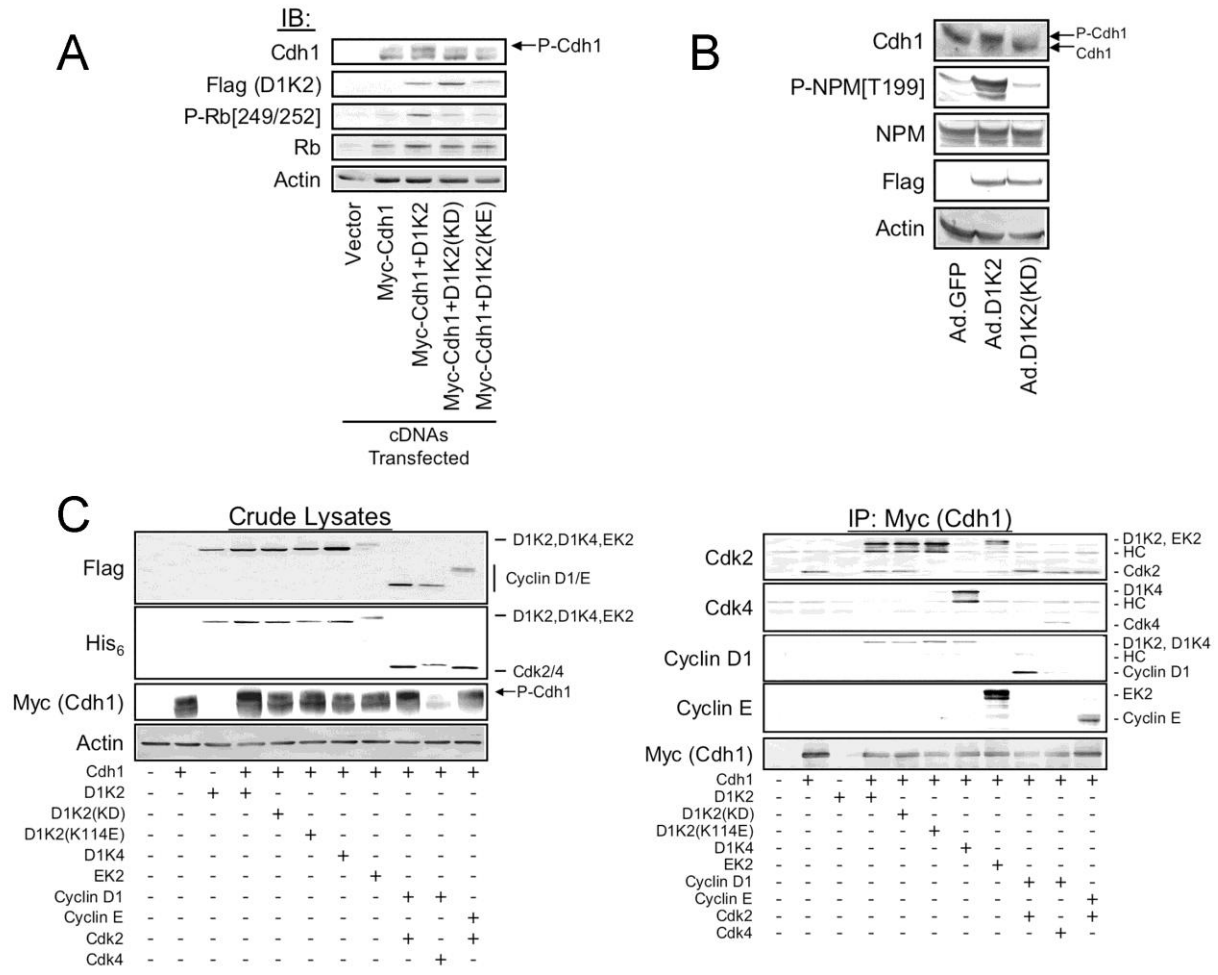

Figure 3-2. Cyclin D1/Cdk2 complexes and the Cyclin D1-Cdk2 fusion protein physically interact with and phosphorylate Cdh1. A) Immunoblot analysis of cell lysates obtained from 293T cells transiently transfected with vectors encoding the indicated proteins. D1K2(KE) is a second kinase-dead form of D1K2. B) Immunoblot analysis of cell lysates from NMuMG cells infected with adenoviruses encoding the indicated proteins. Flag staining denotes the presence of the D1K2 and D1K2(KD) proteins. C) Immunoblot analysis of crude lysates (left panel) and affinity purified Cdh1 complexes (right panel) obtained from 293T cells transiently transfected with constructs for the indicated proteins. The identities of the bands are indicated to the right of some panels. D) Autoradiogram (left panel) and immunoblot analysis (right panel) of kinase assays using D1K2 and D1K2(KD) isolated from NMuMG cells infected with adenovirus and GST-NPM, GST-Cdh1, GST-Rb as substrates, or GST alone as a control to show the relative levels of the GST-fusion proteins substrates, the relative levels of the D1K2 and D1K2(KD) fusion proteins, and to examine the sites of Nucleophosmin and Rb phosphorylation using phospho-specific antibodies.

D

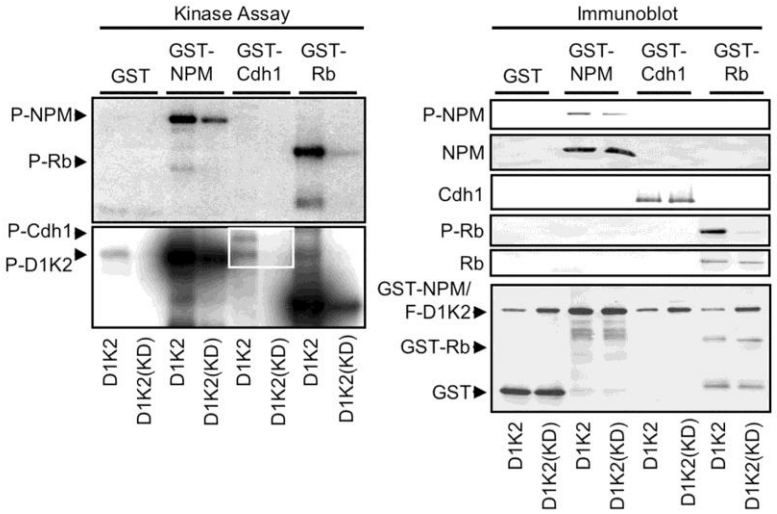

Corsino et al., Fig. 6

Figure 3-2. Continued

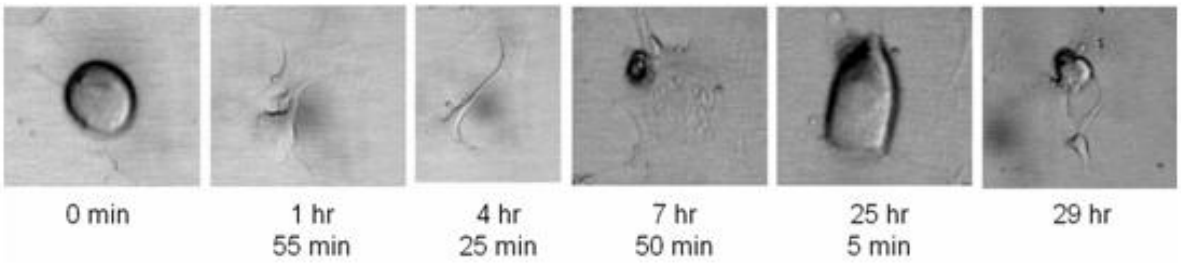

Figure 3-3. D1K2 tumor-derived cell lines exhibit failed cytokinesis. Time lapse images of a D1K2-T2 cell failing cytokinesis and then re-entering mitosis. Cells were incubated with 2.5 mM thymidine for 24 hours prior to release and recorded by microscopy in a temperature, humidity, and CO_2 controlled environment.

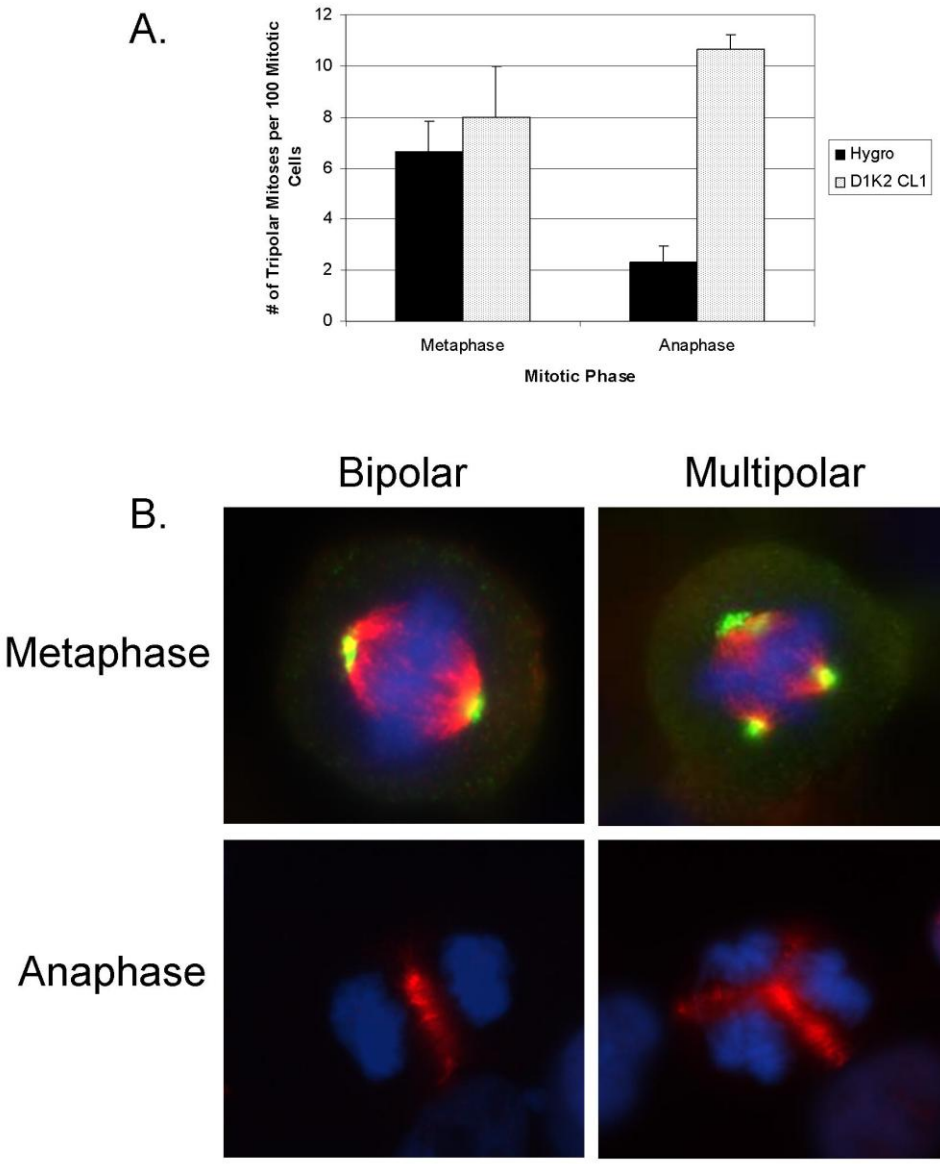

Figure 3-4. D1K2 blocks the bundling of supernumerary centrosomes. A) Quantification of the rate of multipolar metaphase and anaphase in the indicated cell lines. Mitotic figures were scored visually using immunofluorescence of γ-tubulin and INCENP along with DNA staining by DAPI. Values represent the mean and error bars represent the s.d. of three replicate slides. B) Immunofluoresence images of MCF10A D1K2 CL1 cells exhibiting bipolar and multipolar metaphase and anaphase. Blue staining is DAPI, green is pericentrin, and red is γ-tubulin (upper panels) or INCENP (lower panels).

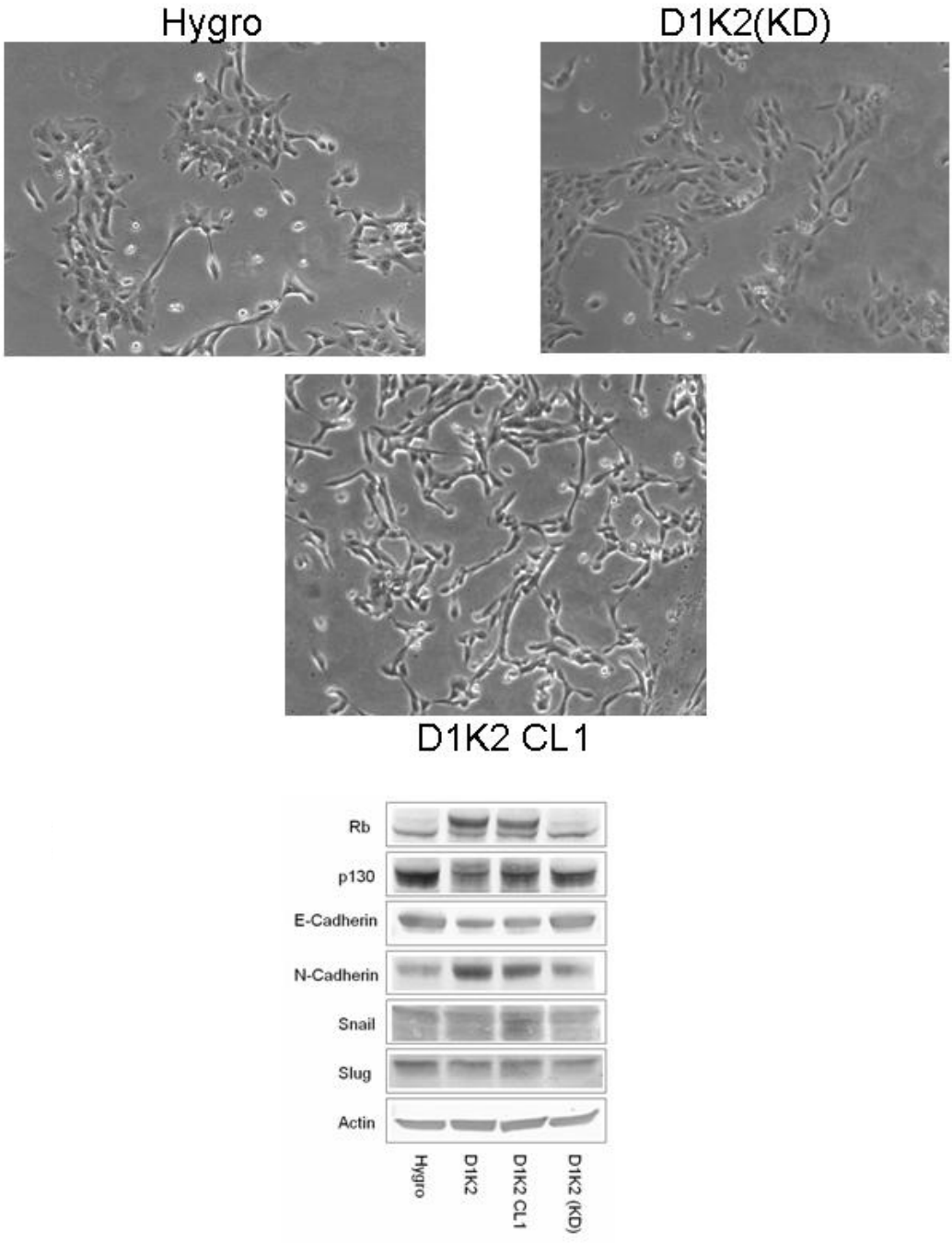

Figure 3-5. D1K2 leads to an epithelial to mesenchymal transition. A) Micrographs of the indicated MCF10A cell lines examining cellular morphology. B) Immunoblot analysis of the indicated cell lines for EMT markers. Actin serves as a loading control.

CHAPTER 4
PSF IS A NOVEL SUBSTRATE OF CDK2

Introduction

The D1K2 fusion protein is not only useful for identifying the roles of overactive Cdk2 in tumor formation, progression, and characteristics, but is also a tool capable of helping to identify novel Cdk substrates. There are likely numerous Cdk substrates that are not yet known and their identification will greatly improve our knowledge of cell biology. In this study we show that polypyrimidine tract binding protein-associated splicing factor (PSF), also known as splicing factor-proline/glutamine rich (SFPQ), is a novel substrate for Cyclin E/Cdk2 and Cyclin D1/Cdk2 complexes. PSF is a multifunctional protein that is usually found in a complex with the PSF homolog, $p54^{nrb}$ (reviewed in [186]).

A 100 kD protein, PSF contains a RNA binding RGG domain, a large proline and glutamine rich segment, two RNA recognition motifs, and a DNA binding domain. It binds to polypyrimidine tracts in pre-mRNA and is indispensable for splicing [187,188], serving as a member of the spliceosome [189] along with p68, also known as DDX5 [190]. PSF also functions in regulation of transcription, binding to the thyroid hormone and retinoid x receptor control elements to control transcriptional activation [191] as well as termination of transcription and the 3' processing of subsequent RNAs [192]. Additionally, the PSF/$p54^{nrb}$ complex has been shown to be involved in the DNA double strand break repair mechanism [193], migrating to sites of DNA damage [194].

Normally located in sub-nuclear speckles, the localization of PSF is controlled by multiple mechanisms. Phosphorylation of c-terminal tyrosines by the Breast Tumor Kinase (BRK) induces a cytoplasmic relocalization that is thought to lead to cell cycle

arrest [195]. Likewise, phosphorylation of serines and threonines by an unknown kinase during apoptosis results in cytoplasmic localization and changes in protein interactions [196]. Changes in splicing regulation can also result from phosphorylation, with glycogen synthase kinase 3 phosphorylating threonine residues that cause alternate splicing of CD45 mRNA in T-cells [197].

Here we show that both Cyclin E/Cdk2 and Cyclin D1/Cdk2 complexes are capable of phosphorylating PSF. The consequences of this phosphorylation are not yet known, however identifying these effects is of great interest. D1K2 expressing cells show a dramatic increase in phosphorylation indicating that it may play a role in the tumorigenesis caused by overactive Cdk2.

Results

Identification of PSF as a Substrate of Cdk2

In an effort to identify the cellular substrates of D1K2, we utilized the previously described MCF10A cell lines expressing D1K2 or D1K2(KD). Immunoprecipitation followed by immunoblot using an antibody that recognizes phosphorylated threonines followed by a proline, potential Cdk2 phosphorylation sites, identified proteins in cell lysates that were preferentially phosphorylated in the cells expressing the kinase active D1K2 (Figure 4-2A left panel). A protein running slightly below the 120 kD marker (denoted by an arrow) was identified by mass spectroscopy as PSF. Further immunoblot analysis confirmed the differential levels of the protein in the samples (Figure 4-2A right panel).

To confirm phosphorylation due to Cdk2, we overexpressed PSF in addition to its binding partners $p54^{nrb}$ and DDX5, along with different combinations of Cyclins and Cdks via transient transfection in the 293T cell line. The coexpression of Cyclin E or

Cyclin D1 and Cdk2 induced the appearance of a second, lower mobility band in SDS-PAGE (Figure 4-2B). This was not seen with a kinase dead mutant of Cdk2. This mobility shift has been used as an indicator of phosphorylation in the past [196] and confirms that Cdk2 can induce phosphorylation of PSF. These results were duplicated in Figure 4-2C, with Cyclin E/Cdk2, Cyclin D1/Cdk2, and D1K2 all inducing a mobility shift. Additionally, this shift is inhibited by co-expression of p21. In all three cases, p21 expression eliminated this shift, presumably by blocking phosphorylation through inhibition of Cdk2 activity.

Previous biochemical analyses have identified three serines or threonines followed by a proline in PSF that are phosphorylated by unknown kinases: S33, S379, and T687 [198]. Mutation of any of these potential Cdk2 phosphorylation sites to alanine results in a notable decrease in the upper, phosphorylated band, but not a total elimination of it (Figure 4-2D). This is complicated by the fact that the endogenous, wild type protein is still present. What is clear is that each site is likely phosphorylated, perhaps leading to other phosphorylation events by Cdks or other kinases.

In order to obviate this problem, we obtained a FLAG-tagged PSF construct, allowing the analysis of only the exogenous PSF. Again, Cyclin E/Cdk2 or D1K2 induced a mobility shift and an analogous construct with all twelve serines and threonines followed by a proline mutated to alanines failed to show a mobility shift regardless of kinase expression (Figure 4-3A). The fact that this mutant, lacking any potential Cdk2 phosphorylation sites, is not phosphorylated is further evidence that PSF is directly phosphorylated by Cdk2. Reverse mutations of A33S, A379S, and A687T, restoring potential phosphorylation sites, failed to restore the shift (Figure 4-3B). These

data with the previous mutation data suggest that these sites are required, but not sufficient, for the observed mobility shift.

Cdk2 Directly Phosphorylates PSF In Vitro

An in vitro kinase assay utilizing bacterially expressed His_6-PSF protein isolated on Talon resin showed that commercial purified Cyclin E/Cdk2, but not Cyclin B/Cdk1 or Cyclin D1/Cdk4 is capable of phosphorylating PSF (Figure 4-4A). D1K2 protein isolated from the previously described D1K2-T2 CL6 cell line [54] was also shown to be capable of phosphorylating PSF (Figure 4-4B, left panel). Cyclin E/Cdk2 showed a much higher level of phosphorylation, even after normalizing based on amount of kinase present, as measured by immunoblot (Figure 4-4B, right panel).

Discussion

While PSF has previously been found to be phosphorylated by BRK, GSK3, and unknown serine/threonine kinases [198], resulting in changes in intracellular localization and splicing activity, it was not known to be a substrate of Cdk2. We have identified PSF as being highly phosphorylated in MCF10A cells expressing the D1K2 fusion protein and have confirmed the protein as a Cdk2 substrate through coexpression experiments utilizing constructs coding for various Cyclins, Cdks, and Cyclin/Cdk fusion proteins. This phosphorylation was also seen to be inhibited by overexpression of p21.

Three potential Cdk2 phosphorylation sites, a serine or threonine followed by a proline, have previously been shown to be phosphorylated by an unknown kinase [198]. Phosphorylation, indicated by a mobility shift in SDS-PAGE, was blocked by the individual mutation of these sites: S33A, S379A, or T687A. In all, PSF contains twelve potential phosphorylation sites, and a construct in which all twelve sites have been mutated to alanine does not show any phosphorylation. Reverse mutation to restore

the phosphorylation sites at residues 33, 379, and 687 failed to restore phosphorylation. Through in vitro kinase assays, both Cyclin E/Cdk2 complexes and the D1K2 fusion protein were shown to directly phosphorylate PSF.

It is not currently known what affect phosphorylation of PSF by Cdk2 has on its function. Our experiments have not shown a change in intracellular localization or complex formation. It is possible that phosphorylation may modulate the RNA splicing or DNA repair functions of PSF and it will be interesting explore in future experiments.

Materials and Methods

Immunoprecipitations

For p-TP immunoprecipitations, cell lysates, in a 1% Triton X-100 buffer, were incubated with a p-TP antibody (9391 Cell Signaling Technology, Inc., Danvers, MA) at 4 ºC overnight. Protein G sepharose was added and allowed to mix at 4 ºC for 2 hours. Beads were washed 3x with 0.1% Triton X-100 buffer and boiled in SDS-PAGE sample buffer. For FLAG immunoprecipitations, cell lysates from D1K2-T2 CL6 were obtained as above and mixed with anti-FLAG agarose (Sigma-Aldrich) for 4 hours at 4 ºC. Beads were washed 3x with 0.1% Triton X-100 buffer and eluted using 200 µg/mL FLAG peptide.

Immunoblots

Immunoblotting was performed as described [170] using antibodies to p-TP (9391 Cell Signaling Technology, Inc.), FLAG (F-3165; Sigma-Aldrich), Actin, PSF, p21 (sc-1616-R, sc-101137, sc-6246; Santa Cruz Biotechnology, Inc., Santa Cruz, CA). His_5 (34660; Qiagen, Valencia, CA).

Transient Transfection

The 293T cell line was transfected using lipofectamine reagent (Invitrogen, Grand Island, NY). Fresh medium was added after incubating overnight and the cells were incubated a further 24 hours before being analyzed.

Expression Constructs

Plasmids encoding WT-PSF, $p54^{nrb}$, and DDX5 were obtained from OriGene Technologies, Inc. (Rockville, MD). The His-PSF construct was a gift from Dr. Stefan Stamm (University of Kentucky, Chandler Medical Center). Nucleotide sequence-optimized constructs for FLAG-PSF and FLAG-PSF(12M) were synthesized de novo and subcloned into the pcDNA3 vector by Bio Basic Canada, Inc. (Markham, ON, Canada). Amino acid mutations were made using the following primers for QuickChange PCR:

S33A Forward 5'-GGCCTCCACGACTTCCGTGCTCCGCCGCCCGGCATGGGC-3'
Reverse 5'-GCCCATGCCGGGCGGCGGAGCACGGAAGTCGTGGAGGCC-3';
S379A Forward 5'-CTTTCTGTTCGTAATCTTGCACCTTATGTTTCCAATGAAC-3',
Reverse 5'-GTTCATTGGAAACATAAGGTGCAAGATTACGAACAGAAAG-3';
T687A Forward 5'-GGAATGGGGCCTGGAGCTCCAGCAGGATATGGTAG-3',
Reverse 5'-CTACCATATCCTGCTGGAGCTCCAGGCCCCATTCC-3' (Sigma Aldrich);
A33S Forward 5'-CATCCCGGGTGGAGGAGACCTAAAGTCATGCAG-3',
Reverse 5'-CTGCATGACTTTAGGTCTCCTCCACCCGGGATG-3';
A379S Forward 5'-GCGTGAGAAATTTGTCGCCCTATGTCTCCAATG-3',
Reverse 5'-CATTGGAGACATAGGGCGACAAATTTCTCACGC-3';
A687T Forward 5'-CCATAACCTGCGGGAGTCCCGGGGCCCATACC-3',
Reverse 5'-GGTATGGGCCCCGGGACTCCCGCAGGTTATGG-3' (Bio Basic Canada).

His-PSF Bacterial Protein Expression

BL21(DE3) *E. coli* were transformed with the pET21a His-PSF vector and cloned on ampicillin-agar plates. The bacteria were grown in LB + ampicillin overnight and then inoculated in LB + ampicillin to an OD_{600} 0.1 – 0.15 and incubated at 37 ºC with shaking until OD_{600} 0.4 – 0.5. Protein expression was induced with 0.4 mM IPTG for 3 hours at 37 ºC.

In Vitro Kinase Assays

Bacteria expressing His-PSF were lysed by sonication in TALON extraction buffer (10 mM MOPS pH 7, 10% glycerin, 100 mM KCl, 10nM microcystin, 5 mM $MgCl_2$, 1% Triton X-100, 1 mM Na_3VO_4, 33 mM $Na_4O_7P_2$), pulled down on TALON resin (Clontech Laboratories Inc., Mountain View, CA), and washed with TALON wash buffer (10 mM MOPS pH 7, 10% glycerin, 100 mM KCl, 10nM microcystin, 5 mM $MgCl_2$, 0.1% CHAPS, 50 mM imidazole). Beads were resuspended in kinase assay buffer (50 mM Hepes pH 7.5, 10 mM $MgCl_2$, 2.5 mM EGTA, 1 mM DTT, 0.1 mM NaF, 0.1 mM Na_3VO_4) and incubated at 37 ºC with Cyclin/Cdk complex, 0.08 µM ATP, and 3.875 µCi [γ-^{32}P]-ATP. Cyclin/Cdk complexes were 0.157 ng either of purchased Cyclin B/Cdk1, Cyclin E/Cdk2, or Cyclin D1/Cdk4 (Cell Signaling Technology, Inc.) or D1K2 purified from the D1K2-T2, CL6 cell line using anti-FLAG agarose. Samples were then mixed with SDS sample buffer and run on 12% polyacrylamide gels. Bands were imaged with autoradiography film and quantitated on a Beckman Coulter LS600SC scintillation counter (Beckman Coulter, Inc., Brea CA) by cutting out the bands.

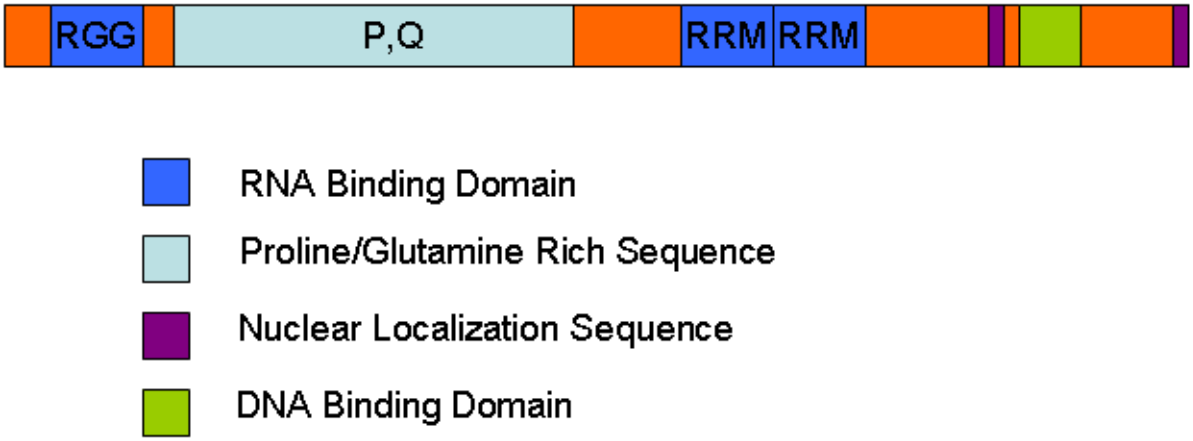

Figure 4-1. Protein structure of PSF. The amino acid sequence contains three RNA binding domains (blue), a DNA binding domain (green), two nuclear localization sequences (violet), and a long proline/glutamine rich segment (light blue).

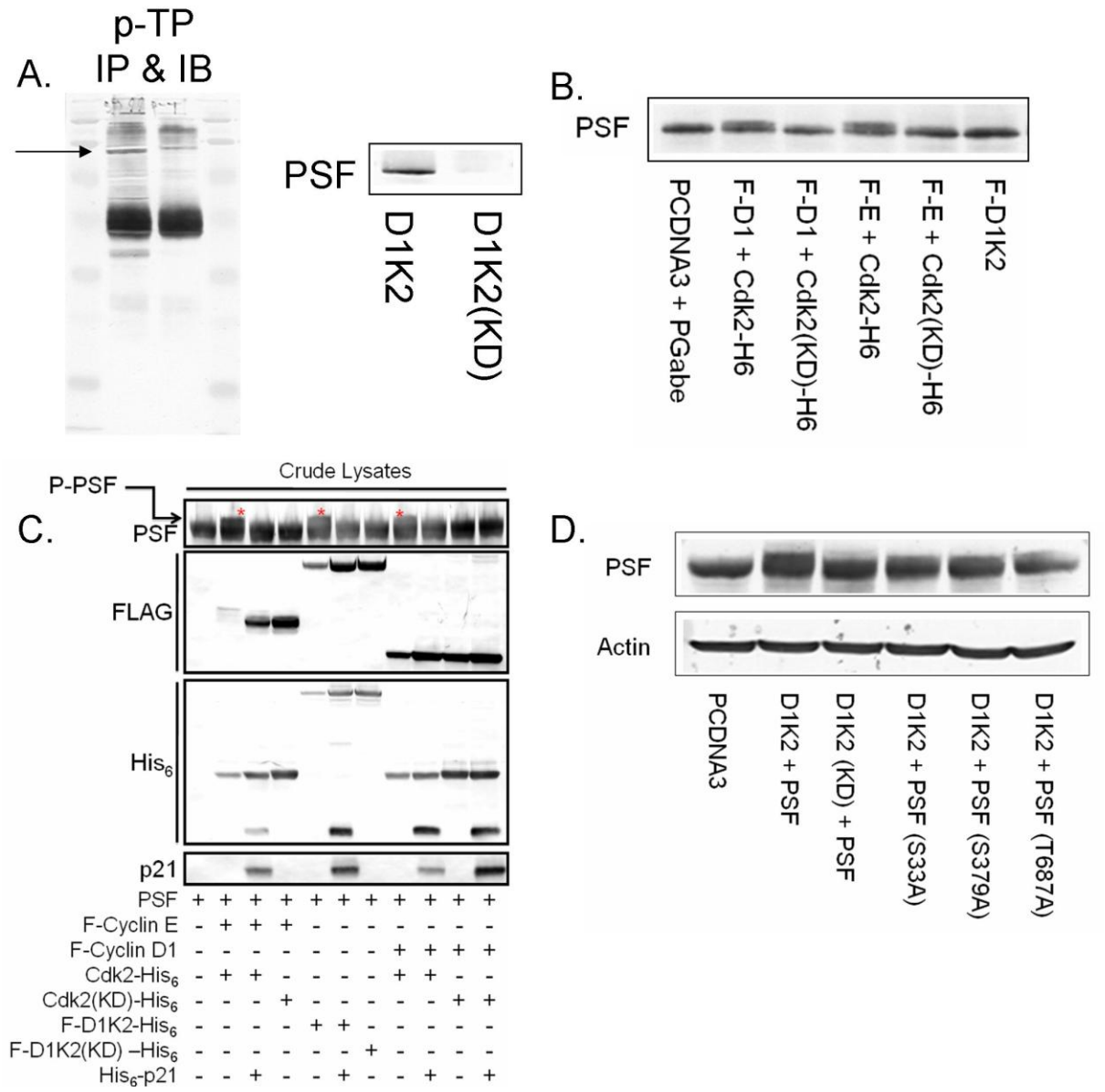

Figure 4-2. Cdk2 phosphorylates PSF. A) Immunoprecipitation of lysates from MCF10A expressing D1K2 or D1K2(KD) using a p-TP antibody and immunoblotted with p-TP (left) and PSF (right). B) Immunoblot analysis showing PSF mobility shift in 293T transiently transfected with PSF and various Cyclins/Cdks. C) Immunoblot analysis of 293T lysates looking at PSF mobility shift in the presence of different Cyclin/Cdk complexes +/- p21. D) Immunoblot analysis of 293T lysates expressing D1K2 and mutants of several potential phosphorylation sites to visualize the PSF mobility shift. Actin serves as a loading control.

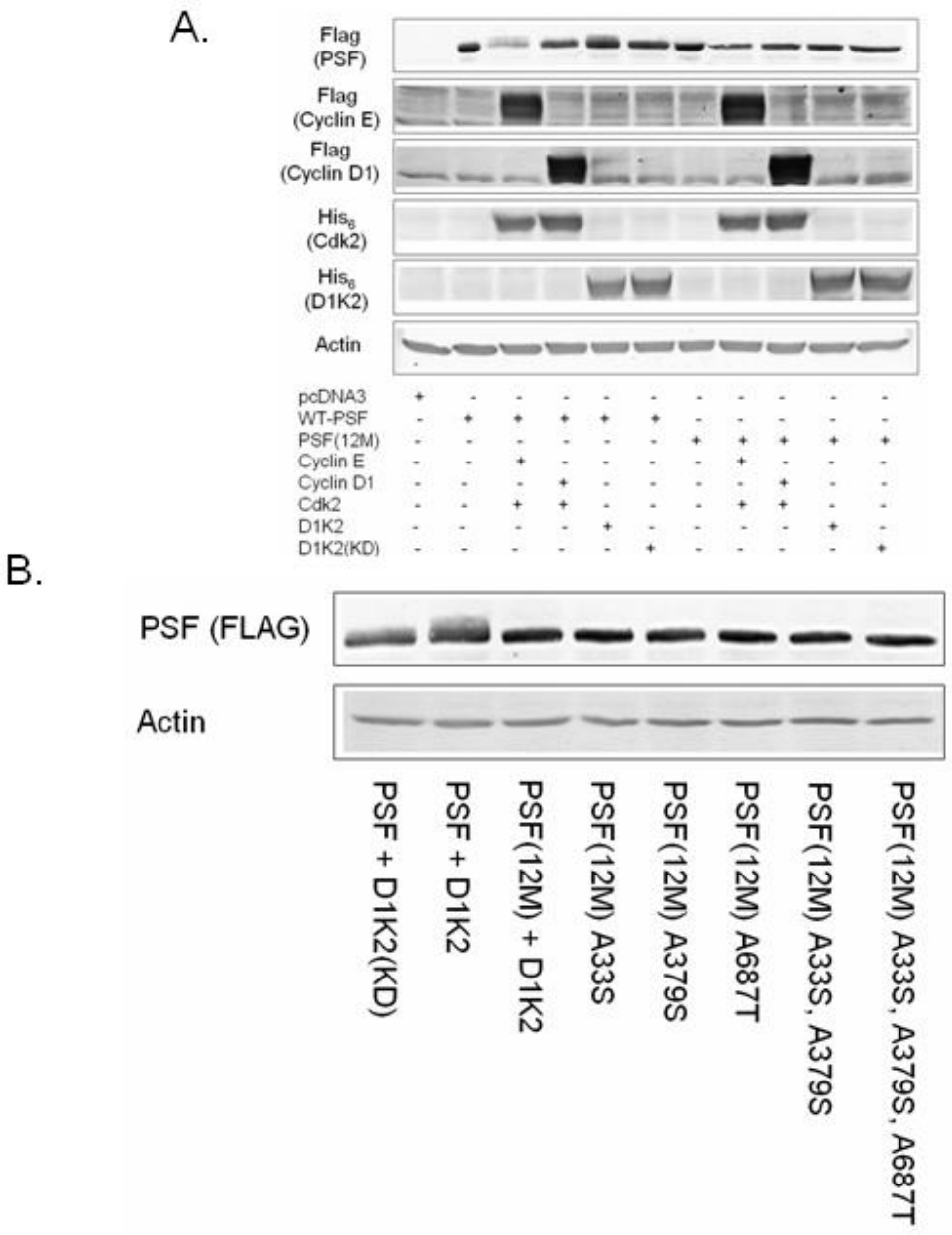

Figure 4-3. Analysis of a non-phosphorylatable PSF mutant. A) Immunoblot analysis of FLAG-PSF expressed with various Cyclin/Cdk complexes. B) Immunoblot analysis of FLAG-PSF containing varying mutations of potential phosphorylation sites expressed with D1K2.

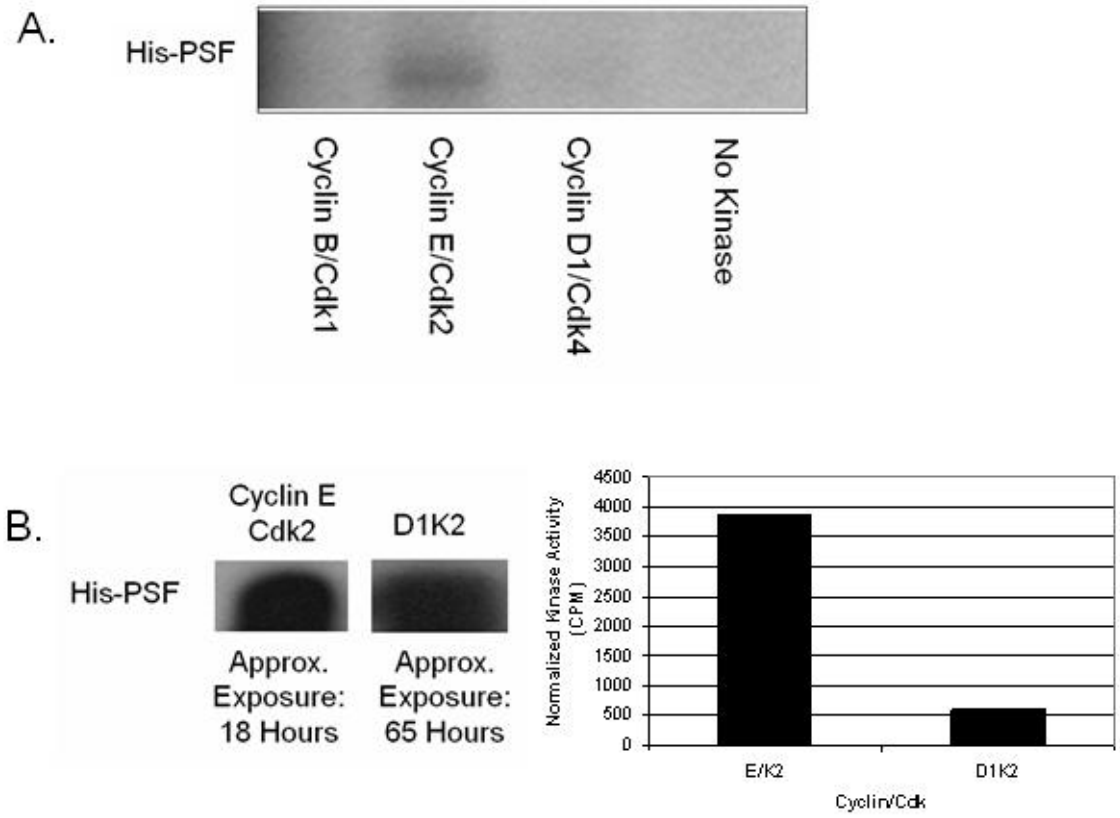

Figure 4-4. In vitro kinase assays of His-PSF and various Cyclin/Cdk complexes. A) Autoradiography of [γ-^{32}P]-phosphorylated His-PSF with differing Cyclin/Cdk complexes. B) Autoradiography of [γ-^{32}P]-phosphorylated His-PSF with either Cyclin E/Cdk2 or D1K2 (left panel) and quantitation of the same bands using a scintillation counter (right panel).

CHAPTER 5
AN IN VIVO MODEL OF EPITHELIAL TO MESENCHYMAL TRANSITION REVEALS A MITOGENIC SWITCH

Introduction

EMT is a pivotal switch in breast cancer progression. During this transition, breast cancer cells transform from an epithelial- to a more migratory, mesenchymal-like phenotype, which is associated with increased motility and invasiveness. Ultimately, these cells metastasize [199,200].

Injection of a MMTV-Her2/neu breast cancer cell line into syngeneic mice results in tumors that undergo EMT in vivo [201]. We employed a similar approach to generate pre- and post-EMT MMTV Her2/neu breast cancer cell lines to examine differences in gene expression in these cells. Here we show that in vivo EMT of MMTV-Her2/neu breast cancer cells is associated with marked changes in receptor tyrosine kinase expression and alterations in signaling through downstream mitogenic cascades. In addition to acquiring responsiveness to PDGF, the post-EMT cells also acquired enhanced responsiveness to hepatocyte growth factor (HGF) and lysophosphatidic acid (LPA), and exhibited constitutive tyrosine phosphorylation of the receptor tyrosine kinase Axl and the transcription factor STAT3. The post-EMT cells were less sensitive than the pre-EMT cells to MEK inhibitor U0126, but more sensitive to the growth inhibitory effects of PDGF, HGF, and LPA receptor inhibitors/antagonists.

Human breast cancer cell lines showed analogous changes in mitogenic protein expression correlating with their EMT status. Inducing a mesenchymal appearance in a normal epithelial cell line, MCF10A, by growth in medium supplemented with 10% fetal bovine serum rather than with the traditional supplements of 5% horse serum, EGF, hydrocortisone, insulin, and cholera toxin [168] caused changes in expression of EMT

markers and mitogenic signaling proteins including PDGFRβ and Axl (further explored in Appendix C). Likewise, treatment of MCF10A cells with TGF-β, which induces a mesenchymal appearance along with an increase in invasiveness dependent on an upregulation of EGFR [202], also caused changes in the expression of EMT markers and mitogenic signaling proteins including PDGFRβ and Axl.

Results

In Vivo EMT as a Function of Tumor Volume

We previously described a cell line derived from a transgenic mouse MMTV-Her2/*neu* tumor, hereafter referred to as neuT [54,179]. NeuT cells are capable of forming tumors with sharp boundaries defined by a capsule and exhibit high levels of E-Cadherin that form functional adherens junctions. In subsequent studies it was observed that when the tumors reach approximately 1 cm in diameter the morphology of the cancer cells changes from a cuboidal shape with little cytoplasm to one in which the cells were elongated and have abundant cytoplasm. Coincident with this change in morphology, the tumors lost their defined border and incorporated inclusions of adipocytes and muscle as they invaded into surrounding tissues (Figure 5-1A). These alterations were consistent with EMT. Cell lines were isolated from large tumors that had undergone this transition and were subjected to microarray analysis to compare their expression profiles to that of the parental neuT cell line. The observed patterns in mRNA expression were consistent with EMT, and expression of several of the corresponding proteins changed in a manner in agreement with the microarray analysis (Figure 5-1B). In contrast to the neuT cells, the clonal post-EMT cell lines expressed the mesenchymal markers N-Cadherin, Zeb1, and SPARC [203-206], and exhibited decreased expression of the epithelial markers E-Cadherin and Occludin. PCR analysis

showed that the post-EMT cells harbored the rat Her2/*neu* transgene, confirming that they were derived from the original neuT cell line (Figure 5-7).

The cells grown in culture maintained a morphology that was consistent with that observed in tumors in vivo. In contrast to the pre-EMT cells, the post-EMT cells did not readily form colonies in culture (Figure 5-1C) and the post-EMT cells exhibited an enhanced ability to invade through Matrigel-impregnated membranes (Figure 5-1D). The invasive properties of the post-EMT cells were apparent when grown as tumors in vivo by the lack of a capsule and defined border, and extensive invasion through the adjacent mammary fat pad (Figure 5-1E). This occurred at a small tumor size (6 mm) at which tumors derived from the pre-EMT neuT cells have not yet undergone EMT and acquired this ability.

Altered Expression of Mitogen Receptors and Mitogen Responsiveness Occurs During EMT

An interesting finding from the microarray analysis was that several of the genes whose expression was altered during EMT in vivo are those encoding receptor tyrosine kinases (RTKs) and other signaling molecules. We pursued this observation further because such changes will likely have important effects on tumor responsiveness to therapeutic agents that target these signaling intermediates. Immunoblot analyses indicated that Her2 and IRS-1 expression were decreased following EMT, and EMT was associated with increased expression of the RTKs Axl, PDGFR, and c-Met (Figure 5-2A). This is consistent with previous observations associating these receptors with EMT [207-210]. We also observed an increased level of c-Met phosphorylation on $Tyr^{1234/1235}$ and constitutive activating phosphorylation of the transcription factor STAT3 on Tyr^{705}, while PDGFR phosphorylation could not be detected (data not shown).

Experiments were performed to determine the functional consequences of these EMT-associated changes in expression. The microarray data also revealed increased mRNA levels of the lysophosphatidic acid receptor LPAR1 in the post-EMT cells. Increasing concentrations of the mitogen LPA dose-dependently increased the proliferation of the post-EMT cells, but had a limited effect on the pre-EMT cells (Figure 5-2B). The mitogenic effects of LPA, and to a lesser extent serum, were inhibited by the LPAR1 and 3 antagonist Ki-16425 (Figure 5-2C). Similarly, HGF and PDGF stimulated the proliferation of the post-EMT cells to a significantly greater extent than that of the pre-EMT cells (Figure 5-3A,C). These effects were blocked by SU11274 and Gleevec, inhibitors of the tyrosine kinase activity of c-Met and PDGFR, respectively (Figure 5-3B,D).

To examine the role of basal signaling in the absence of exogenous ligand, thymidine incorporation experiments were carried out in which pre- and post-EMT neuT cells grown in 1x ITS were treated with Ki-16425, SU11274, or Gleevec (Figure 5-8). Inhibition of LPAR or c-Met resulted in an appreciable decrease, 60-80%, in proliferation in both cell lines, indicating that a basal level of activity may exist in these pathways. Inhibition of PDGFR caused a more modest, 30% decrease in proliferation. This is in agreement with the lack of PDGFR phosphorylation observed in the absence of exogenous PDGF. The observed cellular inhibition could be due to off-target effects of the tyrosine kinase inhibitor.

EMT is Associated with Changes in Cellular Signaling Cascades and Sensitivity to Targeted Therapeutic Agents

The marked changes in growth factor receptor expression during EMT suggests that EMT also is associated with alterations in downstream signaling cascades and cancer cell responsiveness to therapeutic agents that target these pathways. The post-EMT cell lines exhibited diminished levels of steady-state Akt and Erk phosphorylation on activating sites (Figure 5-4A). The decreased Erk and Raf phosphorylation suggested that pre- and post-EMT cells might have differential sensitivity to a MEK inhibitor. Figure 4B shows that the pre-EMT cells are significantly more sensitive to MEK inhibitor U0126 than the post-EMT cells, suggesting that the pre-EMT cells are more dependent on signaling through the Ras/Erk pathway for their proliferation.

Further, immunoblot analysis was carried out on pre- and post-EMT cells treated with the PI3K inhibitor, LY294002, or U0126 in the absence of exogenous ligand or with PDGF, HGF, or LPA in order to examine the effects of these treatments on downstream signaling events. U0126 treatment almost completely abrogated basal and growth factor-induced Erk phosphorylation in both the neuT and $neuT_{EMT, CL2}$ cell lines (Figure 5-4C). These data are in agreement with Figure 4A and 4B and suggest that the increased sensitivity of the pre-EMT cell line to U0126 may be due to its increased basal activation of the Erk pathway. LY294002 blocked AKT phosphorylation caused by PDGF or HGF, demonstrating the role of the PI3K signaling cascade. Figure 5-4C also illustrates that while there is a lack of basal PDGFR phosphorylation in both pre- and post-EMT cell lines, only the cells that have undergone EMT and display increased PDGFR expression are able to activate PDGFR signaling, marked by receptor phosphorylation, in the presence of exogenous PDGF.

Basal-Like Human Breast Cancer Cell Lines Upregulate C-Met, PDGFR, and Axl

EMT is related to the basal-like subtype in human breast cancers [206]. The basal-like subtype in turn overlaps with the triple-negative category of breast tumors that lack Estrogen Receptors, Progesterone Receptors, and Her2 [211-213]. Therefore we examined whether any of the molecular alterations associated with EMT in the neuT mouse model were also present across a panel of human breast cancer cell lines of known subtype based on microarray analysis [214]. An inverse correlation was observed between E-Cadherin levels and the expression of Axl, the Axl ligand GAS-6, and c-Met (Figure 5-5A). However expression of Axl, GAS-6, and c-Met partially overlapped with that of the mesenchymal markers Vimentin, Zeb1, and SPARC. In contrast to the neuT EMT model, there was a reciprocal expression of c-Met and PDGFR in the MDA-MB 157 post-EMT cell line (Figure 5-5A, right half of breast panel). MDA-MB-231, a post-EMT cell line, expressed high levels of GAS-6 and exhibited strong Axl phosphorylation.

We previously showed that E-cadherin function is dysregulated in MDA-MB-231 cells [215] and hypothesized that blocking Axl signaling might restore E-cadherin function, given the role of Axl in inducing EMT and increasing invasion [207]. Stable Axl knockdown did not alter E-cadherin localization or function (data not shown). Interestingly, GAS-6 knockdown blocked Axl phosphorylation, demonstrating that MDA-MB-231 cells have a GAS-6/Axl autocrine loop that may contribute to the aggressive behavior of these cells. Together, these observations in human breast cancer cell lines indicate that upregulation of Axl in the mouse breast cancer cells undergoing EMT is relevant to processes that occur during the progression of human breast cancer.

In Vitro Models of EMT show Analogous Mitogenic Changes

Similar changes in mitogenic signaling were observed in two models of EMT in MCF10A cells. MCF10A, normal human mammary epithelial cells, have a distinctly cuboidal, epithelial morphology when grown in their recommended medium: 50/50 DMEM/F12 supplemented with 5% horse serum, 20 ng/mL EGF, 100 ng/mL cholera toxin, 10 µg/mL insulin, and 500 ng/mL hydrocortisone (Figure 5-6A left panel). When MCF10A cells were grown in 50/50 DMEM/F12 + 10% fetal bovine serum (FBS), the cells assumed a mesenchymal morphology characterized by flattened cells and a lower tendency to form cell-cell contacts (Figure 5-6A right panel). Immunoblot analyses of cells maintained in both growth media (Figure 5-6 B) showed a clear change in the expression of EMT markers, including a switch from E-Cadherin to N-Cadherin and increased expression of Vimentin and Zeb1. Consistent with the models discussed previously, the cells also displayed increased expression of PDGFRβ and Axl and showed a higher level of Axl phosphorylation. The observed decrease in c-Met expression is likely due to the absence of added EGF in the 10% FBS medium, which has been shown to upregulate c-Met expression [216].

Similarly, addition of 2.5 ng/mL TGF-β to complete MCF10A medium induced the cells to undergo EMT, as evidenced by a morphological change (Figure 5-6C), increased Vimentin and Zeb1 expression, and a partial cadherin switch (Figure 5-6D). These cells also showed higher levels of PDGFRβ and Axl. The minor increase in c-Met expression mirrors the neuT tumor model.

Discussion

The investigation of EMT in cancer has primarily focused on this process as a means by which cancer cells acquire the ability to separate from the parent tumor mass,

invade locally, and metastasize to distant sites. EMT has been extensively studied in cell culture systems and is induced by diverse growth factors and cytokines including HGF, TGF-β, TNFα, IL6, and PDGF and combinations thereof [15,217-222]. Each of these factors stimulate different subsets of signaling pathways, making it difficult to dissociate the effects of these factors themselves from changes associated with EMT. Previous work has shown that injection of MMTV-Her2/neu cancer cells into mice that are syngeneic, with the exception of the neu expression in the cancer cells, results in tumors that undergo EMT in vivo [201]. The present results obtained using an in vivo system may be more physiologically relevant than those obtained using in vitro systems because in this model EMT occurs in vivo in an orthotopic setting and in an immune-competent background.

We employed a similar approach to generate pre- and post-EMT MMTV-Her2/neu breast cancer cell lines to study changes in cell signaling that occur during EMT. Microarray analysis indicated that in addition to alterations in the expression of EMT-associated proteins, numerous changes in the expression of elements of mitogenic signaling cascades were also observed. Interestingly, several of the EMT-associated changes in the levels and phosphorylation state of signaling molecules have been implicated either as markers for EMT or as inducers of EMT, including Axl, PDGFR, c-Met, and STAT3 phosphorylation [207,208,222-224]. Importantly, many of these changes also correlate with the expression of EMT markers in human breast cancer cell lines (Figure 5-5).

PDGF and PDGFR are upregulated in several models of EMT. For instance, TGF-β and hyperactive Ras synergize to induce EMT in hepatocytes [222]. In this

model of hepatocellular EMT, the expression of PDGF-A ligand and both the α and β PDGF receptor subunits are highly elevated upon EMT, thus producing a PDGF autocrine loop. Similarly, TGF-β induces a PDGF autocrine loop in MMTV-Neu x MMTV-TGF-β double transgenic mice, and the Ras-transformed murine mammary epithelial cell line EpH4 (EpRas) undergoes TGF-β induced EMT with a concomitant establishment of a PDGF autocrine loop and hyperactivation of PI3K [210]. Our model differs in that the MMTV-Her2/neu cancer cells used for injection into mice were not engineered to overexpress TGF-β although it is possible that these cells [54], or the tumor microenvironment provided sufficient amounts of TGF-β to induce EMT.

Alterations in baseline signaling through mitogenic pathways that occur as a consequence of EMT likely influence how tumor cells respond to targeted anticancer therapeutic agents. Post-EMT neuT cells, for example, exhibited decreased basal Akt, Raf, and Erk phosphorylation, and in comparison to the pre-EMT cells, their proliferation was poorly inhibited by the MEK inhibitor U0126 (Figure 4A,B), which was able to eliminate the high basal level of pre-EMT Erk phosphorylation (Figure 4C). Our model further differed from those cited above since we did not observe hyperactivation of PI3K. It may therefore be important to analyze the PI3K and Erk status of a post-EMT cancer before utilizing treatments that target these signaling pathways.

Increased responsiveness to HGF and LPA was observed in the post-EMT neuT cell lines. It is interesting that both of these factors increase cell motility and invasiveness [225,226], which are traits associated with EMT. This is the first report, to our knowledge, that post-EMT cells become more responsive to LPA. This is an important observation because increased LPAR1 mRNA expression in primary tumors

of breast cancer patients correlates significantly with their positive lymph node status [227]. Furthermore, an LPAR antagonist reduces breast cancer cell migration and invasion in vivo [228]. Additional studies are required to determine to what extent the HGF- and LPA-dependent signaling pathways contribute to EMT and its maintenance, and the motile, invasive properties associated with cells that have undergone EMT.

Tumor cells in vivo may utilize changes in mitogenic signaling in an autocrine (basal) or paracrine manner. Our data suggest that both pre- and post-EMT cells have a basal level of LPAR and c-Met activation, but that the post-EMT cells have a much more dramatic increase in proliferation in response to exogenous LPA or HGF. There was little basal PDGFR activation in either cell line, however, the post-EMT cell lines showed a robust response to the addition of PDGF. These cells increased proliferation and exhibited PDGFR phosphorylation, whereas the pre-EMT cells showed little or no response to PDGF. Therefore, the mitogenic changes associated with EMT may allow post-EMT tumor cells to better exploit growth factors released by the stroma.

It is interesting to note that STAT3 activation increases in the post-EMT MMTV-Her2/neu breast cancer cell lines and in the cells that have undergone EMT in the breast panel. This is not unexpected since STAT3 is activated by an array of cytokines, growth factors (including EGF and PDGF), and some G-protein coupled receptor agonists [229-231]. PDGF or other growth factors or cytokines might activate STAT3 in the post-EMT cells, and this is a subject for future study.

In summary, we characterized a reproducible in vivo model of EMT and find that striking changes in mitogenic signaling take place during this transition. Similar alterations are associated with EMT in a panel of human breast cancer cell lines as well

as in normal human mammary epithelial cells grown in media that induce a mesenchymal phenotype. These changes alter the responsiveness of the cancer cells to both growth factors and to compounds that selectively inhibit their respective downstream signaling pathways. Therapeutic agents targeting c-Met, Axl, and STAT3, are currently under development [232-236], and have the potential to attack the most aggressive breast tumors. Additional studies are required to fully determine the consequences of these observations with respect to the treatment of breast cancer patients with drugs targeting Her2, PDGFR, LPAR, c-Met, and STAT3, and the use of these agents in combination therapies that simultaneously target pre- and post-EMT cancer cells within the same tumor. Further, the observation that tumorigenicity can be maintained in cancer cells initiated by Her2 expression despite loss of detectable Her2/neu expression, presumably through "mitogenic switching," may have important implications for the acquisition of tumor resistance to Her2-targeted therapeutic agents.

Materials and Methods

In Vivo EMT Model

The previously described neuT cancer cell line [6; 7] was injected (10^6 cells) into the inguinal (#4) mammary fat pads of wild type FVB mice. Tumors were allowed to grow to between 1 and 1.5 cm in diameter to permit the tumors to undergo EMT and the tumors were harvested and clonal cancer cell lines were isolated as described previously [6; 7].

Cell Culture

Human cancer cell lines were purchased from ATCC (Manassas, VA). Unless otherwise indicated, all cell lines were cultured in Dulbecco's Modified Eagle's Medium supplemented with 10% fetal bovine serum. Stable knockdown cell lines were

generated by co-transfecting shRNA constructs (Thermo Scientific, Waltham, MA) along with viral packaging plasmids PMD2G and PsPax2 obtained from Addgene (Cambridge, MA) into the 293T cell line using Lipofectamine Reagent (Invitrogen, Grand Island, NY). Medium from the transfected 293T cell line was then used to infect the target cell line, which was subsequently selected using 10 μg/mL Puromycin. The MMTV-D1K2-T2 cell line was described previously [7]

Microarray Analysis

Total RNA was isolated from neuT luminal and neu$T_{EMT,CL2}$ cells using Trizol Reagent (Invitrogen), according to the manufacturer's instructions. Three replicate samples of RNA from each cell line were isolated and analyzed. Microarray analysis was performed using the Affymetrix microarray platform at the Interdisciplinary Center for Biotechnology Research (ICBR) Microarray Core, University of Florida. Total RNA concentration was determined with a NanoDrop Spectrophotometer (NanoDrop Technologies, Inc., Wilmington, DE), and sample quality was assessed using the Agilent 2100 Bioanalyzer (Agilent Technologies, Inc., Santa Clara, CA). All microarray sample preparation reactions used the GeneChip® Whole Transcript (WT) Sense Target Labeling reagents (Affymetrix, Inc., Santa Clara, CA), and reactions were performed following the manufacturer's protocols. The arrays were washed and stained with the reagents supplied in the GeneChip® Hybridization Wash and Stain kit (Affymetrix, Inc) on an Affymetrix Fluidics Station 450, and scanned with a GeneChip® 7G Scanner (Affymetrix, Inc).

Immunoblot analysis

Cell lysates were prepared as described previously [6; 7] and were analyzed by immunoblot with the following antibodies: [Actin (sc-1616-R), Erk1/2 (sc-93), Gas6 (sc-

1936), IRS-1 (sc-559), N-Cadherin (sc-7939), PDGFRß (sc-432), SPARC (sc-25574), Stat3 (sc-7179); Santa Cruz, Santa Cruz, CA)], [Akt (#9272), Axl (#4977), c-Met (#3127), p-Akt S473 (#9271S), p-Akt T308 (#9275S), p-Axl (#5724P), p-Erk T202/Y204 (#9101S), p-Met Y1234/12345 (#3126), p-PDGFRβ Y751 (#4549), p-Stat3 Y705 (#9131S), Zeb1 (#3396S); Cell Signaling, Danvers, MA], [Her2 (MS-730-P0), Vimentin (MS-129-P0); Neomarkers, Freemont, CA], [E-Cadherin (610181); BD Transduction, San Jose, CA], [LPA1 (10005280); Cayman Chemical Company, Ann Arbor, Michigan], [Occludin (711500); Invitrogen Carlsbad, CA].

Proliferation Assays

Proliferation was measured using tritiated thymidine incorporation assays as described [6; 7]. When assessing proliferation induced by HGF, LPA, or PDGF, these factors were applied to the cells diluted in 1x Insulin, Transferrin, and Selenium (ITS) (Roche, Branchburg, NJ). Results are presented as the average ± standard deviation of triplicate determinations.

Invasion Assays

Cells were plated in the inserts of 6-well BD BioCoat Matrigel Invasion Chamber plates (#354480 BD, San Jose, CA) at 125,000 cells per chamber in 0.2% FBS-DMEM. Serum (10% FBS) was added to the lower chambers to act as a chemoattractant. Cells were incubated at 37°C for 48 hours. Following incubation, non-invaded cells were removed from the inserts with cotton swabs. The remaining invaded cells were fixed with ice-cold methanol for 10 minutes, and stained with 0.5% crystal violet/25% methanol for 10 minutes. Invaded cells were counted in three or more randomly chosen fields. Results are presented as the average ± S.D. of triplicate determinations.

MCF10A EMT Models

Unless otherwise stated, MCF10A cells were maintained in a 50/50 mixture of Dulbecco's Modified Eagle's Medium and Ham's F12 medium supplemented with 5% horse serum, 20 ng/mL EGF, 100 ng/mL cholera toxin, 10 µg/mL insulin, and 500 ng/mL hydrocortisone (Sigma-Aldrich, St. Louis, MO). For induction of EMT, cells were grown in 50/50 DMEM/F12 + 10% fetal bovine serum or in the presence of 2.5 ng/mL TGF-β (Millipore, Billerica, MA) for a minimum of four weeks prior to photographing and processing.

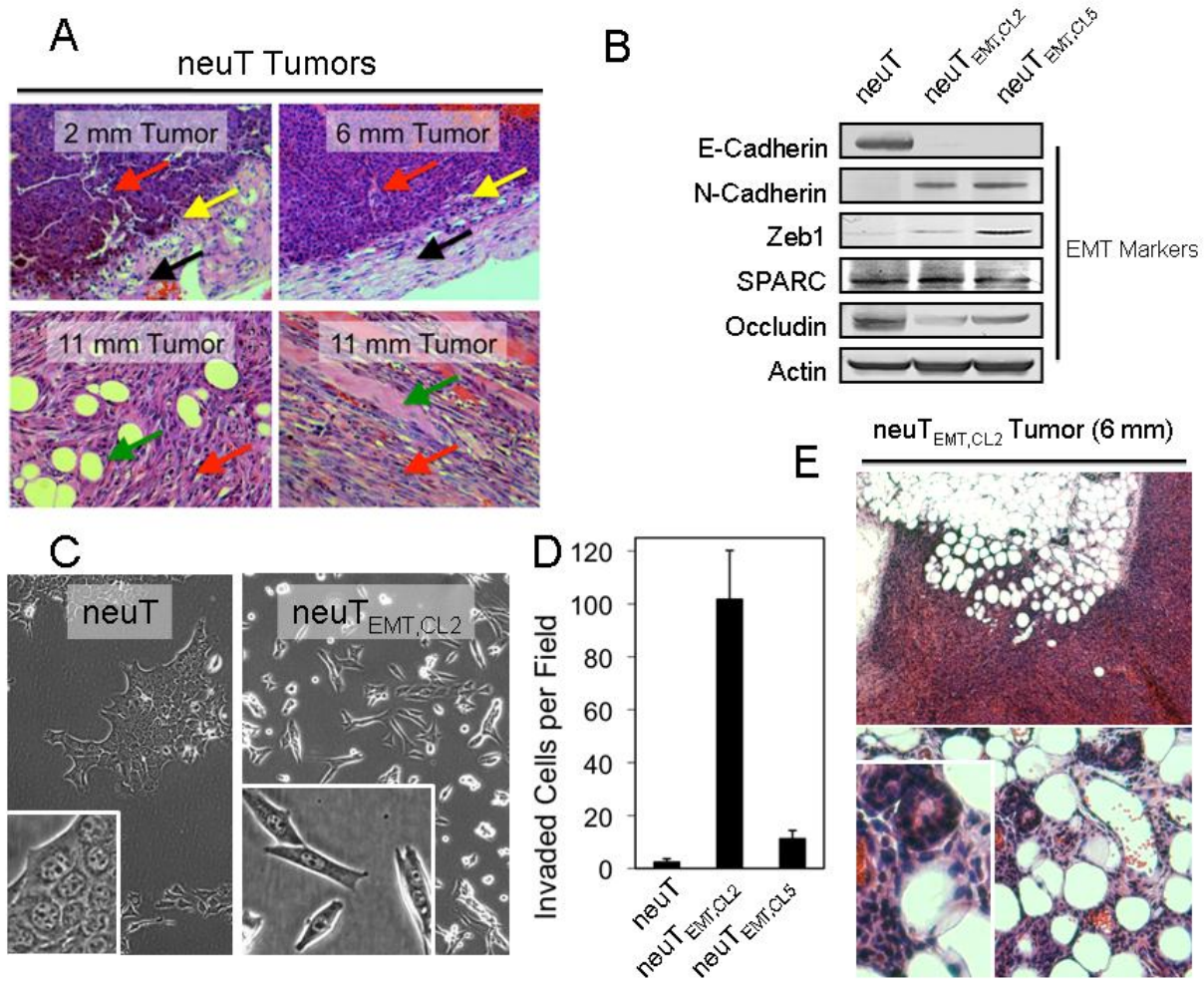

Figure 5-1. Characterization of an in vivo model of EMT. A) Micrographs of hematoxylin and eosin (H&E) stained tumors of the indicated sizes formed from neuT cells. Red arrows point out cancer tissue and cell morphology. Yellow arrows denote tumor boundaries. Black arrows indicate fibroblast capsules. Green arrows show inclusions of adipocytes or muscle tissue in the tumors. B) The original neuT cell line and clonal tumor cell lines derived from neuT cells after having undergone EMT in vivo ($neuT_{EMT,CL2}$ and $neuT_{EMT,CL5}$) cultured in DMEM with 10% FBS and analyzed by immunoblot with the indicated antibodies. Actin served as a loading control. C) Phase contrast micrographs showing cell morphology of neuT and $neuT_{EMT,CL2}$ cells growing in culture. Insets show cells at higher magnification. D) Invasion assays quantifying the number of cells per field permeating a Matrigel impregnated filter. E) Micrograph of an H&E stained 6 mm tumor formed from $neuT_{EMT,CL2}$ cells. Lower panels are higher magnification images showing cancer cell infiltration around mammary adipocytes and ducts.

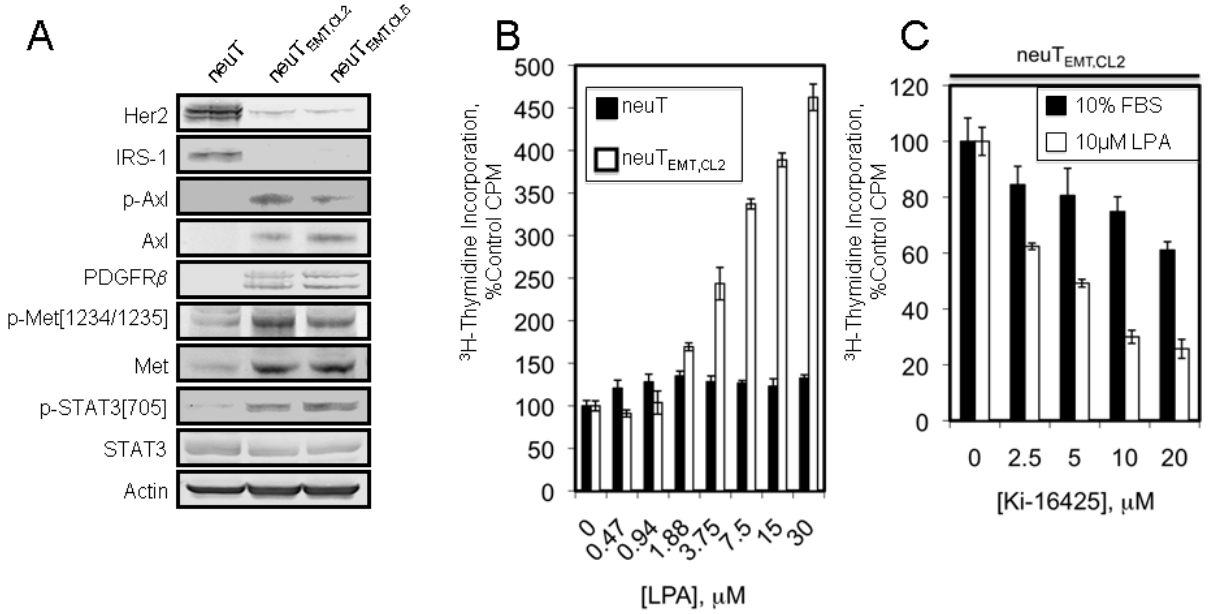

Figure 5-2. EMT is associated with altered growth factor receptor expression and responsiveness to lysophosphatidic acid. A) Immunoblots of extracts prepared as described in Figure 1B were analyzed with the indicated antibodies. B) The neuT and neuT$_{EMT,CL2}$ cells were stimulated with the indicated concentrations of lysophosphatidic acid (LPA) for 24 hours and ^{3}H-thymidine incorporation was measured. C) The neuT and neuT$_{EMT,CL2}$ cells were stimulated with 10 μM LPA or 10% FBS in the presence of the indicated concentrations of Ki-16425 for 24 hours and ^{3}H-thymidine incorporation was quantitated.

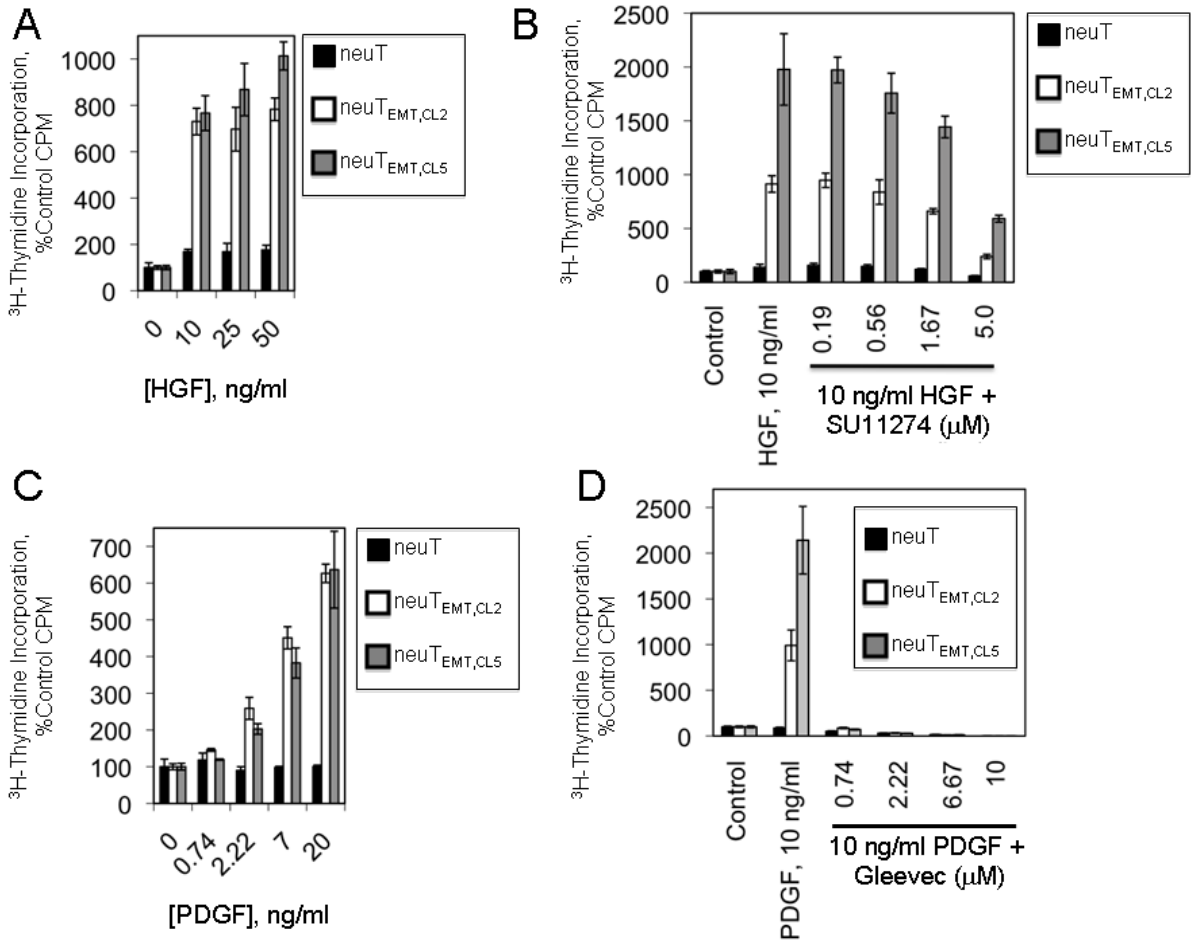

Figure 5-3. Post-EMT cells exhibit enhanced responsiveness to the mitogenic actions of HGF and PDGF. A) The neuT, $neuT_{EMT,CL2,}$ and $neuT_{EMT,CL5}$ cell lines were stimulated with the indicated concentrations of HGF for 24 hours and cell proliferation was measured by ^{3}H-thymidine incorporation. B) The neuT, $neuT_{EMT,CL2,}$ and $neuT_{EMT,CL5}$ cell lines were stimulated with 10 ng/ml HGF in the presence of the indicated concentrations of SU11274 for 24 hours and ^{3}H-thymidine incorporation was quantitated. C) The neuT, $neuT_{EMT,CL2,}$ and $neuT_{EMT,CL5}$ cell lines were stimulated with the indicated concentrations of PDGF for 24 hours and ^{3}H-thymidine incorporation was quantitated. D) The neuT, $neuT_{EMT,CL2,}$ and $neuT_{EMT,CL5}$ cell lines were stimulated for 24 hours with 10 ng/ml PDGF in the presence of the indicated concentrations of Gleevec for 24 hours and ^{3}H-thymidine incorporation was quantitated.

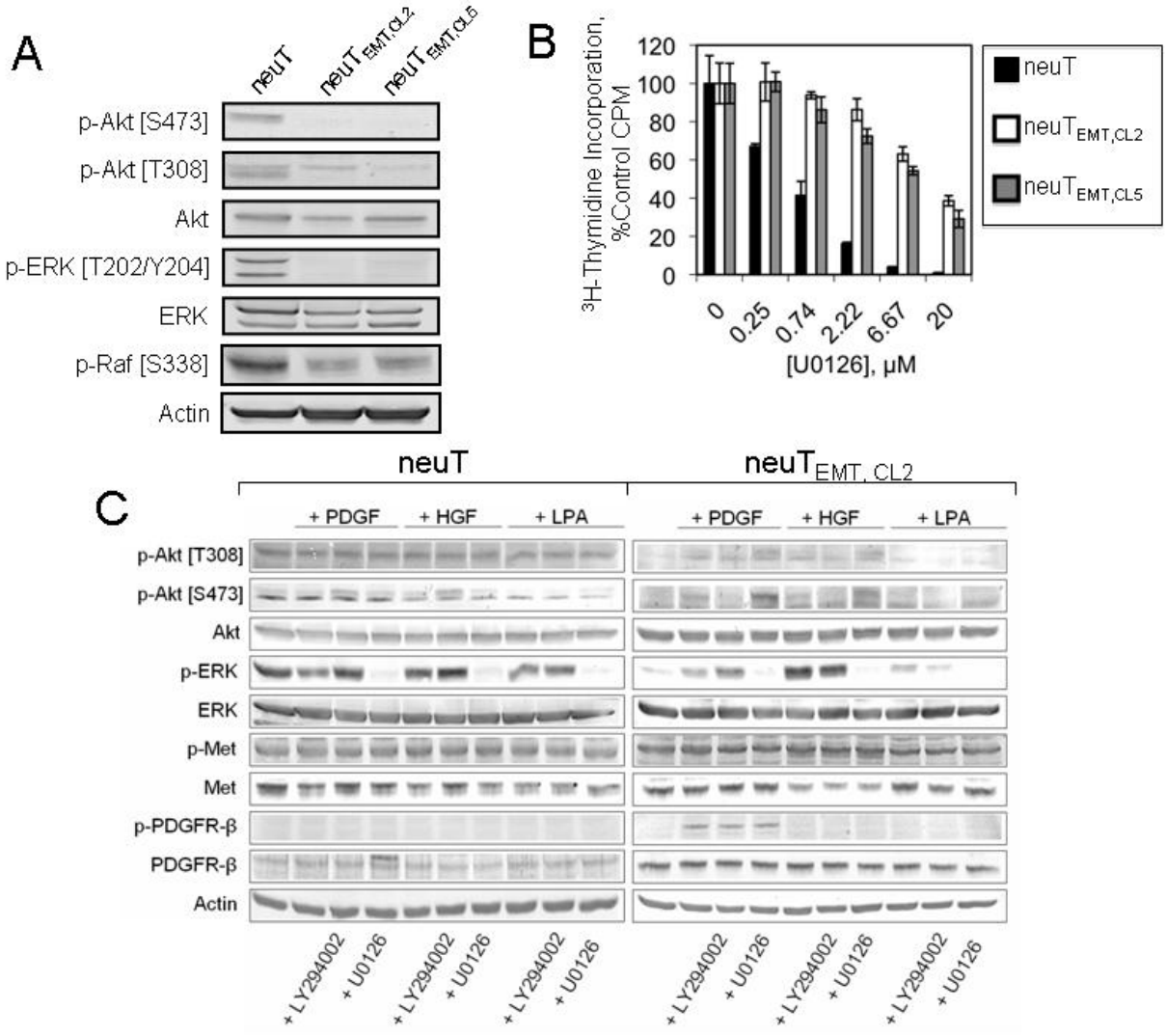

Figure 5-4. EMT is associated with changes in intracellular signal transduction cascades. A) Immunoblot analysis of extracts prepared as in Figure 1B were analyzed with the indicated antibodies. B) The neuT, $neuT_{EMT,CL2,}$ and $neuT_{EMT,CL5}$ cell lines were treated with the indicated concentrations of U0126 in 10% FBS-DMEM growth medium for 24 hours and ^{3}H-thymidine incorporation was quantitated. C) Immunoblot analysis of cell lysates from neuT and $neuT_{EMT, Cl2}$ cells pre-incubated in serum free medium. Cells were pre-treated with inhibitors for 1.5 hours and then co-treated with the inhibitors and growth factors for 30 minutes prior to analysis.

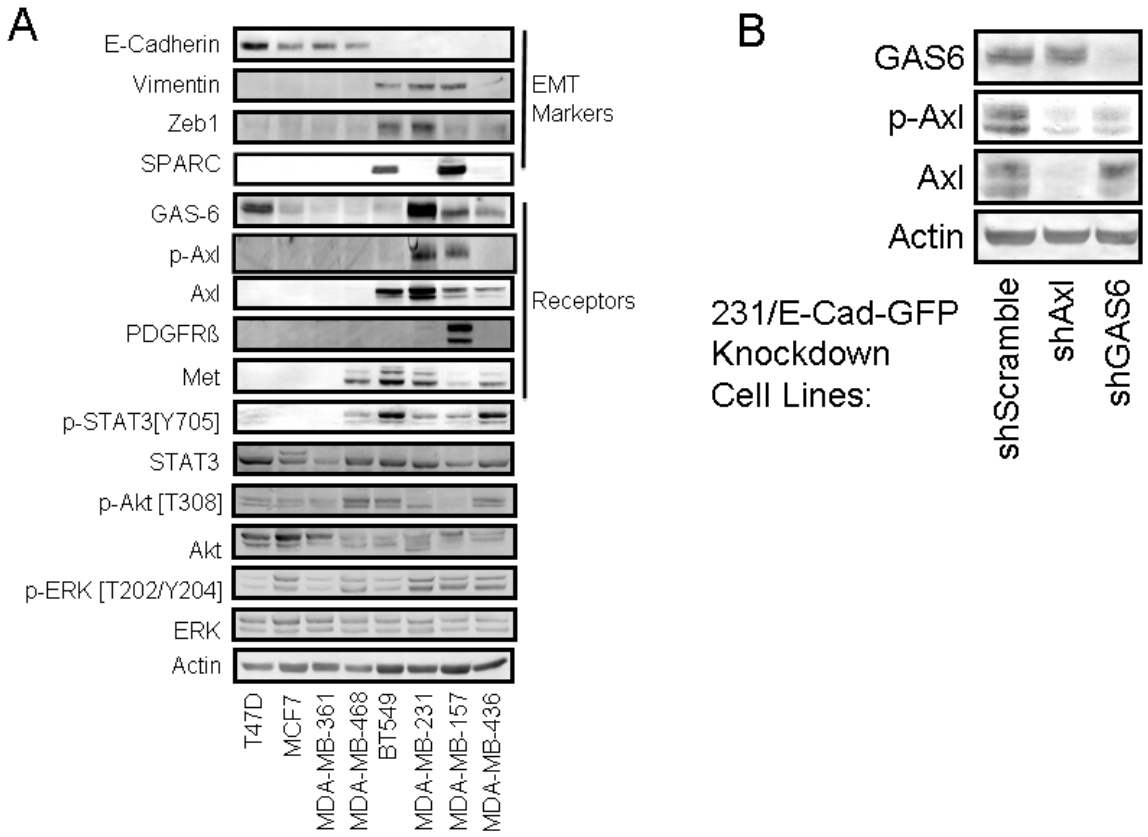

Figure 5-5. Expression of EMT markers in human breast cancer cell lines. A) Immunoblot analysis of human breast cancer cell lines with the indicated antibodies. B) Immunoblot analysis of a MDA-MB-231 cell line stably expressing an E-cadherin-Green Fluorescent Protein fusion protein (231-E-Cad-GFP) transduced with lentiviral vectors encoding short hairpin RNAs targeting Axl, GAS6, or a scrambled control shRNA.

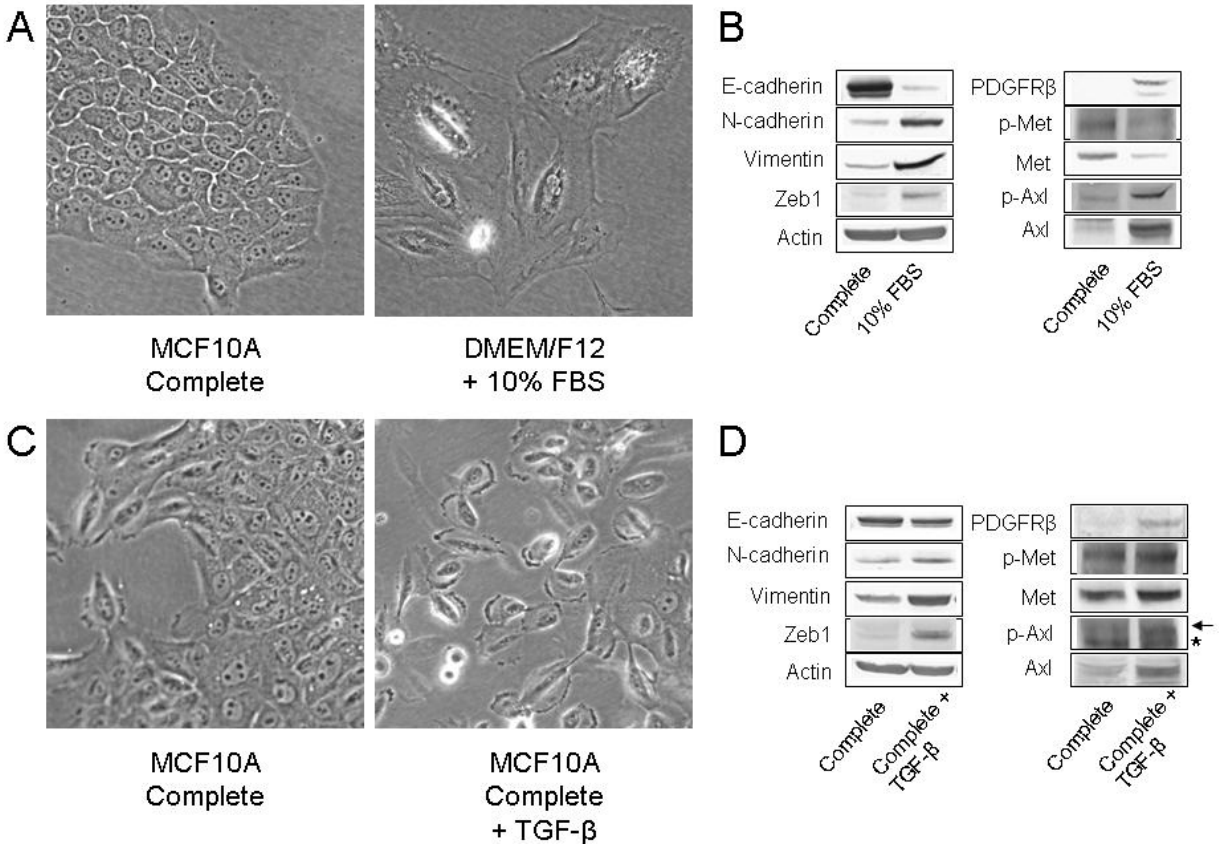

Figure 5-6. EMT of MCF10A cells is associated with altered expression of growth factor receptors. A), Micrographs of MCF10A cells grown in MCF10A complete medium or DMEM/F12 + 10% FBS. B) Immunoblot analysis of MCF10A cells grown in MCF10A complete medium or DMEM/F12 + 10% FBS. C) Micrographs of MCF10A cells grown in MCF10A complete medium with or without 2.5 ng/mL TGF-β. D) Immunoblot analysis of MCF10A cells grown in MCF10A complete medium with or without 2.5 ng/mL TGF-β. The arrow denotes the p-Axl band, while the "*" marks a non-specific band.

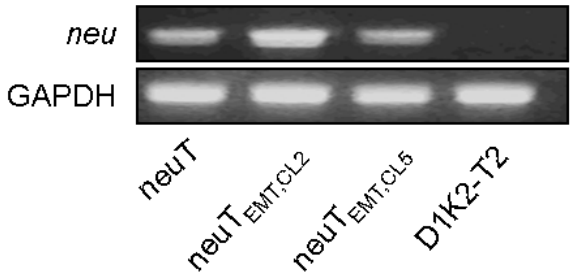

Figure 5-7. Expression of transgenic Her2/neu in isolated cell lines. Pre- and post-EMT cell lines were analyzed by PCR to confirm the presence of the transgenic rat Her2 gene. The primers used are specific to the Her2/neu transgene and do not recognize the endogenous mouse gene (TTTCCTGCAGCAGCCTACGC, CGGAACCCACATCAGGCC). The original neuT cell line served as a positive control and the D1K2-T2 cell line [53] served as a negative control.

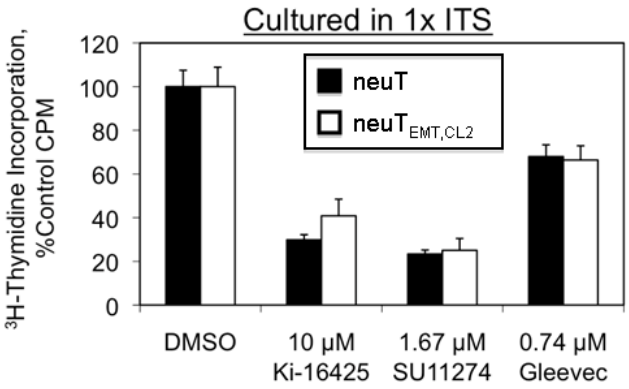

Figure 5-8. Effect of receptor antagonists and kinase inhibitors on basal proliferation. Assessment of thymidine incorporation by neuT or neuT$_{EMT, CL2}$ cells grown in 1x ITS and treated with DMSO, LPAR inhibitor Ki-16425, c-Met inhibitor SU11274, or the PDGFR inhibitor Gleevec.

CHAPTER 6
PERSPECTIVES

Summary

The preceding studies have looked at the role of Cyclin D1/Cdk2 complexes in tumorigenesis and tumor progression. We first showed that mice expressing the D1K2 fusion protein generate spontaneous tumors that exhibit centrosome amplification, chromosomal instability, polyploidy, and aneuploidy. Using the MCF10A cell line as an isogenic background, we determined that D1K2 strengthens the spindle assembly checkpoint through upregulation of Mad2 and weakens the tetraploidy checkpoint by maintaining Rb phosphorylation despite checkpoint activation. This renders cells more sensitive to spindle poisons such as nocodazole and paclitaxel due to a greater mitotic arrest, but permits the polyploidization of cells that undergo mitotic slippage. While it appears these polyploid cells are not viable long-term, the heterogeneous tumor population may contain additional mutations that allow these polyploid cells to persist and become aneuploid.

We next showed that D1K2 is capable of inducing chromosomal instability through other mechanisms as well. Phosphorylation of Nucleophosmin on T199 is required for centrosome duplication and D1K2 causes hyperphosphorylation. Likewise, D1K2 phosphorylates Cdh1, a part of the mitotic and centrosome duplication machineries, and Cdh1 phosphorylation generally induces inactivation. We also saw that cells expressing D1K2 have an observable rate of failed cytokinesis and a reduced ability to bundle supernumerary centrosomes.

It was also discovered that Cdk2, complexed with Cyclin E or D1, is capable of phosphorylating PSF. This protein contains twelve consensus Cdk phosphorylation

sites, of which three have previously been shown to be phosphorylated by unknown kinases. While mutagenesis failed to conclusively identity the residues phosphorylated by Cdk2, the data suggest that multiple sites may be critical in the process.

We finally examined a role of D1K2 in EMT. Both MCF10A cells and mouse tumors expressing D1K2 show characteristics of having undergone EMT, and multiple models of this switch show that stark changes in mitogenic signaling occur during this process. This renders post-EMT cells sensitive to inhibitors of signaling cascades that are not active in the pre-EMT and normal tissues.

Pertinence

The data presented in this study have relevance that may directly or indirectly affect the future treatment of cancer. The results seen with the alteration of the spindle assembly and tetraploidy checkpoints has two-fold importance for the use of spindle poisons. Firstly, it appears that tumors exhibiting overactive Cdk2 may be more sensitive to spindle poisons and other therapeutics that activate the spindle assembly checkpoint. Secondly, these same tumors will likely generate polyploid populations when treated with spindle poisons. Our in vitro studies show that this could potentially increase the efficacy of these treatments as polyploid cells are unviable. In vivo tumors oftentimes behave quite differently, and if these cells were indeed viable, they could become chromosomally unstable, driving tumor evolution and drug resistance.

Similarly, the fact that overactive Cdk2 can lead to chromosomal instability through the above mechanism, NPM or Cdh1 phosphorylation, and failed cytokinesis, as well as promoting EMT, may provide further rationale for the development of specific Cdk2 inhibitors. While single-agent trials of Cdk inhibitors have found limited success, when used in conjunction with other therapies they may serve to block tumor evolution.

This could lead to better patient outcomes through decreased drug resistance and maintaining a localized primary tumor.

The post-EMT tumor population is the most invasive and is likely responsible for the majority of metastases. However, these cells are also generally the most refractory to treatment. Our data on the mitogenic changes that occur during EMT open up potential new avenues for treatment. Post-EMT cells in vitro show greater sensitivity to inhibitors of signaling cascades that are concomitantly turned on such as gleevec, Ki-16425, and SU11274. In vivo studies are needed in order to confirm that this affect is translatable.

Finally, the phosphorylation of PSF by Cdk2 is completely novel. We have yet to identify the consequences of this phosphorylation, however it is possible that phosphorylation affects the RNA splicing or DNA repair functions of PSF. The potential ramifications of either of these to cancer is clear, however the degree of which they contribute to the tumor phenotype is not.

Future Studies

As it is in science, answers are oftentimes simply the reproductive mechanism of questions. While this study answers many questions relating to Cdk2 in cancer, it also raises many more. There has been little work done on the in vivo survival of polyploid tumor populations induced by therapeutic treatment. Studies utilizing the D1K2 mouse strain or xenograft experiments with the D1K2 tumor-derived cell lines could help crystallize the relevance of the in vitro experiments that have been carried out. It would be expected that D1K2 tumors would generate a polyploid population upon paclitaxel treatment that would die out, but the combination of D1K2 expression with p53 mutations may result in viable polyploid cells that are chromosomally stable or unstable.

While completing this work, non-phosphorylatable and phospho-mimic NPM constructs, T199A and T199E, respectively, were generated but not subsequently used. These tools could be used to probe the role that D1K2 phosphorylation of NPM has in centrosome amplification. NPM T199E would be expected to induce centrosome amplification when transfected into the 293T cell line, as would expression of D1K2. The absence of centrosome amplification during expression of D1K2 and NPM T199A would directly implicate D1K2 phosphorylation of T199 in centrosome amplification.

Definitive identification of the Cdk2 phosphorylation sites would prove very useful. While mutation analysis has not given clear results, another possibility would be mass spectroscopy. Doing a cold kinase reaction and running on a gel to separate the phosphorylated protein through the mobility shift may yield a sample sufficient for mass spec analysis to identify the phosphorylated residues. Knowing the phosphorylated residues would give the ability to make phospho-mimic PSF constructs to analyze the effects of phosphorylation.

While we have not been able to show a change in cellular localization of PSF upon phosphorylation by Cdk2, it is possible that the RNA splicing or DNA damage functions may be influenced. An RNA splicing assay, such as has been used elsewhere [237], could determine whether phosphorylation up- or downregulates the splicing activity of PSF. Similarly, the potential of PSF phosphorylation to regulate the DNA damage machinery could be examined using cells expressing non-phosphorylatable or phospho-mimic mutants treated with DNA damaging agents. Alternatively, a more complex DNA damage assay could be utilized [194].

In terms of the EMT data, while we have shown that the mitogenic switch occurs during in vivo EMT, we have not shown that these tumors are sensitized to the inhibitors gleevec, Ki-16425, and SU11274. These inhibitors block the growth induced by exogenous growth factors applied to post-EMT cells in vitro, but fail to show any selectivity on basal proliferation. It is likely that the growth factors secreted by the surrounding tissues in vivo are stimulating proliferation, creating the potential for therapeutic intervention. However, this must be tested in vivo to confirm.

Conclusions

With the advances in treating other leading causes of death, including heart disease and stroke, cancer will soon become the leading cause of death in the United States. Being a disease of age, cancer will become an ever increasing part of our lives as people begin to live longer. While we have made great strides in limiting our exposure to carcinogens and identifying risk factors that predispose individuals to developing cancer, we still know shockingly little about the root cause of the majority of cancer cases.

Considering that a tumor consists of cells derived from a patient's own body, the differences between cancer and normal cells is slight, creating an inherent difficulty in treatment not seen with infectious diseases. This results in a narrow therapeutic window and the oftentimes horrible side-effects commonly associated with cancer treatment. In order to exploit the differences that do exist, we need a greater understanding of them.

This work presents data that expands our knowledge of the development and progression of cancer due to overactive Cdk2 and the epithelial to mesenchymal transition. Future work in the field should continue basic science research with the goal

of developing novel therapeutic strategies. While we are much further from the widespread effective prevention and treatment of cancer than we want and need to be, it is not an unobtainable goal. It is how we proceed that will determine how cancer continues to define our civilization.

“Cancer can take away all of my physical abilities. It cannot touch my mind, it cannot touch my heart, and it cannot touch my soul.” ~ Jim Valvano

APPENDIX A
CDK2 KNOCKDOWN IS LETHAL TO OVARIAN CANCER CELL LINES INFECTED WITH HUMAN PAPILLOMAVIRUS

Results and Discussion

The role of the Human Papilloma Viruses (HPVs) in human cancer has come to light in recent times. They are believed to play a causative role in many forms of cancer, including cervical, anal, and oral cancers, among others (reviewed in [238]). These non-enveloped viruses, approximately 55 nm in diameter, contain a double stranded, circular genome that is about 8 kB in size.

HPVs are only able to replicate in keratinocytes, which make up the outer layer of skin and some mucosal surfaces. Once a host cell is infected, early- and late-viral proteins are produced, promoting viral DNA replication, virion particle production, and subsequent release from the host cell [239]. The proteins E6 and E7 are believed to play the predominant roles in HPV-associated carcinogenesis.

Produced during latent infections, E6 and E7 serve to promote cell growth and survival through inhibition of the p53 and Rb tumor supressors via sequestration through protein-protein interactions and by inducing protein ubiquitination, leading to proteasomal degradation. The subsequent loss of cell-cycle regulation and genome stability lead to uncontrolled cell growth and transformation (reviewed in [240]).

It was noticed in our lab that knockdown of Cdk2 using stable shRNA constructs resulted in the death of the cervical carcinoma cell lines HeLa, CaSki, and SiHa. Cell death was not observed in any other cell lines derived from other tissues, whether transformed or not (data not shown). All three cell lines are infected with HPV [241,242] and it was hypothesized that it is this infection that sensitizes cells to Cdk2 knockdown.

Expression of the viral proteins E6 and E7 in the human colon cancer cell line, HCT116, indeed led to cell death upon Cdk2 knockdown, but failed to sensitize the HPV-negative keratinocyte cell line, HaCaT. Further, expression of E6/E7 in Cdk2$^{-/-}$ HCT116 appeared to have no effect on cell viability (all data not shown). While the results obtained are seemingly contradictory, they raise extremely intriguing questions in the treatment of HPV. It is possible that such cancers would be extremely responsive to Cdk2 inhibition. However, the pharmacological inhibitor CVT313 failed to be more effective at blocking proliferation of the HCT116 cell line expressing E6/E7 than the parental cell line (Figure A-1).

These results indicate that there is a fundamental difference between inhibiting kinase activity and blocking protein expression in this context. Cdk2 knockdown reduces the formation of Cdk2 protein and its associated complexes. This would increase the levels of free Cdk inhibitory proteins in the cell, potentially leading to inhibition of the other Cdks, and the observed cell death. Conversely, pharmacological inhibition blocks only the Cdk2 kinase activity, allowing the protein pool to remain a sink for Cdk inhibitory proteins. Therefore, HPV infection may result in cellular addiction to a Cdk other than Cdk2, paradoxically sensitizing them to Cdk2 knockdown.

Future studies should study the effects of knockdown of the other Cdks in order to determine which are most crucial to survival of HPV infected cells. While the current model presents challenges to its utilization in vivo, siRNA mediated knockdown of Cdk2 may prove to be useful in treating HPV-positive tumors in the future once the great potential of human gene therapy has been harnessed.

Materials and Methods

Cell Culture

Cell lines were purchased from ATCC (Manassas, VA) and cultured in Dulbecco's Modified Eagle's Medium supplemented with 10% fetal bovine serum. Stable knockdown cell lines were generated by co-transfecting shRNA constructs (Thermo Scientific, Waltham, MA) along with viral packaging plasmids PMD2G and PsPax2 obtained from Addgene (Cambridge, MA) into the 293T cell line using Lipofectamine Reagent (Invitrogen, Grand Island, NY). Medium from the transfected 293T cell line was then used to infect the target cell line, which was subsequently selected using 10 μg/mL Puromycin.

Thymidine Incorporation Assays

Proliferation assays were carried out as previously described [54,179].

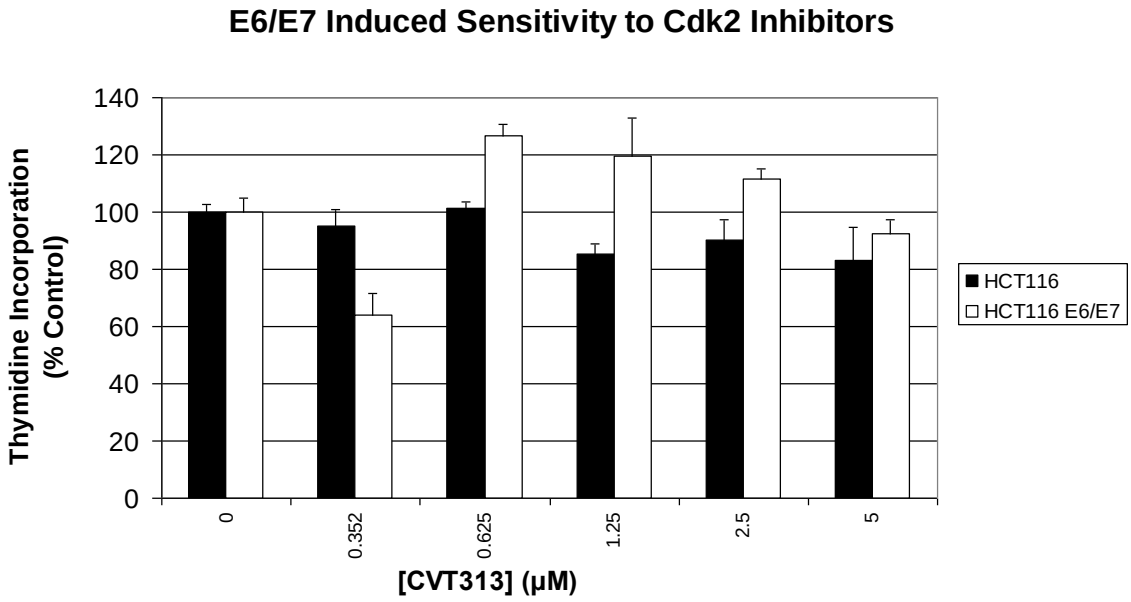

Figure A-1. Lack of E6/E7 induced sensitivity to Cdk2 inhibitor. [^{3}H]-thymidine incorporation of the HCT112 cell line with and with the viral protein E6/E7 after treating with the Cdk2 inhibitor CVT313 for 24 hours.

APPENDIX B
DEVELOPMENT OF A SMALL MOLECULE CDK INHIBITOR

Results and Discussion

As part of his dissertation, a previous student in our lab discovered and classified a new class of Cdk inhibitors [67,148]. While the majority of current Cdk inhibitors are ATP competitive [243], the goal of the project was to use in silico molecular docking to identify compounds that would bind to a pocket present only when Cdks were in the inactive state. The hypothesis was that a compound binding there would prevent conformational changes, locking the protein in its inactive state.

What was discovered was a number of compounds that induced aggregation of Cdks, blocking Cdk kinase activity by reducing the effective amount of protein in the cell [67]. Another of the identified compounds, NSC117024, was seen to inhibit cell proliferation quite potently, with an IC_{50} in the low micromolar range, but did not induce aggregation. Cell lines including the non-transformed MCF10A and NMuMG along with the breast cancer cell lines BT549 and MDA-MB-231 showed differential sensitivity to the compound, with BT549 being inhibited at the lowest concentrations. The cause of the different sensitivities is unclear, however it could be related to the fact the BT549 cell line lacks functional Rb.

NSC117024 was shown to cause a slight G1 arrest but failed to block Cdk2 kinase activity when tested in an in vitro kinase assay. In an effort to optimize the compound as part of the current study, 38 analogs were ordered from the National Cancer Institute's Experimental Therapeutics depository and tested for their efficacy. These analogs differed primarily in the substituents on one of the aromatic rings and showed large variations in efficacy at 2.5 μM in the BT549 cell line (selected

compounds are shown in Figure B-1). Two compounds, NSC116969 and NSC117010 inhibited cell growth better than NSC117024. The structures of these compounds are shown in Figure A2B along with that of NSC117024. A dose response of NSC116969 and NSC117010 shows that, while their efficacy at higher concentrations is similar, NSC117010 is more potent, with an IC_{50} of approximately 200 nM that is almost ten-fold lower than that of NSC117024.

In an attempt to identify the parts of NSC117024 most important for its anti-growth activities, we tested a series of compounds that represent different portions of the parent compound, as well as a few derivatives with changes made to the bicyclic portion of the molecule (Figure B-2). None were as efficacious as NSC117024, indicating that both the upper and lower portions of the molecule are required for the full effect and that derivatization of the upper portion effects its properties.

Experiments showed that NSC117010 failed to block Rb phosphorylation in cell culture and that it is equally efficacious in blocking proliferation of HCT116 and HCT116 $Cdk2^{-/-}$ cell lines (results not shown). These results lead one to believe that it does not inhibit Cdk2 as intended, but it is currently unknown what the cellular target(s) of these compounds is/are. However, their potency, particularly that of NSC117010, make them interesting drug candidates to pursue further. Future studies should focus on determining the targets and possibly include attaching an affinity tag or resin bead to the 5’ position of the lower six-membered ring.

Materials and Methods

Cell Culture

The HCT116 cell line was purchased from ATCC (Manassas, VA) and cultured in Dulbecco's Modified Eagle's Medium supplemented with 10% fetal bovine serum.

Thymidine Incorporation Assays

Proliferation assays were carried out as previously described [54,179].

Compounds

Commercially Obtained

All compounds with an NSC denotation were obtained from the National Cancer Institute's Developmental Therapeutics Program chemical repository (Bethesda, MD). Compounds 3 and 4 were purchased from Sigma Aldrich.

NSC117024

NSC117024 was also synthesized by refluxing 3 (2.000g, 12.6 mmol) with 4 (1.491g, 13.9 mmol) in MeOH (100 mL) for 1 hr with stirring. The mixture was filtered and the red solid was recrystallized from MeOH (300 mL) at room temperature for 3 days to yield 0.730 g of red crystals. M.P. 241 – 252 ˚C.

5

8-amino-2-naphthol (10 g, 62.8 mmol) was dissolved in MeOH (67 mL) and acetic anhydride (6.24 mL, 66.0 mmol) was added over 5 min while stirring in an ice bath. The mixture was refluxed for 90 min and dried to give 12.676 g of a black solid.
^{1}H NMR (300 MHz, methanol-d_4) δ 9.78 (2H, d), 7.78 (1H, d), 7.62 (1H, d), 7.45 (1H, d), 7.30-7.19 (2H, m), 7.14 (1H, d), 2.18 (3H, s).

2

To 5 (1.6 g, 7.95 mmol) dissolved in MeOH (80 mL) was added $K_2(SO_3)NO$ (4.9 g, 19.4 mmol) dissolved in H_2O (280 mL) and 80 mL of 0.167 M KH_2PO_4. The mixture was stirred 20 min at room temperature and 2 hr in an ice bath. Solution was concentrated to 75 mL and filtered. The solid was dissolved in $CHCL_3$, washed 4x with an equal volume of H_2O, and dried over Na_2SO_4. The solution was purified on an alumina

column and dried. The solid was recrystallized from EtOH to give 540 mg of orange-red crystals. M.P. 163 – 165 ˚C.

1

A mixture of 2 (152 mg, 0.706 mmol) and 3 (8.35 mg, 0.779 mmol) was refluxed in MeOH (10 mL) for 2 hr with stirring. The mixture was filtered and the solid was recrystallized from butanol to give 72 mg of copper colored crystals.

^{1}H NMR (300 MHz, D_2O) δ 11.82 (1H, s), 8.8-8.75 (1H, d), 8.02-7.99 (1H, d), 8.85-8.7 (1H, t), 7.32-7.1 (4H, m), 2.57 (1H, s), 2.42 (1H, s), 2.36 (3H, s), 2.22 (3H, s).

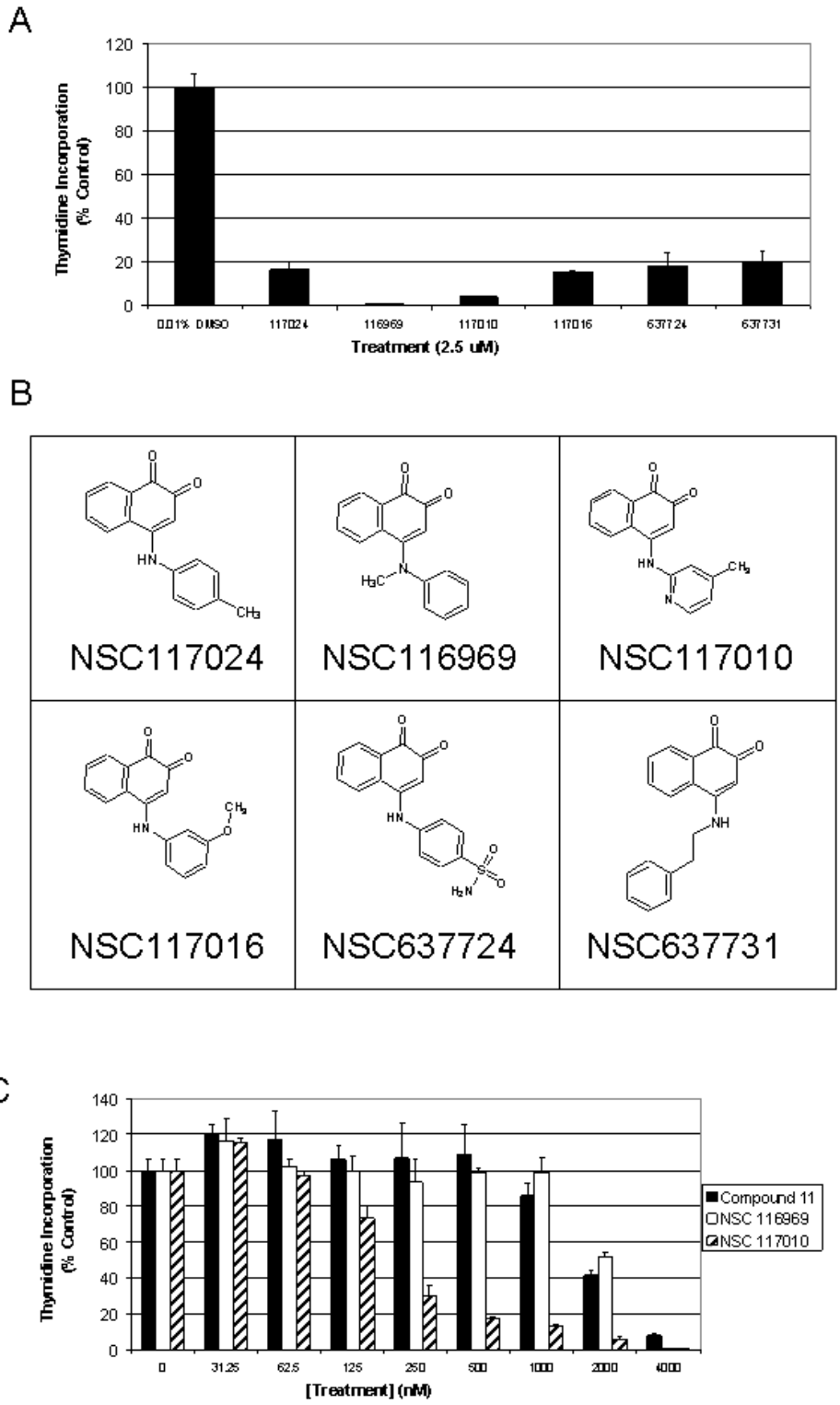

Figure B-1. Screening of NSC117025 analogues. A) Proliferation, as measured by [^{3}H]-thymidine incorporation, of the HCT116 cell line treated with 2.5 μM concentrations of the indicated compounds. B) Chemical structures of the analogues tested in panel A.

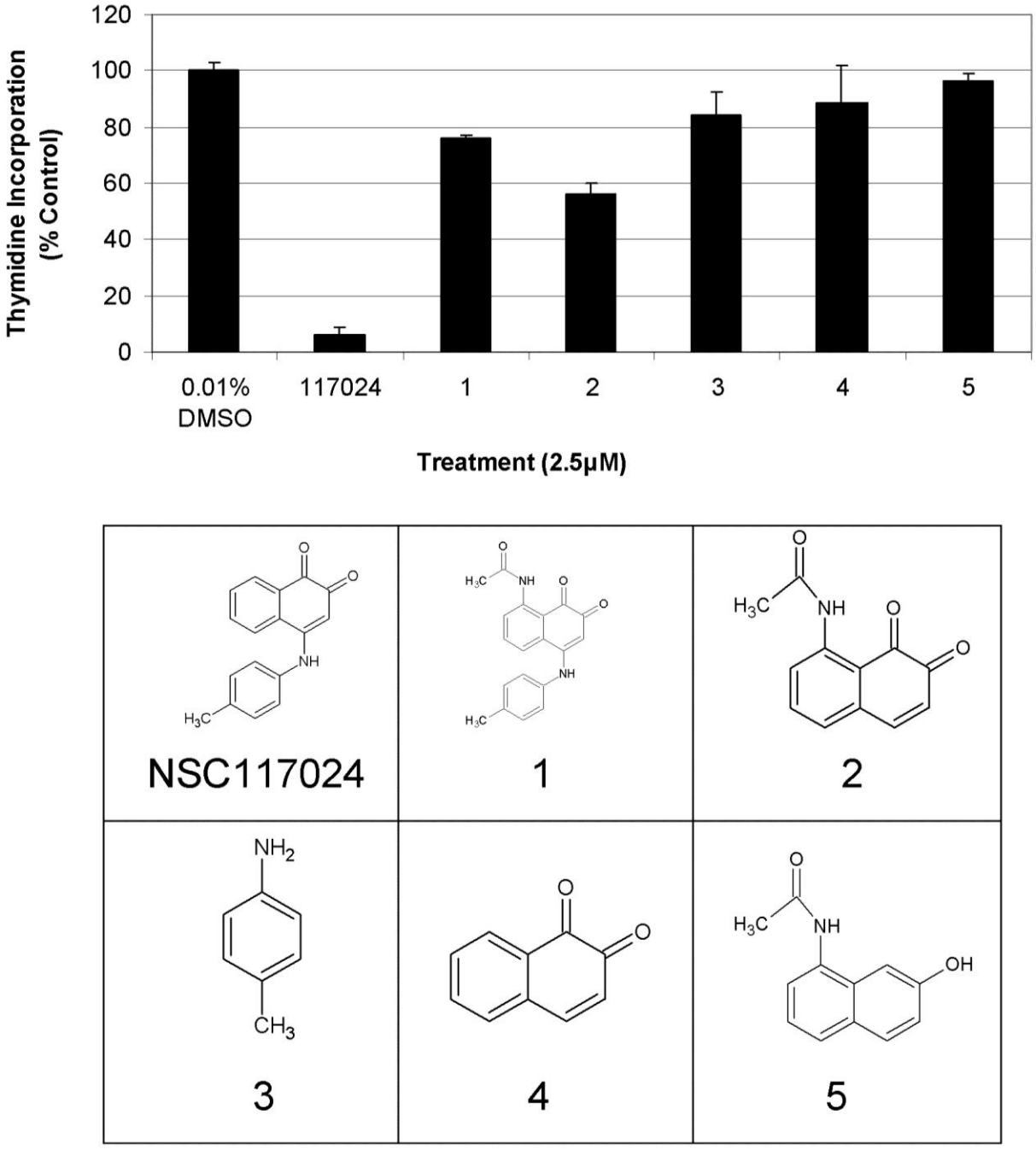

Figure B-2. Testing of NSC117024 molecular parts. A) Proliferation, as measured by [^{3}H]-thymidine incorporation, of the HCT116 cell line treated with 2.5 µM concentrations of the indicated compounds. B) Chemical structures of the compounds tested in panel A.

APPENDIX C
EFFECTS OF GROWTH MEDIUM ON MCF10A CELL MORPHOLOGY

Results and Discussion

Much of the work in this study utilizes the MCF10A cell line. Originally isolated in 1984 from a patient with mammary fibrosis, this cell line was spontaneously immortalized by repeated passaging with trypsin-EDTA [168]. Considered a nontransformed human mammary epithelial cell line, they are commonly used as a "normal" control to compare human mammary epithelial tumor cell lines to. While many cell lines are capable of growing in similar medium, DMEM + FBS for example, MCF10A are not.

During isolation, it was noted that after 3 to 4 years of growth, the cell line would no longer proliferate in the absence of exogenous growth factors. A combination of factors including cortisol (now replaced with hydrocortisone), insulin, cholera toxin, and epidermal growth factor (EGF) that had previously been used with secondary mammary cultures [244-246] was found to promote continued growth. The importance of each additive to growth was measured and found to be cortisol > EGF > insulin > cholera toxin [168]. However, the effects of each additive have not been characterized further, or repeated after what is undoubtedly a large number of passages since the original study.

Through previous experience in our lab, it was known that growing MCF10A in DMEM + 10% FBS resulted in a morphology change. In order to elucidate the importance of each additive in that change, cells were grown in MCF10A complete medium (DMEM/F12 medium supplemented with 5% horse serum, 20 ng/mL EGF, 100 ng/mL cholera toxin, 10 µg/mL insulin, and 500 ng/mL hydrocortisone) minus one

additive at a time and photographed 14 days later. Cells grown in the absence of EGF died in less than one week. No visible difference was seen when insulin or cholera toxin were left out of the medium, whereas a flattening of cells was seen when hydrocortisone was subtracted and the growth rate decreased noticeably. The morphology change seen with DMEM/F12 + 10% FBS was similar to that seen with medium missing hydrocortisone, with the addition of what appears to be stress fibers (Figure C-1).

Analysis of cellular protein levels shows a small increase in N-cadherin in cells grown without hydrocortisone or cholera toxin as well as a decrease in PDGFR and AXL (Figure C-2). Similar effects were seen using immunofluorescence on cells grown in MCF10A complete or DMEM/F12 + 10% FBS. A clear cadherin switch was photographed, showing E-cadherin or N-cadherin at cell-cell junctions when grown in MCF10A complete or DMEM/F12 + 10% FBS, respectively (Figure C-3 top panels). Equally as dramatic of a change, vimentin staining switched from a diffuse pattern to distinct filaments (middle panels) and staining of γ-catenin decreased (bottom panels) when grown in 10% FBS.

These results illustrate the importance of cell culture conditions on the MCF10A cell line. Although used as an epithelial cell line, these cells only maintain their cuboidal morphology and biochemical profile when grown in the presence of exogenous hydrocortisone. This is important to consider when comparing results of different studies since the growth conditions may not be the same. Examination of the signaling pathways activated by the standard additives will give a deeper understanding of the

mechanisms involved, and the effect of different media on other cell lines could prove to be interesting and worthwhile.

Materials and Methods

Cell culture

The MCF10A cell line was maintained in the suggested [168] 50/50 mixture of Dulbecco's Modified Eagle's Medium and Ham's F12 medium supplemented with 5% horse serum, 20 ng/mL EGF, 100 ng/mL cholera toxin, 10 µg/mL insulin, and 500 ng/mL hydrocortisone (Sigma-Aldrich, St. Louis, MO) or various mixtures of these additives with or without 10% FBS.

Immunofluorescence and immunoblot analysis

Immunofluorescence and immunoblotting were performed as in previous chapters. The γ-catenin antibody was obtained from Santa Cruz Biotech (sc-7900).

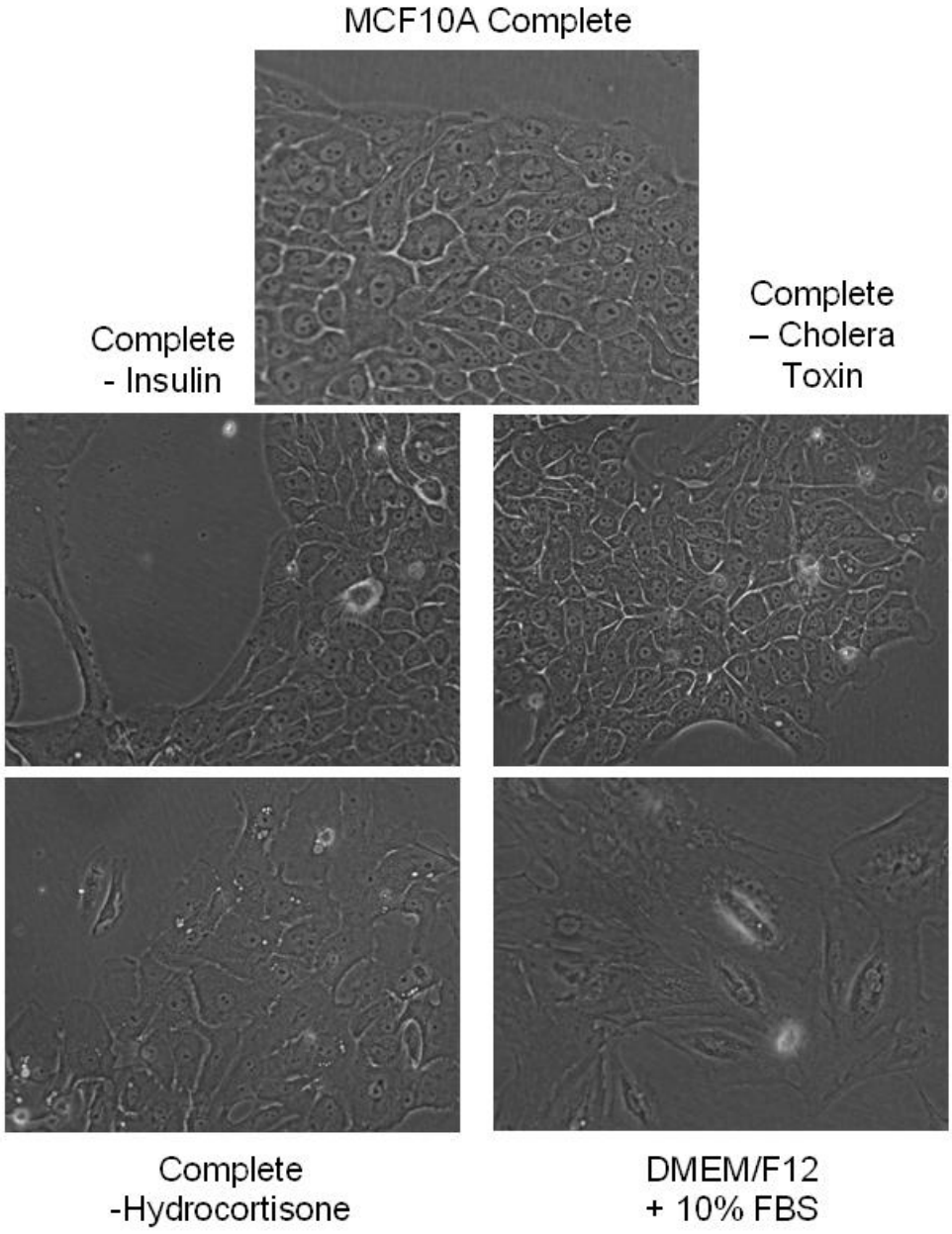

Figure C-1. Growth medium influences morphology of MCF10A cells. Micrographs of MCF10A cells grown in the indicated medium for 14 days.

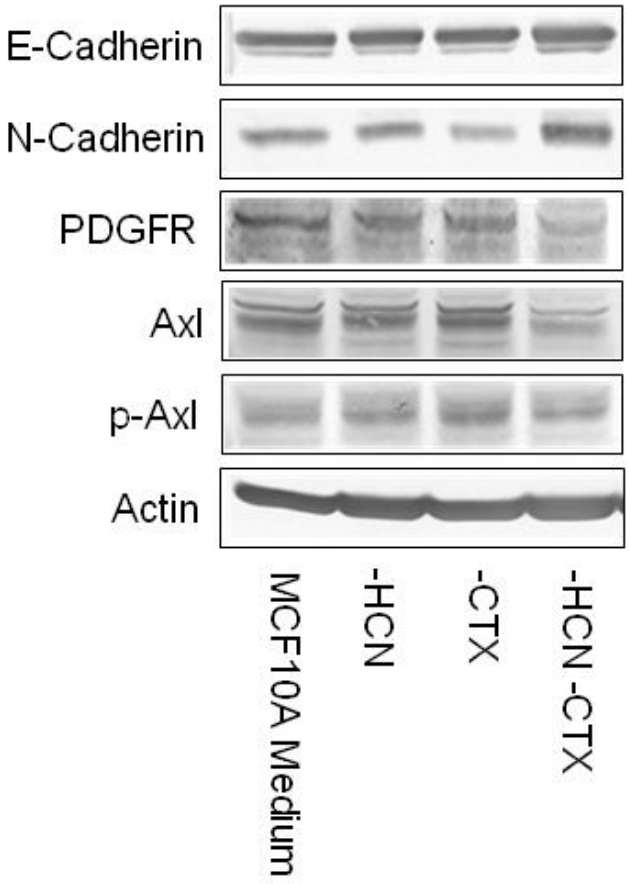

Figure C-2. Biochemical changes in MCF10A cells due to growth media. Immunoblot analysis of MCF10A cells grown in the indicated medium for 14 days.

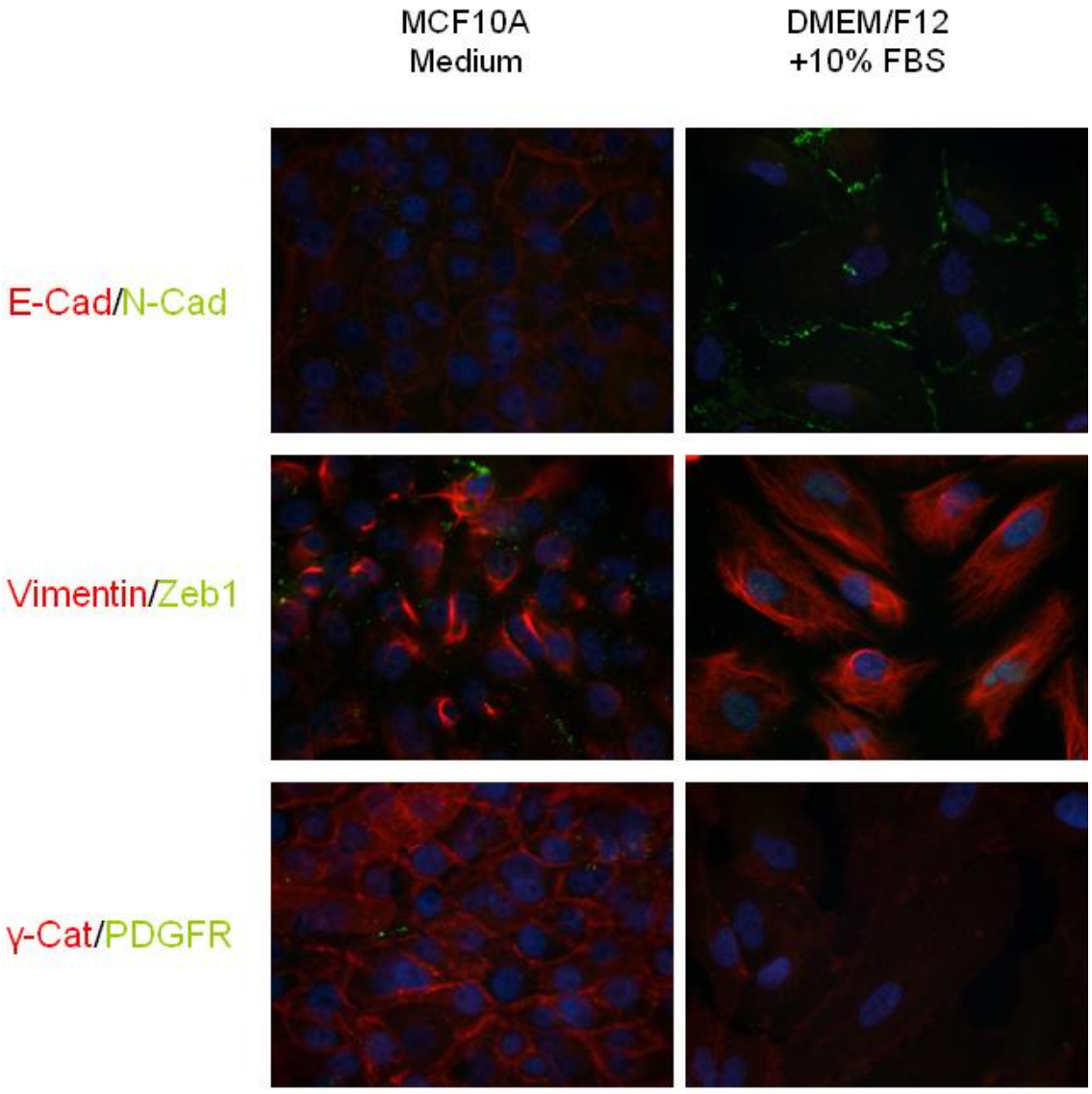

Figure C-3. Growth medium alters intracellular localization of proteins in MCF10A cells. Immunofluorescence of MCF10A cells grown in the indicated medium for 14 days and stained with the indicated antibodies.

LIST OF REFERENCES

[1] American Cancer Society, Cancer Facts & Figures, American Cancer Society, Atlanta, 2012.

[2] A.S. Whittemore, Risk of breast cancer in carriers of BRCA gene mutations, N. Engl. J. Med. 337 (1997) 788-789.

[3] A. McTiernan, Behavioral risk factors in breast cancer: can risk be modified?, Oncologist 8 (2003) 326-334.

[4] V.C. Jordan, Fourteenth Gaddum Memorial Lecture. A current view of tamoxifen for the treatment and prevention of breast cancer, Br. J. Pharmacol. 110 (1993) 507-517.

[5] O. Brouckaert, H. Wildiers, G. Floris, P. Neven, Update on triple-negative breast cancer: prognosis and management strategies, Int J Womens Health 4 (2012) 511-520.

[6] M. Canavese, L. Santo, N. Raje, Cyclin dependent kinases in cancer: Potential for therapeutic intervention, Cancer Biol Ther 13 (2012) 451-457.

[7] A. Schulze, K. Zerfass, D. Spitkovsky, S. Middendorp, J. Berges, K. Helin, P. Jansen-Durr, B. Henglein, Cell cycle regulation of the cyclin A gene promoter is mediated by a variant E2F site, Proc. Natl. Acad. Sci. U. S. A. 92 (1995) 11264-11268.

[8] K. Ohtani, J. DeGregori, J.R. Nevins, Regulation of the cyclin E gene by transcription factor E2F1, Proc. Natl. Acad. Sci. U. S. A. 92 (1995) 12146-12150.

[9] J. DeGregori, T. Kowalik, J.R. Nevins, Cellular targets for activation by the E2F1 transcription factor include DNA synthesis- and G1/S-regulatory genes, Mol. Cell. Biol. 15 (1995) 4215-4224.

[10] N. Dyson, The regulation of E2F by pRB-family proteins, Genes Dev. 12 (1998) 2245-2262.

[11] E.K. Flemington, S.H. Speck, W.G. Kaelin, Jr., E2F-1-mediated transactivation is inhibited by complex formation with the retinoblastoma susceptibility gene product, Proc. Natl. Acad. Sci. U. S. A. 90 (1993) 6914-6918.

[12] J.A. Lees, M. Saito, M. Vidal, M. Valentine, T. Look, E. Harlow, N. Dyson, K. Helin, The retinoblastoma protein binds to a family of E2F transcription factors, Mol. Cell. Biol. 13 (1993) 7813-7825.

[13] H. Aktas, H. Cai, G.M. Cooper, Ras links growth factor signaling to the cell cycle machinery via regulation of cyclin D1 and the Cdk inhibitor p27KIP1, Mol. Cell. Biol. 17 (1997) 3850-3857.

[14] J. Kato, H. Matsushime, S.W. Hiebert, M.E. Ewen, C.J. Sherr, Direct binding of cyclin D to the retinoblastoma gene product (pRb) and pRb phosphorylation by the cyclin D-dependent kinase CDK4, Genes Dev. 7 (1993) 331-342.

[15] S. Bates, L. Bonetta, D. MacAllan, D. Parry, A. Holder, C. Dickson, G. Peters, CDK6 (PLSTIRE) and CDK4 (PSK-J3) are a distinct subset of the cyclin-dependent kinases that associate with cyclin D1, Oncogene 9 (1994) 71-79.

[16] M. Hatakeyama, J.A. Brill, G.R. Fink, R.A. Weinberg, Collaboration of G1 cyclins in the functional inactivation of the retinoblastoma protein, Genes Dev. 8 (1994) 1759-1771.

[17] A. Koff, A. Giordano, D. Desai, K. Yamashita, J.W. Harper, S. Elledge, T. Nishimoto, D.O. Morgan, B.R. Franza, J.M. Roberts, Formation and activation of a cyclin E-cdk2 complex during the G1 phase of the human cell cycle, Science 257 (1992) 1689-1694.

[18] T. Akiyama, T. Ohuchi, S. Sumida, K. Matsumoto, K. Toyoshima, Phosphorylation of the retinoblastoma protein by cdk2, Proc. Natl. Acad. Sci. U. S. A. 89 (1992) 7900-7904.

[19] F. Fang, J.W. Newport, Evidence that the G1-S and G2-M transitions are controlled by different cdc2 proteins in higher eukaryotes, Cell 66 (1991) 731-742.

[20] S.N. Martineau, P.R. Andreassen, R.L. Margolis, Delay of HeLa cell cleavage into interphase using dihydrocytochalasin B: retention of a postmitotic spindle and telophase disc correlates with synchronous cleavage recovery, J. Cell Biol. 131 (1995) 191-205.

[21] D. Desai, Y. Gu, D.O. Morgan, Activation of human cyclin-dependent kinases in vitro, Mol. Biol. Cell 3 (1992) 571-582.

[22] D. Desai, H.C. Wessling, R.P. Fisher, D.O. Morgan, Effects of phosphorylation by CAK on cyclin binding by CDC2 and CDK2, Mol. Cell. Biol. 15 (1995) 345-350.

[23] L.L. Parker, H. Piwnica-Worms, Inactivation of the p34cdc2-cyclin B complex by the human WEE1 tyrosine kinase, Science 257 (1992) 1955-1957.

[24] U. Strausfeld, J.C. Labbe, D. Fesquet, J.C. Cavadore, A. Picard, K. Sadhu, P. Russell, M. Doree, Dephosphorylation and activation of a p34cdc2/cyclin B complex in vitro by human CDC25 protein, Nature 351 (1991) 242-245.

[25] H. Toyoshima, T. Hunter, p27, a novel inhibitor of G1 cyclin-Cdk protein kinase activity, is related to p21, Cell 78 (1994) 67-74.

[26] Y. Xiong, G.J. Hannon, H. Zhang, D. Casso, R. Kobayashi, D. Beach, p21 is a universal inhibitor of cyclin kinases, Nature 366 (1993) 701-704.

[27] M.H. Lee, I. Reynisdottir, J. Massague, Cloning of p57KIP2, a cyclin-dependent kinase inhibitor with unique domain structure and tissue distribution, Genes Dev. 9 (1995) 639-649.

[28] G.J. Hannon, D. Beach, p15INK4B is a potential effector of TGF-beta-induced cell cycle arrest, Nature 371 (1994) 257-261.

[29] M. Serrano, G.J. Hannon, D. Beach, A new regulatory motif in cell-cycle control causing specific inhibition of cyclin D/CDK4, Nature 366 (1993) 704-707.

[30] K.L. Guan, C.W. Jenkins, Y. Li, M.A. Nichols, X. Wu, C.L. O'Keefe, A.G. Matera, Y. Xiong, Growth suppression by p18, a p16INK4/MTS1- and p14INK4B/MTS2-related CDK6 inhibitor, correlates with wild-type pRb function, Genes Dev. 8 (1994) 2939-2952.

[31] T. Okuda, H. Hirai, V.A. Valentine, S.A. Shurtleff, V.J. Kidd, J.M. Lahti, C.J. Sherr, J.R. Downing, Molecular cloning, expression pattern, and chromosomal localization of human CDKN2D/INK4d, an inhibitor of cyclin D-dependent kinases, Genomics 29 (1995) 623-630.

[32] W.S. el-Deiry, T. Tokino, V.E. Velculescu, D.B. Levy, R. Parsons, J.M. Trent, D. Lin, W.E. Mercer, K.W. Kinzler, B. Vogelstein, WAF1, a potential mediator of p53 tumor suppression, Cell 75 (1993) 817-825.

[33] M.L. Rodriguez-Puebla, P.L. Miliani de Marval, M. LaCava, D.S. Moons, H. Kiyokawa, C.J. Conti, Cdk4 deficiency inhibits skin tumor development but does not affect normal keratinocyte proliferation, Am. J. Pathol. 161 (2002) 405-411.

[34] M. Malumbres, R. Sotillo, D. Santamaria, J. Galan, A. Cerezo, S. Ortega, P. Dubus, M. Barbacid, Mammalian cells cycle without the D-type cyclin-dependent kinases Cdk4 and Cdk6, Cell 118 (2004) 493-504.

[35] C. Berthet, E. Aleem, V. Coppola, L. Tessarollo, P. Kaldis, Cdk2 knockout mice are viable, Curr. Biol. 13 (2003) 1775-1785.

[36] E. Aleem, H. Kiyokawa, P. Kaldis, Cdc2-cyclin E complexes regulate the G1/S phase transition, Nat Cell Biol 7 (2005) 831-836.

[37] D. Santamaria, C. Barriere, A. Cerqueira, S. Hunt, C. Tardy, K. Newton, J.F. Caceres, P. Dubus, M. Malumbres, M. Barbacid, Cdk1 is sufficient to drive the mammalian cell cycle, Nature 448 (2007) 811-815.

[38] S.G. Rane, S.C. Cosenza, R.V. Mettus, E.P. Reddy, Germ line transmission of the Cdk4(R24C) mutation facilitates tumorigenesis and escape from cellular senescence, Mol. Cell. Biol. 22 (2002) 644-656.

[39] Z.E. Winters, N.C. Hunt, M.J. Bradburn, J.A. Royds, H. Turley, A.L. Harris, C.J. Norbury, Subcellular localisation of cyclin B, Cdc2 and p21(WAF1/CIP1) in breast cancer. association with prognosis, Eur. J. Cancer 37 (2001) 2405-2412.

[40] M. Hollstein, D. Sidransky, B. Vogelstein, C.C. Harris, p53 mutations in human cancers, Science 253 (1991) 49-53.

[41] R. Mirzayans, B. Andrais, A. Scott, D. Murray, New Insights into p53 Signaling and Cancer Cell Response to DNA Damage: Implications for Cancer Therapy, J Biomed Biotechnol 2012 (2012) 170325.

[42] C. Salon, G. Merdzhanova, C. Brambilla, E. Brambilla, S. Gazzeri, B. Eymin, E2F-1, Skp2 and cyclin E oncoproteins are upregulated and directly correlated in high-grade neuroendocrine lung tumors, Oncogene 26 (2007) 6927-6936.

[43] W.D. Foulkes, J.S. Brunet, I.M. Stefansson, O. Straume, P.O. Chappuis, L.R. Begin, N. Hamel, J.R. Goffin, N. Wong, M. Trudel, L. Kapusta, P. Porter, L.A. Akslen, The prognostic implication of the basal-like (cyclin E high/p27 low/p53+/glomeruloid-microvascular-proliferation+) phenotype of BRCA1-related breast cancer, Cancer Res. 64 (2004) 830-835.

[44] K. Keyomarsi, S.L. Tucker, T.A. Buchholz, M. Callister, Y. Ding, G.N. Hortobagyi, I. Bedrosian, C. Knickerbocker, W. Toyofuku, M. Lowe, T.W. Herliczek, S.S. Bacus, Cyclin E and survival in patients with breast cancer, N. Engl. J. Med. 347 (2002) 1566-1575.

[45] K.K. Hunt, K. Keyomarsi, Cyclin E as a prognostic and predictive marker in breast cancer, Semin. Cancer Biol. 15 (2005) 319-326.

[46] S. Akli, X.Q. Zhang, J. Bondaruk, S.L. Tucker, P.B. Czerniak, W.F. Benedict, K. Keyomarsi, Low molecular weight cyclin E is associated with p27-resistant, high-grade, high-stage and invasive bladder cancer, Cell Cycle 11 (2012) 1468-1476.

[47] R.M. Harwell, B.B. Mull, D.C. Porter, K. Keyomarsi, Activation of cyclin-dependent kinase 2 by full length and low molecular weight forms of cyclin E in breast cancer cells, J. Biol. Chem. 279 (2004) 12695-12705.

[48] K.J. Sweeney, A. Swarbrick, R.L. Sutherland, E.A. Musgrove, Lack of relationship between CDK activity and G1 cyclin expression in breast cancer cells, Oncogene 16 (1998) 2865-2878.

[49] E. Mylona, K. Tzelepis, I. Theohari, I. Giannopoulou, C. Papadimitriou, L. Nakopoulou, Cyclin D1 in invasive breast carcinoma: favourable prognostic significance in unselected patients and within subgroups with an aggressive phenotype, Histopathology 62 (2013) 472-480.

[50] M.A. Parker, N.G. Deane, E.A. Thompson, R.H. Whitehead, S.K. Mithani, M.K. Washington, P.K. Datta, D.A. Dixon, R.D. Beauchamp, Over-expression of cyclin D1 regulates Cdk4 protein synthesis, Cell Prolif. 36 (2003) 347-360.

[51] Q.P. Dou, G. Molnar, A.B. Pardee, Cyclin D1/cdk2 kinase is present in a G1 phase-specific protein complex Yi1 that binds to the mouse thymidine kinase gene promoter, Biochem. Biophys. Res. Commun. 205 (1994) 1859-1868.

[52] V. Dulic, L.F. Drullinger, E. Lees, S.I. Reed, G.H. Stein, Altered regulation of G1 cyclins in senescent human diploid fibroblasts: accumulation of inactive cyclin E-Cdk2 and cyclin D1-Cdk2 complexes, Proc. Natl. Acad. Sci. U. S. A. 90 (1993) 11034-11038.

[53] A. Chytil, M. Waltner-Law, R. West, D. Friedman, M. Aakre, D. Barker, B. Law, Construction of a cyclin D1-Cdk2 fusion protein to model the biological functions of cyclin D1-Cdk2 complexes, J. Biol. Chem. 279 (2004) 47688-47698.

[54] P. Corsino, B. Davis, M. Law, A. Chytil, E. Forrester, P. Norgaard, N. Teoh, B. Law, Tumors initiated by constitutive Cdk2 activation exhibit transforming growth factor beta resistance and acquire paracrine mitogenic stimulation during progression, Cancer Res. 67 (2007) 3135-3144.

[55] F. Bienvenu, S. Jirawatnotai, J.E. Elias, C.A. Meyer, K. Mizeracka, A. Marson, G.M. Frampton, M.F. Cole, D.T. Odom, J. Odajima, Y. Geng, A. Zagozdzon, M. Jecrois, R.A. Young, X.S. Liu, C.L. Cepko, S.P. Gygi, P. Sicinski, Transcriptional role of cyclin D1 in development revealed by a genetic-proteomic screen, Nature 463 (2010) 374-378.

[56] G. Kaur, M. Stetler-Stevenson, S. Sebers, P. Worland, H. Sedlacek, C. Myers, J. Czech, R. Naik, E. Sausville, Growth inhibition with reversible cell cycle arrest of carcinoma cells by flavone L86-8275, J. Natl. Cancer Inst. 84 (1992) 1736-1740.

[57] G.I. Shapiro, Preclinical and clinical development of the cyclin-dependent kinase inhibitor flavopiridol, Clin. Cancer Res. 10 (2004) 4270s-4275s.

[58] A.M. Senderowicz, Small-molecule cyclin-dependent kinase modulators, Oncogene 22 (2003) 6609-6620.

[59] A.M. Senderowicz, D. Headlee, S.F. Stinson, R.M. Lush, N. Kalil, L. Villalba, K. Hill, S.M. Steinberg, W.D. Figg, A. Tompkins, S.G. Arbuck, E.A. Sausville, Phase I trial of continuous infusion flavopiridol, a novel cyclin-dependent kinase inhibitor, in patients with refractory neoplasms, J. Clin. Oncol. 16 (1998) 2986-2999.

[60] L.A. Geddes, W.A. Tacker, P. Cabler, A new electrical hazard associated with the electrocautery, Med. Instrum. 9 (1975) 112-113.

[61] J.E. Karp, E.L. Garrett-Mayer, E.H. Estey, M.A. Rudek, B.D. Smith, J.M. Greer, D.M. Drye, K. Mackey, K.S. Dorcy, S.D. Gore, M.J. Levis, M.A. McDevitt, H.E. Carraway, K.W. Pratz, D.E. Gladstone, M.M. Showell, M. Othus, L.A. Doyle, J.J. Wright, J.M. Pagel, Randomized phase II study of two schedules of flavopiridol given as timed sequential therapy with cytosine arabinoside and mitoxantrone for adults with newly diagnosed, poor-risk acute myelogenous leukemia, Haematologica (2012).

[62] K.C. Bible, P.P. Peethambaram, A.L. Oberg, W. Maples, D.L. Groteluschen, M. Boente, J.K. Burton, L.C. Gomez Dahl, J.D. Tibodeau, C.R. Isham, J.L. Maguire, V. Shridhar, A.K. Kukla, K.J. Voll, M.J. Mauer, A.D. Colevas, J. Wright, L.A. Doyle, C. Erlichman, A Phase 2 Trial of Flavopiridol (Alvocidib) and Cisplatin in Platin-Resistant Ovarian and Primary Peritoneal Carcinoma: MC0261, Gynecol. Oncol. 127 (2012) 55-62.

[63] C. Benson, J. White, J. De Bono, A. O'Donnell, F. Raynaud, C. Cruickshank, H. McGrath, M. Walton, P. Workman, S. Kaye, J. Cassidy, A. Gianella-Borradori, I. Judson, C. Twelves, A phase I trial of the selective oral cyclin-dependent kinase inhibitor seliciclib (CYC202; R-Roscovitine), administered twice daily for 7 days every 21 days, Br. J. Cancer 96 (2007) 29-37.

[64] C. Le Tourneau, S. Faivre, V. Laurence, C. Delbaldo, K. Vera, V. Girre, J. Chiao, S. Armour, S. Frame, S.R. Green, A. Gianella-Borradori, V. Dieras, E. Raymond, Phase I evaluation of seliciclib (R-roscovitine), a novel oral cyclin-dependent kinase inhibitor, in patients with advanced malignancies, Eur. J. Cancer 46 (2010) 3243-3250.

[65] L. Meijer, A. Borgne, O. Mulner, J.P. Chong, J.J. Blow, N. Inagaki, M. Inagaki, J.G. Delcros, J.P. Moulinoux, Biochemical and cellular effects of roscovitine, a potent and selective inhibitor of the cyclin-dependent kinases cdc2, cdk2 and cdk5, Eur. J. Biochem. 243 (1997) 527-536.

[66] E.E. Brooks, N.S. Gray, A. Joly, S.S. Kerwar, R. Lum, R.L. Mackman, T.C. Norman, J. Rosete, M. Rowe, S.R. Schow, P.G. Schultz, X. Wang, M.M. Wick, D. Shiffman, CVT-313, a specific and potent inhibitor of CDK2 that prevents neointimal proliferation, J. Biol. Chem. 272 (1997) 29207-29211.

[67] P. Corsino, N. Horenstein, D. Ostrov, T. Rowe, M. Law, A. Barrett, G. Aslanidi, W.D. Cress, B. Law, A novel class of cyclin-dependent kinase inhibitors identified by molecular docking act through a unique mechanism, J. Biol. Chem. 284 (2009) 29945-29955.

[68] T. Boveri, Concerning the origin of malignant tumours by Theodor Boveri. Translated and annotated by Henry Harris, J. Cell Sci. 121 Suppl 1 (2008) 1-84.

[69] R.E. Zirkle, Ultraviolet-microbeam irradiation of newt-cell cytoplasm: spindle destruction, false anaphase, and delay of true anaphase, Radiat. Res. 41 (1970) 516-537.

[70] M.C. Wani, H.L. Taylor, M.E. Wall, P. Coggon, A.T. McPhail, Plant antitumor agents. VI. The isolation and structure of taxol, a novel antileukemic and antitumor agent from Taxus brevifolia, J. Am. Chem. Soc. 93 (1971) 2325-2327.

[71] C.L. Rieder, R.E. Palazzo, Colcemid and the mitotic cycle, J. Cell Sci. 102 (Pt 3) (1992) 387-392.

[72] J.M. Peters, The anaphase promoting complex/cyclosome: a machine designed to destroy, Nat Rev Mol Cell Biol 7 (2006) 644-656.

[73] A. De Antoni, C.G. Pearson, D. Cimini, J.C. Canman, V. Sala, L. Nezi, M. Mapelli, L. Sironi, M. Faretta, E.D. Salmon, A. Musacchio, The Mad1/Mad2 complex as a template for Mad2 activation in the spindle assembly checkpoint, Curr. Biol. 15 (2005) 214-225.

[74] C.L. Rieder, R.W. Cole, A. Khodjakov, G. Sluder, The checkpoint delaying anaphase in response to chromosome monoorientation is mediated by an inhibitory signal produced by unattached kinetochores, J. Cell Biol. 130 (1995) 941-948.

[75] A.L. Knowlton, W. Lan, P.T. Stukenberg, Aurora B is enriched at merotelic attachment sites, where it regulates MCAK, Curr. Biol. 16 (2006) 1705-1710.

[76] B.A. Pinsky, S. Biggins, The spindle checkpoint: tension versus attachment, Trends Cell Biol. 15 (2005) 486-493.

[77] E. Hernando, I. Orlow, V. Liberal, G. Nohales, R. Benezra, C. Cordon-Cardo, Molecular analyses of the mitotic checkpoint components hsMAD2, hBUB1 and hBUB3 in human cancer, Int. J. Cancer 95 (2001) 223-227.

[78] L.S. Michel, V. Liberal, A. Chatterjee, R. Kirchwegger, B. Pasche, W. Gerald, M. Dobles, P.K. Sorger, V.V. Murty, R. Benezra, MAD2 haplo-insufficiency causes

premature anaphase and chromosome instability in mammalian cells, Nature 409 (2001) 355-359.

[79] D.J. Baker, K.B. Jeganathan, J.D. Cameron, M. Thompson, S. Juneja, A. Kopecka, R. Kumar, R.B. Jenkins, P.C. de Groen, P. Roche, J.M. van Deursen, BubR1 insufficiency causes early onset of aging-associated phenotypes and infertility in mice, Nat. Genet. 36 (2004) 744-749.

[80] W. Dai, Q. Wang, T. Liu, M. Swamy, Y. Fang, S. Xie, R. Mahmood, Y.M. Yang, M. Xu, C.V. Rao, Slippage of mitotic arrest and enhanced tumor development in mice with BubR1 haploinsufficiency, Cancer Res. 64 (2004) 440-445.

[81] J.R. Babu, K.B. Jeganathan, D.J. Baker, X. Wu, N. Kang-Decker, J.M. van Deursen, Rae1 is an essential mitotic checkpoint regulator that cooperates with Bub3 to prevent chromosome missegregation, J. Cell Biol. 160 (2003) 341-353.

[82] K. Tsukasaki, C.W. Miller, E. Greenspun, S. Eshaghian, H. Kawabata, T. Fujimoto, M. Tomonaga, C. Sawyers, J.W. Said, H.P. Koeffler, Mutations in the mitotic check point gene, MAD1L1, in human cancers, Oncogene 20 (2001) 3301-3305.

[83] G.J. Kops, D.R. Foltz, D.W. Cleveland, Lethality to human cancer cells through massive chromosome loss by inhibition of the mitotic checkpoint, Proc. Natl. Acad. Sci. U. S. A. 101 (2004) 8699-8704.

[84] M. Malumbres, M. Barbacid, Cell cycle kinases in cancer, Curr. Opin. Genet. Dev. 17 (2007) 60-65.

[85] P. Silva, J. Barbosa, A.V. Nascimento, J. Faria, R. Reis, H. Bousbaa, Monitoring the fidelity of mitotic chromosome segregation by the spindle assembly checkpoint, Cell Prolif. 44 (2011) 391-400.

[86] R.W. Wilkinson, R. Odedra, S.P. Heaton, S.R. Wedge, N.J. Keen, C. Crafter, J.R. Foster, M.C. Brady, A. Bigley, E. Brown, K.F. Byth, N.C. Barrass, K.E. Mundt, K.M. Foote, N.M. Heron, F.H. Jung, A.A. Mortlock, F.T. Boyle, S. Green, AZD1152, a selective inhibitor of Aurora B kinase, inhibits human tumor xenograft growth by inducing apoptosis, Clin. Cancer Res. 13 (2007) 3682-3688.

[87] C. Wong, T. Stearns, Mammalian cells lack checkpoints for tetraploidy, aberrant centrosome number, and cytokinesis failure, BMC Cell Biol 6 (2005) 6.

[88] P.R. Andreassen, O.D. Lohez, F.B. Lacroix, R.L. Margolis, Tetraploid state induces p53-dependent arrest of nontransformed mammalian cells in G1, Mol. Biol. Cell 12 (2001) 1315-1328.

[89] C.L. Rieder, H. Maiato, Stuck in division or passing through: what happens when cells cannot satisfy the spindle assembly checkpoint, Dev Cell 7 (2004) 637-651.

[90] M. Castedo, A. Coquelle, S. Vivet, I. Vitale, A. Kauffmann, P. Dessen, M.O. Pequignot, N. Casares, A. Valent, S. Mouhamad, E. Schmitt, N. Modjtahedi, W. Vainchenker, L. Zitvogel, V. Lazar, C. Garrido, G. Kroemer, Apoptosis regulation in tetraploid cancer cells, EMBO J. 25 (2006) 2584-2595.

[91] Y. Uetake, G. Sluder, Cell cycle progression after cleavage failure: mammalian somatic cells do not possess a "tetraploidy checkpoint", J. Cell Biol. 165 (2004) 609-615.

[92] A. Krzywicka-Racka, G. Sluder, Repeated cleavage failure does not establish centrosome amplification in untransformed human cells, J. Cell Biol. 194 (2011) 199-207.

[93] K. Mikule, B. Delaval, P. Kaldis, A. Jurcyzk, P. Hergert, S. Doxsey, Loss of centrosome integrity induces p38-p53-p21-dependent G1-S arrest, Nat Cell Biol 9 (2007) 160-170.

[94] D. Hanahan, R.A. Weinberg, Hallmarks of cancer: the next generation, Cell 144 (2011) 646-674.

[95] S. Raptis, B. Bapat, Genetic instability in human tumors, EXS (2006) 303-320.

[96] A. Meindl, N. Ditsch, K. Kast, K. Rhiem, R.K. Schmutzler, Hereditary breast and ovarian cancer: new genes, new treatments, new concepts, Dtsch Arztebl Int 108 (2011) 323-330.

[97] N.J. Ganem, S.A. Godinho, D. Pellman, A mechanism linking extra centrosomes to chromosomal instability, Nature 460 (2009) 278-282.

[98] M. Paintrand, M. Moudjou, H. Delacroix, M. Bornens, Centrosome organization and centriole architecture: their sensitivity to divalent cations, J. Struct. Biol. 108 (1992) 107-128.

[99] J. Azimzadeh, W.F. Marshall, Building the centriole, Curr. Biol. 20 (2010) R816-825.

[100] R. Habedanck, Y.D. Stierhof, C.J. Wilkinson, E.A. Nigg, The Polo kinase Plk4 functions in centriole duplication, Nat Cell Biol 7 (2005) 1140-1146.

[101] M. Bettencourt-Dias, A. Rodrigues-Martins, L. Carpenter, M. Riparbelli, L. Lehmann, M.K. Gatt, N. Carmo, F. Balloux, G. Callaini, D.M. Glover, SAK/PLK4 is required for centriole duplication and flagella development, Curr. Biol. 15 (2005) 2199-2207.

[102] Y. Tokuyama, H.F. Horn, K. Kawamura, P. Tarapore, K. Fukasawa, Specific phosphorylation of nucleophosmin on Thr(199) by cyclin-dependent kinase 2-cyclin E and its role in centrosome duplication, J. Biol. Chem. 276 (2001) 21529-21537.

[103] Z. Chen, V.B. Indjeian, M. McManus, L. Wang, B.D. Dynlacht, CP110, a cell cycle-dependent CDK substrate, regulates centrosome duplication in human cells, Dev Cell 3 (2002) 339-350.

[104] E.A. Nigg, Centrosome aberrations: cause or consequence of cancer progression?, Nat Rev Cancer 2 (2002) 815-825.

[105] K. Kawamura, H. Izumi, Z. Ma, R. Ikeda, M. Moriyama, T. Tanaka, T. Nojima, L.S. Levin, K. Fujikawa-Yamamoto, K. Suzuki, K. Fukasawa, Induction of centrosome amplification and chromosome instability in human bladder cancer cells by p53 mutation and cyclin E overexpression, Cancer Res. 64 (2004) 4800-4809.

[106] C.J. Tang, S.Y. Lin, W.B. Hsu, Y.N. Lin, C.T. Wu, Y.C. Lin, C.W. Chang, K.S. Wu, T.K. Tang, The human microcephaly protein STIL interacts with CPAP and is required for procentriole formation, EMBO J. 30 (2011) 4790-4804.

[107] S. Leidel, M. Delattre, L. Cerutti, K. Baumer, P. Gonczy, SAS-6 defines a protein family required for centrosome duplication in C. elegans and in human cells, Nat Cell Biol 7 (2005) 115-125.

[108] J.C. Macmillan, J.W. Hudson, S. Bull, J.W. Dennis, C.J. Swallow, Comparative expression of the mitotic regulators SAK and PLK in colorectal cancer, Ann. Surg. Oncol. 8 (2001) 729-740.

[109] A. Erez, M. Perelman, S.M. Hewitt, G. Cojacaru, I. Goldberg, I. Shahar, P. Yaron, I. Muler, S. Campaner, N. Amariglio, G. Rechavi, I.R. Kirsch, M. Krupsky, N. Kaminski, S. Izraeli, Sil overexpression in lung cancer characterizes tumors with increased mitotic activity, Oncogene 23 (2004) 5371-5377.

[110] S. La Terra, C.N. English, P. Hergert, B.F. McEwen, G. Sluder, A. Khodjakov, The de novo centriole assembly pathway in HeLa cells: cell cycle progression and centriole assembly/maturation, J. Cell Biol. 168 (2005) 713-722.

[111] Y. Uetake, J. Loncarek, J.J. Nordberg, C.N. English, S. La Terra, A. Khodjakov, G. Sluder, Cell cycle progression and de novo centriole assembly after centrosomal removal in untransformed human cells, J. Cell Biol. 176 (2007) 173-182.

[112] K. Neben, B. Tews, G. Wrobel, M. Hahn, F. Kokocinski, C. Giesecke, U. Krause, A.D. Ho, A. Kramer, P. Lichter, Gene expression patterns in acute myeloid leukemia correlate with centrosome aberrations and numerical chromosome changes, Oncogene 23 (2004) 2379-2384.

[113] K. Neben, G. Ott, S. Schweizer, J. Kalla, B. Tews, T. Katzenberger, M. Hahn, A. Rosenwald, A.D. Ho, H.K. Muller-Hermelink, P. Lichter, A. Kramer, Expression of centrosome-associated gene products is linked to tetraploidization in mantle cell lymphoma, Int. J. Cancer 120 (2007) 1669-1677.

[114] H. Nagase, Y. Nakamura, Mutations of the APC (adenomatous polyposis coli) gene, Hum. Mutat. 2 (1993) 425-434.

[115] C.M. Caldwell, R.A. Green, K.B. Kaplan, APC mutations lead to cytokinetic failures in vitro and tetraploid genotypes in Min mice, J. Cell Biol. 178 (2007) 1109-1120.

[116] W.M. Zhao, G. Fang, Anillin is a substrate of anaphase-promoting complex/cyclosome (APC/C) that controls spatial contractility of myosin during late cytokinesis, J. Biol. Chem. 280 (2005) 33516-33524.

[117] C. Lindon, J. Pines, Ordered proteolysis in anaphase inactivates Plk1 to contribute to proper mitotic exit in human cells, J. Cell Biol. 164 (2004) 233-241.

[118] S. Stewart, G. Fang, Destruction box-dependent degradation of aurora B is mediated by the anaphase-promoting complex/cyclosome and Cdh1, Cancer Res. 65 (2005) 8730-8735.

[119] A.J. Piekny, M. Glotzer, Anillin is a scaffold protein that links RhoA, actin, and myosin during cytokinesis, Curr. Biol. 18 (2008) 30-36.

[120] J. Li, J. Wang, H. Jiao, J. Liao, X. Xu, Cytokinesis and cancer: Polo loves ROCK'n' Rho(A), J Genet Genomics 37 (2010) 159-172.

[121] T. Saeki, M. Ouchi, T. Ouchi, Physiological and oncogenic Aurora-A pathway, Int J Biol Sci 5 (2009) 758-762.

[122] D. Chen, Y. Zhang, Q. Yi, Y. Huang, H. Hou, Q. Hao, H.J. Cooke, L. Li, Q. Sun, Q. Shi, Regulation of asymmetrical cytokinesis by cAMP during meiosis I in mouse oocytes, PLoS One 7 (2012) e29735.

[123] L.L. Satterwhite, M.J. Lohka, K.L. Wilson, T.Y. Scherson, L.J. Cisek, J.L. Corden, T.D. Pollard, Phosphorylation of myosin-II regulatory light chain by cyclin-p34cdc2: a mechanism for the timing of cytokinesis, J. Cell Biol. 118 (1992) 595-605.

[124] D. Ring, R. Hubble, M. Kirschner, Mitosis in a cell with multiple centrioles, J. Cell Biol. 94 (1982) 549-556.

[125] M. Kwon, S.A. Godinho, N.S. Chandhok, N.J. Ganem, A. Azioune, M. Thery, D. Pellman, Mechanisms to suppress multipolar divisions in cancer cells with extra centrosomes, Genes Dev. 22 (2008) 2189-2203.

[126] D. Cimini, Merotelic kinetochore orientation, aneuploidy, and cancer, Biochim. Biophys. Acta 1786 (2008) 32-40.

[127] B.A. Weaver, A.D. Silk, C. Montagna, P. Verdier-Pinard, D.W. Cleveland, Aneuploidy acts both oncogenically and as a tumor suppressor, Cancer Cell 11 (2007) 25-36.

[128] R. Sotillo, E. Hernando, E. Diaz-Rodriguez, J. Teruya-Feldstein, C. Cordon-Cardo, S.W. Lowe, R. Benezra, Mad2 overexpression promotes aneuploidy and tumorigenesis in mice, Cancer Cell 11 (2007) 9-23.

[129] R.M. Ricke, K.B. Jeganathan, J.M. van Deursen, Bub1 overexpression induces aneuploidy and tumor formation through Aurora B kinase hyperactivation, J. Cell Biol. 193 (2011) 1049-1064.

[130] C.J. Sherr, Cancer cell cycles, Science 274 (1996) 1672-1677.

[131] E. Hernando, Z. Nahle, G. Juan, E. Diaz-Rodriguez, M. Alaminos, M. Hemann, L. Michel, V. Mittal, W. Gerald, R. Benezra, S.W. Lowe, C. Cordon-Cardo, Rb inactivation promotes genomic instability by uncoupling cell cycle progression from mitotic control, Nature 430 (2004) 797-802.

[132] A. Walther, R. Houlston, I. Tomlinson, Association between chromosomal instability and prognosis in colorectal cancer: a meta-analysis, Gut 57 (2008) 941-950.

[133] A.J. Lee, D. Endesfelder, A.J. Rowan, A. Walther, N.J. Birkbak, P.A. Futreal, J. Downward, Z. Szallasi, I.P. Tomlinson, M. Howell, M. Kschischo, C. Swanton, Chromosomal instability confers intrinsic multidrug resistance, Cancer Res. 71 (2011) 1858-1870.

[134] D. Liu, G. Vader, M.J. Vromans, M.A. Lampson, S.M. Lens, Sensing chromosome bi-orientation by spatial separation of aurora B kinase from kinetochore substrates, Science 323 (2009) 1350-1353.

[135] D.S. Boss, P.O. Witteveen, J. van der Sar, M.P. Lolkema, E.E. Voest, P.K. Stockman, O. Ataman, D. Wilson, S. Das, J.H. Schellens, Clinical evaluation of AZD1152, an i.v. inhibitor of Aurora B kinase, in patients with solid malignant tumors, Ann. Oncol. 22 (2011) 431-437.

[136] R. Kuriyama, M. Kofron, R. Essner, T. Kato, S. Dragas-Granoic, C.K. Omoto, A. Khodjakov, Characterization of a minus end-directed kinesin-like motor protein from cultured mammalian cells, J. Cell Biol. 129 (1995) 1049-1059.

[137] V. Mountain, C. Simerly, L. Howard, A. Ando, G. Schatten, D.A. Compton, The kinesin-related protein, HSET, opposes the activity of Eg5 and cross-links microtubules in the mammalian mitotic spindle, J. Cell Biol. 147 (1999) 351-366.

[138] P.C. Nowell, The clonal evolution of tumor cell populations, Science 194 (1976) 23-28.

[139] T. Fujiwara, M. Bandi, M. Nitta, E.V. Ivanova, R.T. Bronson, D. Pellman, Cytokinesis failure generating tetraploids promotes tumorigenesis in p53-null cells, Nature 437 (2005) 1043-1047.

[140] G. Sluder, J.J. Nordberg, The good, the bad and the ugly: the practical consequences of centrosome amplification, Curr. Opin. Cell Biol. 16 (2004) 49-54.

[141] P. Deangelis, T. Stokke, L. Smedshammer, R. Lothe, G. Meling, M. Rofstad, Y. Chen, O. Clausen, P53 expression is associated with a high-degree of tumor DNA aneuploidy and incidence of p53 gene mutation, and is localized to the aneuploid component in colorectal carcinomas, Int. J. Oncol. 3 (1993) 305-312.

[142] P. Collecchi, T. Santoni, E. Gnesi, A. Giuseppe Naccarato, A. Passoni, M. Rocchetta, R. Danesi, G. Bevilacqua, Cyclins of phases G1, S and G2/M are overexpressed in aneuploid mammary carcinomas, Cytometry 42 (2000) 254-260.

[143] C.J. Nelsen, R. Kuriyama, B. Hirsch, V.C. Negron, W.L. Lingle, M.M. Goggin, M.W. Stanley, J.H. Albrecht, Short term cyclin D1 overexpression induces centrosome amplification, mitotic spindle abnormalities, and aneuploidy, J. Biol. Chem. 280 (2005) 768-776.

[144] X. Zeng, F.Y. Shaikh, M.K. Harrison, A.M. Adon, A.J. Trimboli, K.A. Carroll, N. Sharma, C. Timmers, L.A. Chodosh, G. Leone, H.I. Saavedra, The Ras oncogene signals centrosome amplification in mammary epithelial cells through cyclin D1/Cdk4 and Nek2, Oncogene 29 (2010) 5103-5112.

[145] S. Ussar, T. Voss, MEK1 and MEK2, different regulators of the G1/S transition, J. Biol. Chem. 279 (2004) 43861-43869.

[146] A.M. Adon, X. Zeng, M.K. Harrison, S. Sannem, H. Kiyokawa, P. Kaldis, H.I. Saavedra, Cdk2 and Cdk4 regulate the centrosome cycle and are critical

mediators of centrosome amplification in p53-null cells, Mol. Cell. Biol. 30 (2010) 694-710.

[147] E.A. Hanse, C.J. Nelsen, M.M. Goggin, C.K. Anttila, L.K. Mullany, C. Berthet, P. Kaldis, G.S. Crary, R. Kuriyama, J.H. Albrecht, Cdk2 plays a critical role in hepatocyte cell cycle progression and survival in the setting of cyclin D1 expression in vivo, Cell Cycle 8 (2009) 2802-2809.

[148]P. Corsino, Cyclin-Dependent Kinases as Tumor Initiators and Therapeutic Targets, University of Florida, 2008.

[149] E.H. Hinchcliffe, C. Li, E.A. Thompson, J.L. Maller, G. Sluder, Requirement of Cdk2-cyclin E activity for repeated centrosome reproduction in Xenopus egg extracts, Science 283 (1999) 851-854.

[150] Y. Matsumoto, K. Hayashi, E. Nishida, Cyclin-dependent kinase 2 (Cdk2) is required for centrosome duplication in mammalian cells, Curr. Biol. 9 (1999) 429-432.

[151] Z.A. Stewart, S.D. Leach, J.A. Pietenpol, p21(Waf1/Cip1) inhibition of cyclin E/Cdk2 activity prevents endoreduplication after mitotic spindle disruption, Mol. Cell. Biol. 19 (1999) 205-215.

[152] T. Nishimura, M. Takahashi, H.S. Kim, H. Mukai, Y. Ono, Centrosome-targeting region of CG-NAP causes centrosome amplification by recruiting cyclin E-cdk2 complex, Genes Cells 10 (2005) 75-86.

[153] A. Duensing, Y. Liu, M. Tseng, M. Malumbres, M. Barbacid, S. Duensing, Cyclin-dependent kinase 2 is dispensable for normal centrosome duplication but required for oncogene-induced centrosome overduplication, Oncogene 25 (2006) 2943-2949.

[154] R. Balczon, L. Bao, W.E. Zimmer, K. Brown, R.P. Zinkowski, B.R. Brinkley, Dissociation of centrosome replication events from cycles of DNA synthesis and mitotic division in hydroxyurea-arrested Chinese hamster ovary cells, J. Cell Biol. 130 (1995) 105-115.

[155] M. Okuda, H.F. Horn, P. Tarapore, Y. Tokuyama, A.G. Smulian, P.K. Chan, E.S. Knudsen, I.A. Hofmann, J.D. Snyder, K.E. Bove, K. Fukasawa, Nucleophosmin/B23 is a target of CDK2/cyclin E in centrosome duplication, Cell 103 (2000) 127-140.

[156] A.J. Minn, L.H. Boise, C.B. Thompson, Expression of Bcl-xL and loss of p53 can cooperate to overcome a cell cycle checkpoint induced by mitotic spindle damage, Genes Dev. 10 (1996) 2621-2631.

[157] J.S. Lanni, T. Jacks, Characterization of the p53-dependent postmitotic checkpoint following spindle disruption, Mol. Cell. Biol. 18 (1998) 1055-1064.

[158] A. Janssen, G.J. Kops, R.H. Medema, Elevating the frequency of chromosome mis-segregation as a strategy to kill tumor cells, Proc. Natl. Acad. Sci. U. S. A. 106 (2009) 19108-19113.

[159] L. Kabeche, D.A. Compton, Checkpoint-independent stabilization of kinetochore-microtubule attachments by Mad2 in human cells, Curr. Biol. 22 (2012) 638-644.

[160] T. Sudo, M. Nitta, H. Saya, N.T. Ueno, Dependence of paclitaxel sensitivity on a functional spindle assembly checkpoint, Cancer Res. 64 (2004) 2502-2508.

[161] X. Hao, Z. Zhou, S. Ye, T. Zhou, Y. Lu, D. Ma, S. Wang, Effect of Mad2 on paclitaxel-induced cell death in ovarian cancer cells, J Huazhong Univ Sci Technolog Med Sci 30 (2010) 620-625.

[162] A.A. Ahmed, A.D. Mills, A.E. Ibrahim, J. Temple, C. Blenkiron, M. Vias, C.E. Massie, N.G. Iyer, A. McGeoch, R. Crawford, B. Nicke, J. Downward, C. Swanton, S.D. Bell, H.M. Earl, R.A. Laskey, C. Caldas, J.D. Brenton, The extracellular matrix protein TGFBI induces microtubule stabilization and sensitizes ovarian cancers to paclitaxel, Cancer Cell 12 (2007) 514-527.

[163] Y.X. Chen, Y. Wang, C.C. Fu, F. Diao, L.N. Song, Z.B. Li, R. Yang, J. Lu, Dexamethasone enhances cell resistance to chemotherapy by increasing adhesion to extracellular matrix in human ovarian cancer cells, Endocr Relat Cancer 17 (2010) 39-50.

[164] J.M. Westendorf, P.N. Rao, L. Gerace, Cloning of cDNAs for M-phase phosphoproteins recognized by the MPM2 monoclonal antibody and determination of the phosphorylated epitope, Proc. Natl. Acad. Sci. U. S. A. 91 (1994) 714-718.

[165] G.M. Chin, R. Herbst, Induction of apoptosis by monastrol, an inhibitor of the mitotic kinesin Eg5, is independent of the spindle checkpoint, Mol Cancer Ther 5 (2006) 2580-2591.

[166] M.O. Trielli, P.R. Andreassen, F.B. Lacroix, R.L. Margolis, Differential Taxol-dependent arrest of transformed and nontransformed cells in the G1 phase of the cell cycle, and specific-related mortality of transformed cells, J. Cell Biol. 135 (1996) 689-700.

[167] A.W. Duncan, R.D. Hickey, N.K. Paulk, A.J. Culberson, S.B. Olson, M.J. Finegold, M. Grompe, Ploidy reductions in murine fusion-derived hepatocytes, PLoS Genet 5 (2009) e1000385.

[168] H.D. Soule, T.M. Maloney, S.R. Wolman, W.D. Peterson, Jr., R. Brenz, C.M. McGrath, J. Russo, R.J. Pauley, R.F. Jones, S.C. Brooks, Isolation and characterization of a spontaneously immortalized human breast epithelial cell line, MCF-10, Cancer Res. 50 (1990) 6075-6086.

[169] J. Bayani, Preparation of Cytogenetic Specimens from Tissue Samples, John Wiley and Sons, Inc., Hoboken, NJ, 2004.

[170] B.K. Law, A. Chytil, N. Dumont, E.G. Hamilton, M.E. Waltner-Law, M.E. Aakre, C. Covington, H.L. Moses, Rapamycin potentiates transforming growth factor beta-induced growth arrest in nontransformed, oncogene-transformed, and human cancer cells, Mol. Cell. Biol. 22 (2002) 8184-8198.

[171] I. Garcia-Higuera, E. Manchado, P. Dubus, M. Canamero, J. Mendez, S. Moreno, M. Malumbres, Genomic stability and tumour suppression by the APC/C cofactor Cdh1, Nat Cell Biol 10 (2008) 802-811.

[172] P. Tarapore, K. Shinmura, H. Suzuki, Y. Tokuyama, S.H. Kim, A. Mayeda, K. Fukasawa, Thr199 phosphorylation targets nucleophosmin to nuclear speckles and represses pre-mRNA processing, FEBS Lett. 580 (2006) 399-409.

[173] M.E. Cuomo, A. Knebel, N. Morrice, H. Paterson, P. Cohen, S. Mittnacht, p53-Driven apoptosis limits centrosome amplification and genomic instability downstream of NPM1 phosphorylation, Nat Cell Biol 10 (2008) 723-730.

[174] M.F. Buckley, K.J. Sweeney, J.A. Hamilton, R.L. Sini, D.L. Manning, R.I. Nicholson, A. deFazio, C.K. Watts, E.A. Musgrove, R.L. Sutherland, Expression and amplification of cyclin genes in human breast cancer, Oncogene 8 (1993) 2127-2133.

[175] M. Loden, M. Stighall, N.H. Nielsen, G. Roos, S.O. Emdin, H. Ostlund, G. Landberg, The cyclin D1 high and cyclin E high subgroups of breast cancer: separate pathways in tumorogenesis based on pattern of genetic aberrations and inactivation of the pRb node, Oncogene 21 (2002) 4680-4690.

[176] T. Lindahl, G. Landberg, J. Ahlgren, H. Nordgren, T. Norberg, S. Klaar, L. Holmberg, J. Bergh, Overexpression of cyclin E protein is associated with specific mutation types in the p53 gene and poor survival in human breast cancer, Carcinogenesis 25 (2004) 375-380.

[177] R.D. Coletta, K. Christensen, K.J. Reichenberger, J. Lamb, D. Micomonaco, L. Huang, D.M. Wolf, C. Muller-Tidow, T.R. Golub, K. Kawakami, H.L. Ford, The Six1 homeoprotein stimulates tumorigenesis by reactivation of cyclin A1, Proc. Natl. Acad. Sci. U. S. A. 101 (2004) 6478-6483.

[178] J.M. Keck, M.K. Summers, D. Tedesco, S. Ekholm-Reed, L.C. Chuang, P.K. Jackson, S.I. Reed, Cyclin E overexpression impairs progression through mitosis by inhibiting APC(Cdh1), J. Cell Biol. 178 (2007) 371-385.

[179] P.E. Corsino, B.J. Davis, P.H. Norgaard, N.N. Parker, M. Law, W. Dunn, B.K. Law, Mammary tumors initiated by constitutive Cdk2 activation contain an invasive basal-like component, Neoplasia 10 (2008) 1240-1252.

[180] Y. Arima, Y. Inoue, T. Shibata, H. Hayashi, O. Nagano, H. Saya, Y. Taya, Rb depletion results in deregulation of E-cadherin and induction of cellular phenotypic changes that are characteristic of the epithelial-to-mesenchymal transition, Cancer Res. 68 (2008) 5104-5112.

[181] I. Cozar-Castellano, G. Harb, K. Selk, K. Takane, R. Vasavada, B. Sicari, B. Law, P. Zhang, D.K. Scott, N. Fiaschi-Taesch, A.F. Stewart, Lessons from the first comprehensive molecular characterization of cell cycle control in rodent insulinoma cell lines, Diabetes 57 (2008) 3056-3068.

[182] C.M. Pfleger, E. Lee, M.W. Kirschner, Substrate recognition by the Cdc20 and Cdh1 components of the anaphase-promoting complex, Genes Dev 15 (2001) 2396-2407.

[183] W. Wang, A. Budhu, M. Forgues, X.W. Wang, Temporal and spatial control of nucleophosmin by the Ran-Crm1 complex in centrosome duplication, Nat Cell Biol 7 (2005) 823-830.

[184] M. Law, E. Forrester, A. Chytil, P. Corsino, G. Green, B. Davis, T. Rowe, B. Law, Rapamycin disrupts cyclin/cyclin-dependent kinase/p21/proliferating cell nuclear antigen complexes and cyclin D1 reverses rapamycin action by stabilizing these complexes, Cancer Res. 66 (2006) 1070-1080.

[185] S.C. Jahn, M.E. Law, P.E. Corsino, N.N. Parker, K. Pham, B.J. Davis, J. Lu, B.K. Law, An in vivo model of epithelial to mesenchymal transition reveals a mitogenic switch, Cancer Lett. 326 (2012) 183-190.

[186] Y. Shav-Tal, D. Zipori, PSF and p54(nrb)/NonO--multi-functional nuclear proteins, FEBS Lett. 531 (2002) 109-114.

[187] J.G. Patton, E.B. Porro, J. Galceran, P. Tempst, B. Nadal-Ginard, Cloning and characterization of PSF, a novel pre-mRNA splicing factor, Genes Dev. 7 (1993) 393-406.

[188] E. Rosonina, J.Y. Ip, J.A. Calarco, M.A. Bakowski, A. Emili, S. McCracken, P. Tucker, C.J. Ingles, B.J. Blencowe, Role for PSF in mediating transcriptional activator-dependent stimulation of pre-mRNA processing in vivo, Mol. Cell. Biol. 25 (2005) 6734-6746.

[189] O. Gozani, J.G. Patton, R. Reed, A novel set of spliceosome-associated proteins and the essential splicing factor PSF bind stably to pre-mRNA prior to catalytic step II of the splicing reaction, EMBO J. 13 (1994) 3356-3367.

[190] S. Liang, C.S. Lutz, p54nrb is a component of the snRNP-free U1A (SF-A) complex that promotes pre-mRNA cleavage during polyadenylation, RNA 12 (2006) 111-121.

[191] A. Emili, M. Shales, S. McCracken, W. Xie, P.W. Tucker, R. Kobayashi, B.J. Blencowe, C.J. Ingles, Splicing and transcription-associated proteins PSF and p54nrb/nonO bind to the RNA polymerase II CTD, RNA 8 (2002) 1102-1111.

[192] S. Kaneko, O. Rozenblatt-Rosen, M. Meyerson, J.L. Manley, The multifunctional protein p54nrb/PSF recruits the exonuclease XRN2 to facilitate pre-mRNA 3' processing and transcription termination, Genes Dev. 21 (2007) 1779-1789.

[193] C.L. Bladen, D. Udayakumar, Y. Takeda, W.S. Dynan, Identification of the polypyrimidine tract binding protein-associated splicing factor.p54(nrb) complex as a candidate DNA double-strand break rejoining factor, J. Biol. Chem. 280 (2005) 5205-5210.

[194] K. Ha, Y. Takeda, W.S. Dynan, Sequences in PSF/SFPQ mediate radioresistance and recruitment of PSF/SFPQ-containing complexes to DNA damage sites in human cells, DNA Repair (Amst) 10 (2011) 252-259.

[195] K.E. Lukong, M.E. Huot, S. Richard, BRK phosphorylates PSF promoting its cytoplasmic localization and cell cycle arrest, Cell. Signal. 21 (2009) 1415-1422.

[196] Y. Shav-Tal, M. Cohen, S. Lapter, B. Dye, J.G. Patton, J. Vandekerckhove, D. Zipori, Nuclear relocalization of the pre-mRNA splicing factor PSF during apoptosis involves hyperphosphorylation, masking of antigenic epitopes, and changes in protein interactions, Mol. Biol. Cell 12 (2001) 2328-2340.

[197] F. Heyd, K.W. Lynch, Phosphorylation-dependent regulation of PSF by GSK3 controls CD45 alternative splicing, Mol. Cell 40 (2010) 126-137.

[198] V. Mayya, D.H. Lundgren, S.I. Hwang, K. Rezaul, L. Wu, J.K. Eng, V. Rodionov, D.K. Han, Quantitative phosphoproteomic analysis of T cell receptor signaling reveals system-wide modulation of protein-protein interactions, Sci Signal 2 (2009) ra46.

[199] B. Hollier, K. Evans, S. Mani, The Epithelial-to-Mesenchymal Transition and Cancer Stem Cells: A Coalition Against Cancer Therapies, J. Mammary Gland Biol. Neoplasia 14 (2009) 29-43.

[200] M. Iwatsuki, K. Mimori, T. Yokobori, H. Ishi, T. Beppu, S. Nakamori, H. Baba, M. Mori, Epithelial–mesenchymal transition in cancer development and its clinical significance, Cancer Sci. 101 (2010) 293-299.

[201] M. Santisteban, J.M. Reiman, M.K. Asiedu, M.D. Behrens, A. Nassar, K.R. Kalli, P. Haluska, J.N. Ingle, L.C. Hartmann, M.H. Manjili, D.C. Radisky, S. Ferrone, K.L. Knutson, Immune-Induced Epithelial to Mesenchymal Transition In vivo Generates Breast Cancer Stem Cells, Cancer Res. 69 (2009) 2887-2895.

[202] M.K. Wendt, J.A. Smith, W.P. Schiemann, Transforming growth factor-[beta]-induced epithelial-mesenchymal transition facilitates epidermal growth factor-dependent breast cancer progression, Oncogene 29 (2010) 6485-6498.

[203] K. Aigner, B. Dampier, L. Descovich, M. Mikula, A. Sultan, M. Schreiber, W. Mikulits, T. Brabletz, D. Strand, P. Obrist, W. Sommergruber, N. Schweifer, A. Wernitznig, H. Beug, R. Foisner, A. Eger, The transcription factor ZEB1 (deltaEF1) promotes tumour cell dedifferentiation by repressing master regulators of epithelial polarity, Oncogene 26 (2007) 6979-6988.

[204] T.R. Graham, H.E. Zhau, V.A. Odero-Marah, A.O. Osunkoya, K.S. Kimbro, M. Tighiouart, T. Liu, J.W. Simons, R.M. O'Regan, Insulin-like growth factor-I-dependent up-regulation of ZEB1 drives epithelial-to-mesenchymal transition in human prostate cancer cells, Cancer Res. 68 (2008) 2479-2488.

[205] H.C. Lien, Y.H. Hsiao, Y.S. Lin, Y.T. Yao, H.F. Juan, W.H. Kuo, M.C. Hung, K.J. Chang, F.J. Hsieh, Molecular signatures of metaplastic carcinoma of the breast by large-scale transcriptional profiling: identification of genes potentially related to epithelial-mesenchymal transition, Oncogene 26 (2007) 7859-7871.

[206] D. Sarrio, S.M. Rodriguez-Pinilla, D. Hardisson, A. Cano, G. Moreno-Bueno, J. Palacios, Epithelial-mesenchymal transition in breast cancer relates to the basal-like phenotype, Cancer Res. 68 (2008) 989-997.

[207] C. Gjerdrum, C. Tiron, T. Hoiby, I. Stefansson, H. Haugen, T. Sandal, K. Collett, S. Li, E. McCormack, B.T. Gjertsen, D.R. Micklem, L.A. Akslen, C. Glackin, J.B. Lorens, Axl is an essential epithelial-to-mesenchymal transition-induced regulator of breast cancer metastasis and patient survival, Proc. Natl. Acad. Sci. U. S. A. 107 (2010) 1124-1129.

[208] M.G. Ponzo, R. Lesurf, S. Petkiewicz, F.P. O'Malley, D. Pinnaduwage, I.L. Andrulis, S.B. Bull, N. Chughtai, D. Zuo, M. Souleimanova, D. Germain, A. Omeroglu, R.D. Cardiff, M. Hallett, M. Park, Met induces mammary tumors with diverse histologies and is associated with poor outcome and human basal breast cancer, Proc. Natl. Acad. Sci. U. S. A. 106 (2009) 12903-12908.

[209] S. Thomson, F. Petti, I. Sujka-Kwok, D. Epstein, J.D. Haley, Kinase switching in mesenchymal-like non-small cell lung cancer lines contributes to EGFR inhibitor resistance through pathway redundancy, Clin. Exp. Metastasis 25 (2008) 843-854.

[210] M. Jechlinger, A. Sommer, R. Moriggl, P. Seither, N. Kraut, P. Capodiecci, M. Donovan, C. Cordon-Cardo, H. Beug, S. Grünert, Autocrine PDGFR signaling promotes mammary cancer metastasis, The Journal of Clinical Investigation 116 (2006) 1561-1570.

[211] A.A. Thike, J. Iqbal, P.Y. Cheok, A.P. Chong, G.M. Tse, B. Tan, P. Tan, N.S. Wong, P.H. Tan, Triple negative breast cancer: outcome correlation with immunohistochemical detection of basal markers, Am. J. Surg. Pathol. 34 (2010) 956-964.

[212] S.E. Elsheikh, A.R. Green, E.A. Rakha, R.M. Samaka, A.A. Ammar, D. Powe, J.S. Reis-Filho, I.O. Ellis, Caveolin 1 and Caveolin 2 are associated with breast cancer basal-like and triple-negative immunophenotype, Br. J. Cancer 99 (2008) 327-334.

[213] J.S. Reis-Filho, A.N. Tutt, Triple negative tumours: a critical review, Histopathology 52 (2008) 108-118.

[214] R.M. Neve, K. Chin, J. Fridlyand, J. Yeh, F.L. Baehner, T. Fevr, L. Clark, N. Bayani, J.P. Coppe, F. Tong, T. Speed, P.T. Spellman, S. DeVries, A. Lapuk, N.J. Wang, W.L. Kuo, J.L. Stilwell, D. Pinkel, D.G. Albertson, F.M. Waldman, F. McCormick, R.B. Dickson, M.D. Johnson, M. Lippman, S. Ethier, A. Gazdar, J.W. Gray, A collection of breast cancer cell lines for the study of functionally distinct cancer subtypes, Cancer Cell 10 (2006) 515-527.

[215] M.E. Law, P.E. Corsino, S.C. Jahn, B.J. Davis, S. Chen, B. Patel, K. Pham, J. Lu, B. Sheppard, P. Norgaard, J. Hong, P. Higgins, J.S. Kim, H. Luesch, B.K. Law, Glucocorticoids and histone deacetylase inhibitors cooperate to block the invasiveness of basal-like breast cancer cells through novel mechanisms, Oncogene (2012).

[216] L. Xu, M.B. Nilsson, P. Saintigny, T. Cascone, M.H. Herynk, Z. Du, P.G. Nikolinakos, Y. Yang, L. Prudkin, D. Liu, J.J. Lee, F.M. Johnson, K.K. Wong, L. Girard, A.F. Gazdar, J.D. Minna, J.M. Kurie, I.I. Wistuba, J.V. Heymach, Epidermal growth factor receptor regulates MET levels and invasiveness through hypoxia-inducible factor-1[alpha] in non-small cell lung cancer cells, Oncogene 29 (2010) 2616-2627.

[217] P. Savagner, K.M. Yamada, J.P. Thiery, The zinc-finger protein slug causes desmosome dissociation, an initial and necessary step for growth factor-induced epithelial-mesenchymal transition, J. Cell Biol. 137 (1997) 1403-1419.

[218] M. Oft, K.H. Heider, H. Beug, TGFbeta signaling is necessary for carcinoma cell invasiveness and metastasis, Curr. Biol. 8 (1998) 1243-1252.

[219] M.J. Chuang, K.H. Sun, S.J. Tang, M.W. Deng, Y.H. Wu, J.S. Sung, T.L. Cha, G.H. Sun, Tumor-derived tumor necrosis factor-alpha promotes progression and epithelial-mesenchymal transition in renal cell carcinoma cells, Cancer Sci 99 (2008) 905-913.

[220] N.J. Sullivan, A.K. Sasser, A.E. Axel, F. Vesuna, V. Raman, N. Ramirez, T.M. Oberyszyn, B.M. Hall, Interleukin-6 induces an epithelial-mesenchymal transition phenotype in human breast cancer cells, Oncogene 28 (2009) 2940-2947.

[221] Y. Li, M.M. Bhargava, A. Joseph, L. Jin, E.M. Rosen, I.D. Goldberg, Effect of hepatocyte growth factor/scatter factor and other growth factors on motility and morphology of non-tumorigenic and tumor cells, In Vitro Cell. Dev. Biol. Anim. 30A (1994) 105-110.

[222] J. Gotzmann, A.N.M. Fischer, M. Zojer, M. Mikula, V. Proell, H. Huber, M. Jechlinger, T. Waerner, A. Weith, H. Beug, W. Mikulits, A crucial function of PDGF in TGF-[beta]-mediated cancer progression of hepatocytes, Oncogene 25 (2006) 3170-3185.

[223] S. Zhao, K. Venkatasubbarao, J.W. Lazor, J. Sperry, C. Jin, L. Cao, J.W. Freeman, Inhibition of STAT3 Tyr705 phosphorylation by Smad4 suppresses transforming growth factor beta-mediated invasion and metastasis in pancreatic cancer cells, Cancer Res. 68 (2008) 4221-4228.

[224] H.W. Lo, S.C. Hsu, W. Xia, X. Cao, J.Y. Shih, Y. Wei, J.L. Abbruzzese, G.N. Hortobagyi, M.C. Hung, Epidermal growth factor receptor cooperates with signal transducer and activator of transcription 3 to induce epithelial-mesenchymal transition in cancer cells via up-regulation of TWIST gene expression, Cancer Res. 67 (2007) 9066-9076.

[225] L. Beviglia, K. Matsumoto, C.S. Lin, B.L. Ziober, R.H. Kramer, Expression of the c-Met/HGF receptor in human breast carcinoma: correlation with tumor progression, Int. J. Cancer 74 (1997) 301-309.

[226] C.R. Stadler, P. Knyazev, J. Bange, A. Ullrich, FGFR4 GLY388 isotype suppresses motility of MDA-MB-231 breast cancer cells by EDG-2 gene repression, Cell. Signal. 18 (2006) 783-794.

[227] M. David, J. Ribeiro, F. Descotes, C.M. Serre, M. Barbier, M. Murone, P. Clezardin, O. Peruchaud, Targeting lysophosphatidic acid receptor type 1 with Debio 0719 inhibits spontaneous metastasis dissemination of breast cancer cells

independently of cell proliferation and angiogenesis., Int. J. Oncol. 40 (2011) 1133-1141.

[228] H. Zhang, X. Xu, J. Gajewiak, R. Tsukahara, Y. Fujiwara, J. Liu, J.I. Fells, D. Perygin, A.L. Parrill, G. Tigyi, G.D. Prestwich, Dual Activity Lysophosphatidic Acid Receptor Pan-Antagonist/Autotaxin Inhibitor Reduces Breast Cancer Cell Migration In vitro and Causes Tumor Regression In vivo, Cancer Res. 69 (2009) 5441-5449.

[229] A.H. Brivanlou, J.E. Darnell, Signal Transduction and the Control of Gene Expression, Science 295 (2002) 813-818.

[230] D.E. Levy, J.E. Darnell, STATs: transcriptional control and biological impact, Nat Rev Mol Cell Biol 3 (2002) 651-662.

[231] J.J. O'Shea, M. Gadina, R.D. Schreiber, Cytokine Signaling in 2002: New Surprises in the Jak/Stat Pathway, Cell 109 (2002) S121-S131.

[232] S.J. Holland, A. Pan, C. Franci, Y. Hu, B. Chang, W. Li, M. Duan, A. Torneros, J. Yu, T.J. Heckrodt, J. Zhang, P. Ding, A. Apatira, J. Chua, R. Brandt, P. Pine, D. Goff, R. Singh, D.G. Payan, Y. Hitoshi, R428, a selective small molecule inhibitor of Axl kinase, blocks tumor spread and prolongs survival in models of metastatic breast cancer, Cancer Res. 70 (2010) 1544-1554.

[233] H.Y. Zou, Q. Li, J.H. Lee, M.E. Arango, S.R. McDonnell, S. Yamazaki, T.B. Koudriakova, G. Alton, J.J. Cui, P.P. Kung, M.D. Nambu, G. Los, S.L. Bender, B. Mroczkowski, J.G. Christensen, An orally available small-molecule inhibitor of c-Met, PF-2341066, exhibits cytoreductive antitumor efficacy through antiproliferative and antiangiogenic mechanisms, Cancer Res. 67 (2007) 4408-4417.

[234] K.L. Lin, J.C. Su, C.M. Chien, C.H. Tseng, Y.L. Chen, L.S. Chang, S.R. Lin, Naphtho[1,2-b]furan-4,5-dione disrupts Janus kinase-2 and induces apoptosis in breast cancer MDA-MB-231 cells, Toxicol In Vitro 24 (2010) 1158-1167.

[235] Z. Duan, J. Bradner, E. Greenberg, R. Mazitschek, R. Foster, J. Mahoney, M.V. Seiden, 8-benzyl-4-oxo-8-azabicyclo[3.2.1]oct-2-ene-6,7-dicarboxylic acid (SD-1008), a novel janus kinase 2 inhibitor, increases chemotherapy sensitivity in human ovarian cancer cells, Mol. Pharmacol. 72 (2007) 1137-1145.

[236] K. Siddiquee, S. Zhang, W.C. Guida, M.A. Blaskovich, B. Greedy, H.R. Lawrence, M.L. Yip, R. Jove, M.M. McLaughlin, N.J. Lawrence, S.M. Sebti, J. Turkson, Selective chemical probe inhibitor of Stat3, identified through structure-based virtual screening, induces antitumor activity, Proc. Natl. Acad. Sci. U. S. A. 104 (2007) 7391-7396.

[237] A.A. Melton, J. Jackson, J. Wang, K.W. Lynch, Combinatorial control of signal-induced exon repression by hnRNP L and PSF, Mol. Cell. Biol. 27 (2007) 6972-6984.

[238] M. Schiffman, P.E. Castle, J. Jeronimo, A.C. Rodriguez, S. Wacholder, Human papillomavirus and cervical cancer, Lancet 370 (2007) 890-907.

[239] J. Doorbar, The papillomavirus life cycle, J. Clin. Virol. 32 Suppl 1 (2005) S7-15.

[240] C.A. Moody, L.A. Laimins, Human papillomavirus oncoproteins: pathways to transformation, Nat Rev Cancer 10 (2010) 550-560.

[241] D.K. Shibata, N. Arnheim, W.J. Martin, Detection of human papilloma virus in paraffin-embedded tissue using the polymerase chain reaction, J. Exp. Med. 167 (1988) 225-230.

[242] C.C. Baker, W.C. Phelps, V. Lindgren, M.J. Braun, M.A. Gonda, P.M. Howley, Structural and transcriptional analysis of human papillomavirus type 16 sequences in cervical carcinoma cell lines, J. Virol. 61 (1987) 962-971.

[243] J. Cicenas, M. Valius, The CDK inhibitors in cancer research and therapy, J. Cancer Res. Clin. Oncol. 137 (2011) 1409-1418.

[244] C.M. McGrath, H.D. Soule, Calcium regulation of normal human mammary epithelial cell growth in culture, In Vitro 20 (1984) 652-662.

[245] J. Yang, J. Richards, P. Bowman, R. Guzman, J. Enami, K. McCormick, S. Hamamoto, D. Pitelka, S. Nandi, Sustained growth and three-dimensional organization of primary mammary tumor epithelial cells embedded in collagen gels, Proc. Natl. Acad. Sci. U. S. A. 76 (1979) 3401-3405.

[246] J. Yang, A. Balakrishnan, S. Hamamoto, J.J. Elias, W. Rosenau, C.W. Beattie, T.K. Das Gupta, S.R. Wellings, S. Nandi, Human breast epithelial cells in serum-free collagen gel primary culture: growth, morphological, and immunocytochemical analysis, J. Cell. Physiol. 133 (1987) 228-234, 254-225.

BIOGRAPHICAL SKETCH

Stephan Christopher Jahn was born in Saginaw, Michigan. He received his high school diploma from Arthur Hill High School in 2004, after which he obtained a Bachelor of Science degree in biochemistry from Saginaw Valley State University in 2008. His undergraduate honors thesis was titled “Completing the Cycle: Formation of Cloud Point Depressants from Glycerin Obtained in the Production of Biodiesel,” and concurrently worked in Dow Dispersion Sciences and subsequently Amerchol at The Dow Chemical Company. Upon graduation, he began the Interdisciplinary Program in Biomedical Science at the University of Florida and obtained his Ph.D. from the College of Medicine working with Dr. Brian Law in the Department of Pharmacology and Therapeutics.